STRUCTURAL AND FUNCTIONAL RELATIONSHIP OF PIN1

SONG PEI CHEE

(BACHELOR OF SCIENCE (HONOURS), NUS)

A THESIS SUBMITTED

FOR THE DEGREE OF MASTER OF SCIENCE

DEPARTMENT OF BIOCHEMISTRY

NATIONAL UNIVERSITY OF SINGAPORE

2007

ACKNOWLEDGEMENTS

♣ I would like to sincerely thank my supervisors, Dr. Liou Yih-Cherng and Dr Tang Bor Luen, for giving me this opportunity to work on this project, and for their patient guidance. I would like to thank Dr Wu Xueji for crystal growing and encouragement. Without his help, I would not have had the protein crystals for X-ray crystallography. I would like to thank Dr. Jayaraman Sivaraman for support and advice on X-ray crystallography. I would like to thank my fellow postgraduate student, Jobichen Chacko, for his practical help on X-ray diffraction and structure refinements, and his time spent to help solving my problems on the structural biology softwares and the LINUX system; and to Liu Yang for his help on MOLMOL to draw structure figures during the very critical time. I would like to thank our friend in the Department of Mathematics, Xu Yuhong, for his help on writing a Matlab script to analyze and plot graphs for the CD data. Without his help, those thousand sets of data would have made me crazy to analyze for the Pin1 mutants' melting temperature. I would also like to thank our lab manager, Shirley, all the fellow members in Dr Liou's and Dr. Tang's labs, members in Dr. Sivaraman's lab, and fellows along the Structural Biology Lab corridor. I would like to thank Mr Suwato from the Bio-Rad company in assisting the setting up of FPLC system. Last but not the least, I would like to thank my sisters in Christ for interceding and praying with me in love for the project and thesis writing, and to my dear husband for his never ever failing support which is beyond any words to express. *–Phoebe, December 2006*

TABLE OF CONTENTS

SUMMARY

Peptidyl-prolyl isomerase Pin1 is a key protein in many regulatory processes in the mammalian cell. By catalyzing conformational changes in over 50 critical proteins, it participates in a diverse array of cellular processes, including cell cycle control, transcription / splicing regulation, DNA replication checkpoint control, DNA damage response, neuronal survival, and germ cell development. Deregulation of Pin1 has been implicated in several human diseases. Notably, overexpression of Pin1 is prevalent in many human cancers; whereas its inhibition induces apoptosis and contributes to neuronal death in Alzheimer's disease. Pin1 specifically catalyzes *cis*/*trans*-isomerization of proline in the target sequence of phosphorylated Ser/Thr-Pro. Very little is known about its catalytic mechanism and its interaction with its biological substrates.

In the current studies, crystal structures of seven Pin1 mutants of previously reported functionally important residues, including R14A, F25A, S32A, W34A, K63A, C113A, and M130A, are solved and compared to the published wild-type structures. Structures of R14A, F25A, and S32A mutants exhibited side chain shifts in residues Arg-14, Arg-17, His-27, Arg-21, Gln-66, and Lys-117, suggesting the formers' potential roles in substrate binding. Conformation at the active site of the C113A and M130A structures was identical to the wild-type structure even though without a bound substrate at the site. Our CD analyses show a decreased melting

temperature for C113A and M130A. Together, these suggest that Cys-113 and Met-130 contribute to the stability of Pin1's core structure. This region could be very rigid to serve as a critical selectivity filter for substrate binding. The α1/β1 loops of all the mutants are in a closed conformation although there is no sulphate or phosphate ion recruited to the PPIase catalytic site. This observation contradicts a previously proposed "induced-fit" model. Here, we propose a "two-step induced-fit" binding model. In this model, substrate binding to the WW domain induces the opening of the α1/β1 loop through Arg-14 and Phe-25 for the recruitment of a second recognition motif to the catalytic site. This second binding in turn induces the closure of α1/β1 loop, followed by substrate conformational change through *cis/trans*-isomerization of proline. Lastly, Pin1 nuclear localization could result from its interaction with cellular substrates. Interestingly, the W34A mutant caused Pin1 translocation to the cytosol in all cell cycle stages, indicating the *in vivo* relevance of Trp-34 in substrate binding.

In summary, the work reported in this dissertation provided new information on certain key residues with their contribution to Pin1 core structure stability, local secondary structures and its subcellular distribution. These revealed novel insights of how Pin1 interacts with its biological target proteins, which could perhaps aid effective rational drug design.

Keywords: Pin1, isomerization, α1/β1 loop, "two-step induced-fit" binding model, melting temperature, translocation

LIST OF TABLES

LIST OF FIGURES

LIST OF ABBREVIATIONS

Aβ	Amyloid β peptides
AD	Alzheimer's disease
AICD	APP intracellular domain
APC	Adenomatous polyposis protein
APP	Amyloid precursor protein
APS	Ammonium persulphate
ATCC	American Type Culture Collection
CD	Circular dichroism
Cdk2	Cyclin-dependent protein kinase 2
Chk2	Checkpoint kinase 2
CHO	Chinese hamster ovary
CHT-I	Bio-Scale ceramic hydroxyapatite Type I
CsA	Cyclosporine A
CTD	C-terminal repeated domain
CTF	Carboxy-terminal fragments
CyP	Cyclophilin
DMEM	Dulbeco's Minimum Eagles Medium
E. coli	*Escherichia coli*
EGF	Epidermal growth factor
EGFP	Enhanced green fluorencence protein

FKBP	FK506-binding protein
FPLC	Fast performance liquid chromatography
HRP	Horse radish peroxidase
IPTG	Isopropyl β-D-1-thiogalactopyranoside
IRF3	Interferon-regulatory factor 3
JIP3	JNK-interacting protein 3
JNK	Jun N-terminal protein kinase
LB	Luria Bertani broth
LPS	Lipopolysaccharide
MAPK	Mitogen-activated protein kinase
MRW	Mean residue weight
MS	Mass spectrometry
NFTs	Neurofibrillary tangles
NHERF-1	Na^+/H^+ exchanger regulatory factor 1
NIMA	Never-In-Mitosis A
NMR	Nuclear magnetic resonance
PCR	Polymerase chain reaction
PEG	Polyethylene glycol
PHFs	Paired helical filaments
pI	Isoelectric point
Pin1	Peptidyl-prolyl isomerase 1
PPC	Protein and Proteomic Center

PPIase	Peptidyl-prolyl isomerase
PPII	Polyproline II
PP2A	Protein phosphatase 2A
pSer/Thr-Pro	Phosphorylated serine or threonine followed by a proline
SDS-PAGE	Sodium dodecyl sulphate polyacrylamide gel electrophoresis
SH3	Src homology 3
SRC-3	Steroid receptor coactivator-3
TB	Terrific broth
TCF	Ternary complex factor
TEMED	N,N,N,N,-Tetramethyl-Ethylenediamine
TLR	Toll-like receptor
Tm	Melting temperature
WT	Wild type

LIST OF SYMBOLS

$[\Theta]$	Mean residue ellipticity
λ	Wavelength
θ_λ	Measured ellipticity in degree at wavelength λ
ω	Angular frequency
Kd	Dissociation constant
Ka	Association constant

CHAPTER 1: A LITERATURE REVIEW ON THE STRUCTURE AND FUNCTION RELATIONSHIP OF PIN1

1.1 Introduction

Peptidyl-prolyl isomerase (PPIase) Pin1 (EC 5.2.1.8) is an essential protein in regulating entry into mitosis by catalyzing the conformational change of a number of critical regulatory proteins. Structurally and functionally, Pin1 is a novel prolyl isomerase and specifically catalyzes *cis*/*trans*-isomerization of proline in the sequence of phosphorylated Ser/Thr-Pro (pSer/Thr-Pro). Ser/Thr-Pro is a major regulatory phosphorylation motif that functions in diverse cellular processes, and it has long been believed that Ser/Thr phosphorylation regulates the function of proteins by inducing conformational changes. Yet, little is known about how phosphorylation actually induces the conformational change. The identification of Pin1 has revealed a novel post-phosphorylation regulatory mechanism, in which Pin1 induces the conformational change of proteins through its specific isomerase activity towards pSer/Thr-Pro motifs, thereby regulating protein function (Lu et al., 2002a; Lu et al., 1996b; Ranganathan et al., 1997; Yaffe et al., 1997).

Intensive studies on Pin1 had revealed a wide range of critical proteins essential in cell cycle regulation to be its biological substrates. Deregulation of Pin1 has been implicated in pathological conditions including cancers and neurodegenerative diseases (Wulf et al., 2005). Hence, comprehensive biochemical, cellular, functional and structural studies have been carried out to understand the

mechanism of Pin1 in regulating the activity of its biological substrates.

1.2 The peptidyl-prolyl isomerase (PPIase) family

Peptidyl-prolyl isomerases (PPIases) are ubiquitous proteins expressed in prokaryotic and eukaryotic cells. They are enzymes that catalyze the interconversion of *cis/trans* conformations of certain peptidyl prolyl bonds in proline-containing peptide chains. These enzymes were originally identified as helper enzymes for accelerating the restructuring of polypeptide backbones to promote native folding of newly synthesized proteins (Fischer et al., 1998; Schiene and Fischer, 2000). To date, based on sequence homology and drug specificity, PPIases have been classified into three families, namely cyclophilins (CyPs), FK506-binding protein (FKBPs), and parvulins. CyPs and FKBPs selectively bind the immunosuppressant drugs cyclosporine A (CsA) and FK506 / rapamycin, respectively. CyPs and FKBPs are hence also known as immunophilins, and they are implicated in immune functions. Recent studies have recognized that they act by sequestering calcineurin, rather than having an immune system-specific action (Shaw, 2002). Moreover, CyPs and FKBPs are also involved in neuroprotection or neuroregeneration activities, Ca^{2+}-mediated intracellular signaling, chaperone activities, and HIV infection (Wang and Etzkorn, 2006). On the other hand, unlike CyPs and FKBPs, members of the parvulin family, which include the *Escherichia coli* (*E. coli*) protein parvulin, the *Drosophila dodo* gene product, the *Arabidopsis* protein At-Pin1at, human protein hPar14 and the focus of the thesis, Pin1, do not bind immunosuppressant drugs. They have instead been

shown to be important for cell cycle progression (Shaw, 2002).

These three families of PPIases are also structurally distinct. CyPs consist of eight antiparallel β-strands wrapping around a barrel surface that forms a compact hydrophobic pocket in which CsA binds (Ke et al., 1991). FKBPs, in contrast, are characterized by an amphipathic, five-stranded β-sheet that wraps around a single short α-helix (Van Duyne et al., 1991; Michnick et al., 1991). PPIase domain of parvulins folds into a half β-barrel, consisting of four antiparallel β-strands surrounded by four α-helices (Ranganathan et al., 1997).

1.3 Pin1 discovery and historical perspectives

The human PPIase Pin1 was first identified in 1996 by yeast two-hybrid screens as a protein that binds to and suppresses the toxicity of Never-In-Mitosis A (NIMA), a fungal mitotic kinase that is phosphorylated on multiple pSer/Thr-Pro motifs and induces mitotic catastrophe in eukaryotic cells (Lu et al., 1996a; Lu and Hunter, 1995; Ye et al., 1995). Hence, it is given the name as Pin1 (Protein (peptidyl-prolyl cis/trans isomerase) NIMA-interacting 1). Subsequent studies revealed that Pin1 specifically binds to and isomerizes pSer/Thr-Pro motifs, in a large and defined subset of phosphoproteins (Lu et al., 1999b; Ranganathan et al., 1997; Yaffe et al., 1997). This specificity of Pin1 is not observed for other two well-known families of PPIases. Hence, Pin1 was classified into the parvulin family of PPIases, whose enzymatic activity can be irreversibly inhibited by the compound juglone (5-hydroxy-1,4-naphthoquinone) (Rahfeld et al., 1994b; Rudd et al., 1995; Lu et al.,

1996b). Interestingly, within the parvulin family of PPIases, bacterial and mouse parvulins, as well as human hPar14 have no activity towards pSer/Thr-Pro bonds, and their phosphorylated function remains unknown (Uchida et al., 1999). Thus, the parvulin family can be further subdivided into Pin1-type PPIases and Parvulin-type PPIases (Lu et al., 2002a).

Human Pin1 encodes a polypeptide of 163 amino acid residues in length with a molecular weight of 18,000 Dalton and is ubiquitously expressed (Lu et al., 1996b). It is a nuclear protein and mainly localizes at nuclear speckles. Pin1 is highly conserved among the eukaryotes. Among its homologues, human Pin1 shares 95% identity to mouse Pin1, 87% to *Xenopus* Pin1, 57% to *Drosophila* Dodo, 46% to yeast Ptf1/Ess1, 51% to fungi Ssp1, and 51% to plant At-Pin1at (Fujimori et al., 1999; Hani et al., 1995; Landrieu et al., 2002; Maleszka et al., 1996; Kops et al., 1998; Winkler et al., 2000). In contrast to cyclophilins and FKBPs for which deletion in yeast is non-lethal, Ptf1/Ess1 or Pin1 is essential for growth in several genetic backgrounds in budding yeast and in several human cancer cell lines. For examples, the depletion of Pin1 or inhibition of its PPIase activity in these cells result in mitotic arrest and apoptosis (Rippmann et al., 2000). In *Xenopus* extracts, Pin1 depletion causes premature G2/M transition and a DNA replication defect (Winkler et al., 2000). In mouse, disruption of *Pin1* gene results in a range of severe cell proliferative defects. On the other hand, overexpression of Pin1 causes G2/M arrest in HeLa cells and in *Xenopus* extracts (Lu et al., 1996b; Shen et al., 1998; Osmani et al., 1988). These observations have

initiated interest on Pin1, and Pin1 was first suggested to be an essential cell cycle regulator involved in G2/M transition and M-phase exit (Albert et al., 2004).

Nevertheless, some findings which question Pin1's essentiality have emerged. For example, disruption of *Pin1* gene in mice, and of its homologues in *Drosophila* and fission yeast, is not lethal, although the mutants do display some interesting phenotypes (Maleszka et al., 1996; Campbell et al., 1997). For example, Pin1 null *Drosophila* displays a severe oogenic defect, and fission yeast mutation has a synthetic growth defect with mutations of Cdc25 or Wee1. The mutant fission yeast is also hypersensitive to inhibitors of phosphatase or cyclophilins. Interestingly, in one strain of budding yeast, Ptf1/Ess1 disruption permits the mutant cells to grow more slowly compared to wild-type cells and the mutant displays elevated level of cyclophilin A, as in the case in Ptf1/Ess1 knockout fission yeast. Furthermore, overexpression of cyclophilin A can rescue the *Pin1* phenotype. These results suggest that Pin1 and cyclophilin A might have some overlapping functions under certain conditions. Besides, there are multiple *Pin1*-like genes in plants and more than one *Pin1*-related gene in Drosophila. Thus, other functionally overlapping *Pin1*-like genes or even other structurally distinct phosphorylation-specific PPIases may exist in higher eukaryotic cells to explain why *Pin1* gene is not essential in some model organisms (Campbell et al., 1997).

1.4 A unique role in the pSer/Thr-Pro conformational switch

Proline has a distinctive five-carbonyl ring structure, where its three-carbon side

chain is linked back to the nitrogen atom of its backbone. Thus, the peptide bond of the prolyl residue in relation to an adjacent phosphorylated site in a native protein is able to populate two markedly distinct *cis* and *trans* conformations (Figure 1-1) (Wulf et al., 2005). Typically, the pSer/Thr-Pro peptide bond that is stable in the *cis* conformation in a protein is estimated to be ~10-20% (Zhou et al., 2000). Moreover, rotation around the prolyl peptide bonds is energetically unfavored, with a ~22 kcal/mol energy barrier due to their partial double-bond character (Ranganathan et al., 1997). Thus, interconversion between the *cis* and *trans* onformations could be a major rate-limiting step for many biological processes because the distinct isomeric structures may interact with different cellular proteins. Phosphorylation on Ser/Thr-Pro motifs further restrains this conversion.

Isomerization of the pSer/Thr-Pro motifs is important because they are the only phosphorylation motifs known for almost all proline-directed protein kinases. Proline-directed phosphorylation mediated by the kinases plays an essential role in normal cell proliferation and in malignant transformation. In fact, many oncogenes and tumour suppressors are directly regulated by proline-directed phosphorylation (Lu, 2003). Degenerated peptide screen demonstrated that Pin1 specifically catalyzes *cis*/*trans*-isomerization of proline in the sequence of pSer/Thr-Pro motif (Yaffe et al., 1997). This motif specificity implies that Pin1 plays a unique and excellent role in the regulation of signaling cascades associated with proline-directed phosphorylation. Isomerization of pSer/Thr-Pro motifs between *cis* and *trans* conformation mediated

by Pin1 can significantly affect the local or even the global tertiary structure of the target protein. This could have profound effects on the target molecules, allowing the turning on and off of signaling cascades with high efficiency and precise timing, in dynamic cellular processes such as cell division. This post-phosphorylation regulatory machinery provided another layer of post-translational regulation upon phosphorylation-dependent regulation (Lu et al., 2002a). Interestingly, most pSer/Thr-Pro motifs in Pin1 targets are located in the regulatory domains of the proteins and these would have critical regulatory roles in cell signaling (Lu et al., 2003c).

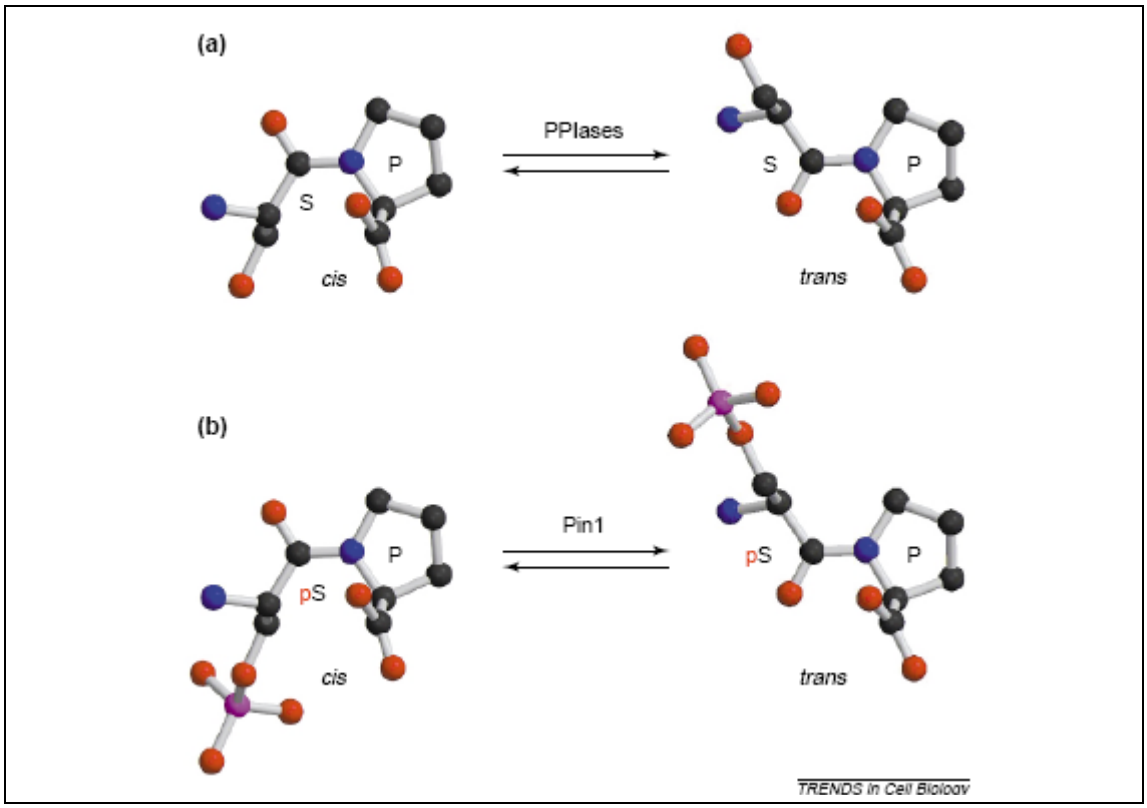

Figure 1-1: Peptidyl-prolyl *cis/trans* isomerization and PPIases. (Adapted from Lu *et al.* (2002), *Trends in Cell Biology*, 12(4): 164-172)

The biological significance of such post-phosphorylation regulatory mechanism

becomes even more obvious as seen in the conformation specificity of proline-directed protein kinases and phosphatases. Indeed, protein kinases such as mitogen-activated protein kinases (MAPKs), cyclin-dependent protein kinase 2 (Cdk2), and a major phosphatase, protein phosphatase 2A (PP2A), phosphorylate or dephosphorylate preferentially the *trans* conformation of Ser/Thr-Pro motifs. pSer/Thr-Pro motifs in the *cis* conformation are energetically less favourable, but as mentioned earlier, exist at a level of ~10-20 % physiologically, as a result of spontaneous isomerization. Thus, PPIases are needed to convert these conformers to *trans* isomers. A novel regulatory mechanism for phosphorylation signaling has been revealed, whereby a protein kinase deposits a phosphate group onto a protein, the isomerase induces a conformational change that facilitates removal of the phosphate group by a phosphatase to control the function and activity of the phosphoproteins with efficiency and precise timing (Lu et al., 2002a).

1.5 Biological substrates of Pin1

Comprehensive studies have revealed that Pin1 participates in many essential cellular processes, including mitotic regulation, DNA replication checkpoint control, DNA damage response, transcription / splicing regulation, cell survival / apoptosis, germ cell development, and immune response. This is done by Pin1's interaction with a wide range of target proteins, whereby it regulates a spectrum of activities such as catalysis, protein-protein interactions, subcellular localization, protein dephosphorylation, and protein stability amongst its targets (Wulf et al., 2005).

There are more than 50 Pin1 substrates identified so far through recent comprehensive biochemical, biological and structural studies. These include cell cycle regulated protein Raf-1 (Dougherty et al., 2005), Cdc25 (Zhou et al., 2000; Stukenberg and Kirschner, 2001), Cyclin D1 (Liou et al., 2002), Cyclin E (Yeh et al., 2006), GTP-binding protein Rab4 (Yaffe et al., 1997; Gerez et al., 2000), anti-apoptotic protein Bcl-2 (Basu et al., 2002; Basu and Haldar, 2002; Pathan et al., 2001), transcription factors c-Jun (Wulf et al., 2001), β-catenin (Ryo et al., 2001), NFAT (Liu et al., 2001), p53 (Berger et al., 2005; Zheng et al., 2002; Zacchi et al., 2002; Wulf et al., 2002), c-Myc (Yeh et al., 2004), p73 (Mantovani et al., 2004), c-fos (Monje et al., 2005), and Alzheimer's disease related proteins APP (Pastorino et al., 2006), and Tau (Lu et al., 1999a; Smet et al., 2004). This list is of course not exhaustive, and is summarized in Table 1-1.

1.6 Regulation of Pin1 expression and activity

While Pin1 is participating in such a diverse cellular processes, it is known to be tightly regulated at both transcriptional and post-translational levels. At the transcriptional level, growth factors or other stimulating factors such as the activated Neu or Ras stimulate the E2F family of transcription factors. E2F in turn enhance transcription of *Pin1* gene. Like many other E2F target genes, Pin1 transcripts and its protein levels fluctuate during cell cycle progression in non-transformed cells. In transformed cells, however, Pin1 level is constitutively high (Shen et al., 1998; Ryo et al., 2002).

At the post-translational level, regulation of Pin1 activity is mediated by its phosphorylation at Ser-16 of its WW domain. Phosphorylation of Ser-16 or substitution of Ser-16 with glutamine to mimic phosphorylation abolishes Pin1's ability to interact with its substrates, thereby inhibiting its physiological activities (Lu et al., 2002b). Interestingly, Pin1 is found to be hypophosphorylated in breast cancer, indicating that phosphorylation of Pin1 indeed inactivates Pin1 *in vivo* (Wulf et al., 2001). However, it is still not known which kinases and phosphatases are responsible for this regulation *in vivo*, although protein kinase A has been shown to be able to phosphorylate Pin1 *in vitro* (Wulf et al., 2005). A recent study has shown that phosphorylation of Pin1 is reversely correlated with phosphorylated GSK3β, indicating that GSK3β may be responsible for Pin1 phosphorylation. This data is not yet conclusive and deserves further investigation (Min et al., 2005).

1.7 Pin1 in pathological conditions

Pin1-mediated conformational changes following phosphorylation can have profound effects on cell signaling by regulating a spectrum of target activities. Pin1 activity, in turn, is tightly regulated by multiple mechanisms and its deregulation has an important role in pathological conditions.

1.7.1 Cancers

Overexpression of Pin1 is prevalently found in many human cancers， including breast, prostate, cervical, brain, lung, and colon cancers (Lu, 2003). Overexpression of Pin1 could therefore be a primary event in human cancers.

Table 1-1 Pin1 substrates and their regulation by Pin1.

Protein	Substrate activity	Target sites for Pin1	Pin1 Functional domains	What Pin1 does to the proteins	References
Mitotic regulation					
NIMA	Mitotic kinase	--	--	Genetic interaction	(Lu et al., 1996b; Lu and Hunter, 1995; Ye et al., 1995)
Nek6	Mitotic kinase	--	--	--	(Chen et al., 2006)
Wee1	Mitotic kinase	--	--	Genetic interaction	(Shen et al., 1998)
Myt1	Mitotic kinase	--	--	--	(Shen et al., 1998; Wells et al., 1999)
Plk1	Mitotic kinase	--	WW domain binds substrate	--	(Eckerdt et al., 2005; Crenshaw et al., 1998; Shen et al., 1998)
Raf-1	Mitotic kinase	pSer29-Pro; pSer43-Pro^; pSer289-Pro; pSer296-Pro; pSer301-Pro; pSer642-Pro	PPIase activity is required for the dephosphorylation	Dephosphorylation by PP2A	(Dougherty et al., 2005)
P70/S6 kinase	Protein kinase	--	--	--	(Yaffe et al., 1997)
Cdc25	Mitotic phosphatase	pThr48-Pro; pThr67-Pro; pThr138-Pro; pSer205-Pro; pSer285-Pro	WW domain bind, PPIase domain catalyze	Phosphatase activity, protein dephosphorylation by PP2A, genetic interaction	(Zhou et al., 2000; Stukenberg and Kirschner, 2001)
Btk	Nonreceptor tyrosine kinase	pSer115-Pro; pSer21-Pro		Dephosphorylation, stability	(Yu et al., 2006)
Cyclin D1	G1/S regulator	pThr286-Pro	--	Protein expression, promote protein stability, nuclear localization	(Liou et al., 2002)

Cyclin E	G1/S regulator	Ser384^	--	Promote protein degradation by 26S proteosome-mediated proteolysis	(Yeh et al., 2006)
CENP-F	Kinetochore protein	--	--	--	(Shen et al., 1998)
Incenp	Inner centromere protein	--	--	--	(Shen et al., 1998)
Cdc27	Anaphase-promoting complex	--	--	--	(Yaffe et al., 1997; Shen et al., 1998)
Rab4	GTP-binding protein	pSer196		Localization, protein-protein interaction	(Yaffe et al., 1997; Gerez et al., 2000)
Anti-apoptotic proteins					
Bcl-2	Anti-apoptotic protein	pSer70-Pro*; pSer87-Pro*		Dephosphorylation, nuclear translocation	(Basu et al., 2002; Basu and Haldar, 2002; Pathan et al., 2001)
BIM_{EL}	Apoptotic protein	pSer65-Pro	WW domain binds substrate	Promote protein stability	(Becker and Bonni, 2006)
Tis/BTG2/pc3	Antiproliferative protein	pSer147-Pro	--	--	(Hong et al., 2005)
JIP3	Neuron-specific JNK signaling scaffold protein	--	WW domain binds	--	(Becker and Bonni, 2006)
Transcription factors / Gene regulation					
c-Jun	Transciptional activator	pSer63-Pro; pSer73-Pro	Both domains required for the activity	Transcriptional activity	(Wulf et al., 2001)
β-catenin	Transcriptional activator	pSer246-Pro		Promote protein stability, localization, transcriptional activity	(Ryo et al., 2001)

RNA Pol II	Transcriptional initiator	pSer5-Pro (in repeated sequence)			(Jacobs et al., 2003; Verdecia et al., 2000; Shen et al., 1998; Wu et al., 2000)
NFAT	Transcriptional activator	pSer5-Pro (in repeated sequence)	WW domain binds substrate	Inhibit dephosphorylation by calcineurin, localization in cytosol	(Liu et al., 2001)
p53	Transcriptional activator	pSer33-Pro; pSer46-Pro; pThr81-Pro; pSer315-Pro		Promote protein stability, transcriptional activity	(Berger et al., 2005; Zheng et al., 2002; Zacchi et al., 2002; Wulf et al., 2002)
NF-κB	Transcriptional activator	pThr254-Pro		Nuclear translocation, transcriptional activity, promote protein stability	(Ryo et al., 2003)
c-Myc	Transcriptional activator	pThr58-Pro#; pSer62-Pro	WW domain binds substrate	Promote degradation by 28S proteosome, dephosphorytion by PP2A	(Yeh et al., 2004)
IRF3	Transcriptional activator	pSer339-Pro	WW domain binds substrate	Protein stability, transcriptional activity	(Saitoh et al., 2006)
p73	Transcriptional activator	pSer412-Pro; pThr442-Pro; pThr482-Pro	PPIase is required for the protection from proteolytic cleavage	Promote stability, transcriptional activity	(Mantovani et al., 2004)
c-fos	Transcriptional activator	pThr232-Pro#;pThr325-Pro pThr331-Pro; pSer374-Pro		Transcriptional activity	(Monje et al., 2005)
SRC-3/AIB1	Transcriptional coactivator	pThr24-Pro; pSer505-Pro; pSer543-Pro; S860-Pro; pSer867-Pro	WW domain binds substrate	Promote degradation, protein-protein interaction, transcriptional activity	(Yi et al., 2005; Wu et al., 2004)
Cf-2	Transcriptional repressor	pThr40-P		Promote protein degradation, transcriptional activity	(Hsu et al., 2001)

RARalpha	Transcriptional regulator	pSer77-Pro	--	Promote degradation by 26S proteosome	(Brondani et al., 2005)
Alzheimer's disease related					
Tau	Microtubule-binding protein	pThr212-Pro; pThr231-Pro		Protein-protein interaction, protein dephosphorylation	(Lu et al., 1999a; Smet et al., 2004)
APP	May involved in the survival and differentiation of neuronal cells	pThr668-Pro	WW domain binds		(Pastorino et al., 2006)
Others					
Synphilin-1	Trafficking-related protein	pSer211-Pro; pSer215-Pro		Protein-protein interaction	(Ryo et al., 2006)
Lipofuscin	Lysosomal accumulated granule of fluorescent retinoid, lipid and protein debris	--	--	--	(Hashemzadeh-Bonehi et al., 2006)
Sin3-Rpd3	Histone deacetylase	--		Genetic interaction	(revalo-Rodriguez et al., 2000)
p54nrb	Nuclear factor	pThr412-Pro; pThr430-Pro; pThr452-Pro	WW domain binds	--	(Proteau et al., 2005)
NHERF-1	Na+/H+ exchanger regulatory factor	pSer279-Pro; pSer301-Pro		Dephosphorylation by PP2A/PP1	(He et al., 2001)
KRMP1	Kinesin-related protein	--	WW domain binds substrate	--	(Kamimoto et al., 2001)
Sil	Intermediate-early protein essential for embryonic development	pThr574-Pro; pSer643-Pro; pSer656-Pro; pSer664-Pro; pThr686-Pro; pSer699-Pro; pSer760-Pro	WW domain bind substrate	--	(Campaner et al., 2005)

* no actual proof # major binding site ^ not pSer/Thr-Pro motif

Pin1 is a critical catalyst at multiple steps in oncogenic pathways. Most importantly, Pin1 regulates the function of Cyclin D1, an essential protein upregulated during breast cancer development. Pin1 stabilizes and upregulates Cyclin D1 on both transcriptional and post-translational levels (Wulf et al., 2005). At the transcriptional level, Pin1 promotes *Cyclin D1* gene expression through Ras/JNK and Wnt/β-catenin signaling pathways to stabilize transcription factors c-Jun and β-catenin, respectively. Pin1 also activates and stabilizes NF-κB in response to cytokine stimulation to enhance the transcriptional activity of NF-κB towards *Cyclin D1* gene. Moreover, c-Myc, which is a substrate of Pin1, upregulates Cdk4. Cdk4 in turn activates the *E2F* genes to enhance the transcriptional level of Cyclin D1 as well as of Pin1 itself. This positive feedback loop suggests that deregulation of Rb/E2F pathway, as seen in many cancers, may be a cause for the elevated Pin1 levels in many cancers. At the protein level, Pin1 stabilizes cyclin D1 directly by preventing its nuclear export and proteolysis in the cytoplasm. Hence, Pin1 raises Cyclin D1 levels, which will lead to cell proliferation and transformation (Figure 1-2).

Pin1 can be a cancer prognostic marker. Increased Pin1 levels are indeed highly predictive of cancer recurrence after prostatectomy (Wulf et al., 2005). Moreover, Pin1 can also be a molecular target for cancer therapies. Specific Pin1 inhibitors are currently being developed. Juglone is an effective Pin1 inhibitor, acting by covalently inactivating Cys-113 residue at the active site of Pin1. However, it also potently inhibits other Parvulin-type PPIases and many other proteins and enzymes. Other Pin1

inhibitors are designed mainly based on competitive binding, with the chemicals inhibiting the interaction between Pin1's WW domain and the phosphopeptides at the binding surface, such as PiB and its analogs. PiB and its analogs have been shown to inhibit cell growth, but they inhibit non-phosphorylation-specifc prolyl isomerases such as Par14 as well. Thus, more specific Pin1 inhibitors needs to be developed (Lu, 2003).

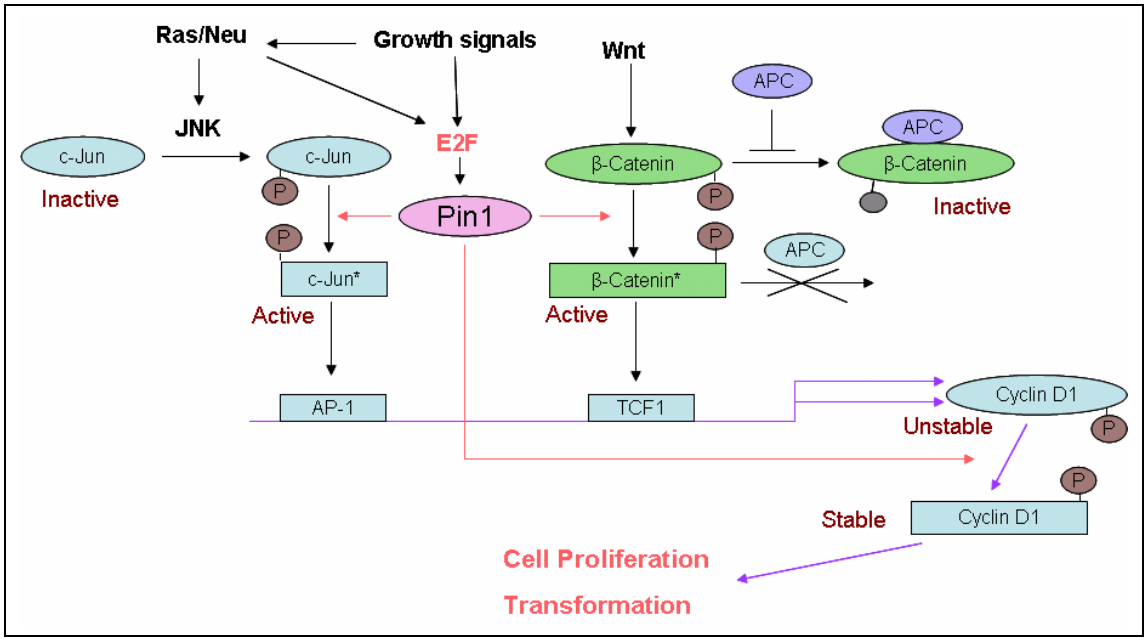

Figure1-2: Roles of Pin1 in the regulation of Cyclin D1 in cell proliferation and oncogenesis. (Adapted from Lu (2003), *Cancer Cell*, 4: 175-180)

1.7.2 Alzheimer's disease

Pin1 is implicated in Alzheimer's disease (AD). So far, there is no definitive clinical diagnosis and effective treatment available for the disease. This disease is clinically characterized by a progressive loss of memory, dementia and eventually death, with an average survival time being about ~8 years after the onset of the disease (Lu et al., 2003b). Its neuropathological hallmarks consist of intracellular neurofibrillary tangles (NFTs) and extracellular neuritic plaques, with neuronal cell

death in specific areas of the brain such as the hippocampus (Lu et al., 2003a).

NFTs contain paired helical filaments (PHFs) composed of aggregates of phosphorylated and ubiquitinated Tau, which forms a β-pleated sheet structure. Tau is a microtubule-binding protein that promotes microtubule assembly in neurons. Under normal circumstances, mitotic events phosphorylate Tau and such phosphorylation would abolish Tau's ability to bind microtubule for microtubule assembly, thereby inhibiting normal neuronal functions. However, interaction of Pin1 with Tau at its pThr212-Pro and pThr231-Pro motifs causes a conformational change, making Tau accessible to PP2A for dephosphorylation. In this way, Pin1 restores Tau's function in binding to microtubules. In AD's brains, abnormal activation of mitosis causes Tau to be hyperphosphorylated. Hyperphosphorylation of Tau creates excess Pin1 binding sites. Pin1 could thus be redirected from nucleus to the cytoplasm and trapped in the NFTs. Thus, functional Pin1 becomes depleted in the nucleus as well as subcellular compartments, which could lead to mitotic arrest and eventually neuronal cell death.

AD neuritic plaques are composed of massive accumulation of amyloid β peptides (Aβ), derived from the amyloid precursor protein (APP). Full-length APP is a transmembrane protein and it undergoes sequential proteolytic cleavage by at least three proteases called α-, β-, and γ-secretases. α-secretase and β-secretase cleave APP within the extracellular domain to shed off large soluble APP derivatives called α-APPs and β-APPs, respectively. The remaining membrane-tethered α- or β-carboxy-terminal fragments (APP-CTFα and APP-CTFβ, respectively) are then

cleaved by γ-secretase within the transmembrane domain, producing either a 3 kDa product (p3 for APP-CTFα) or Aβ (for APP-CTFβ), and the APP intracellular domain (AICD) (Figure 1-3). Aβ has long been postulated as the primary etiology agent of AD. Accumulation of insoluble, extracellular Aβ forms neuritic plaques in AD's brains (Katzman and Saitoh, 1991; Kerr and Small, 2005).

A

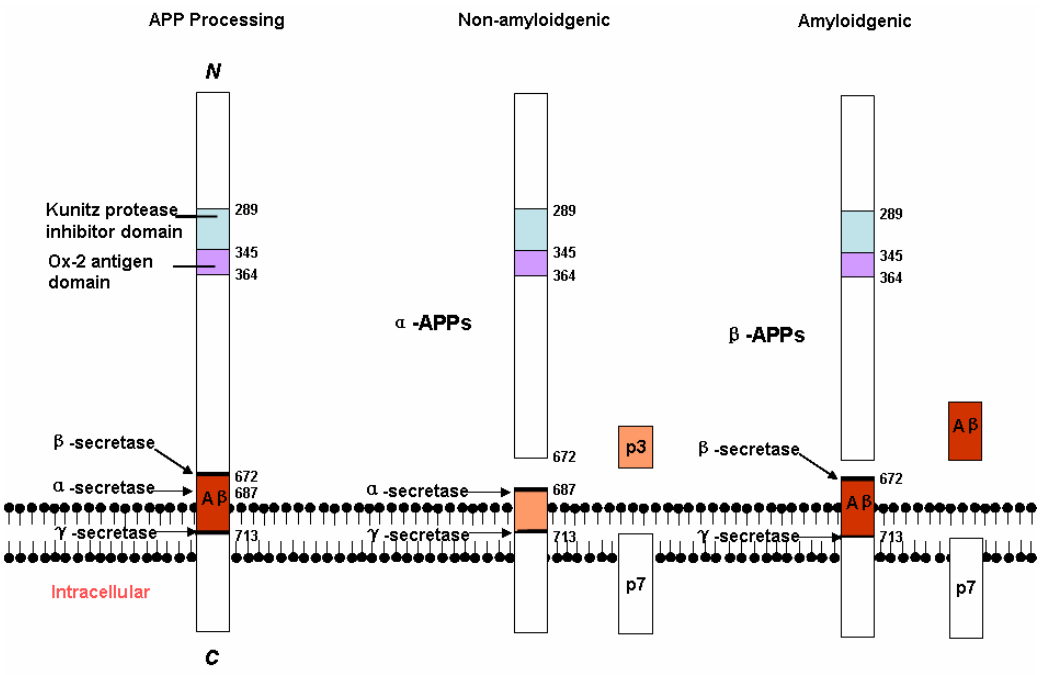

B

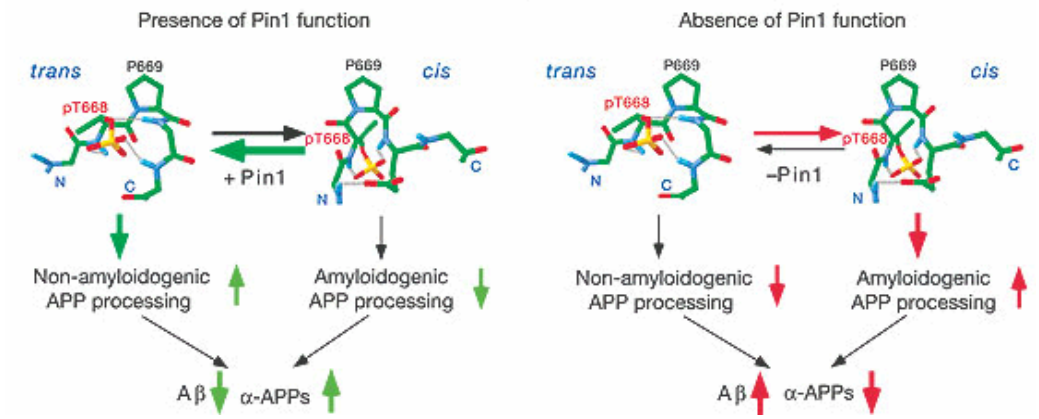

Figure 1-3: Pin1 in APP processing and its role in forming amyloidogenic Aβ in Alzheimer's disease. (A) APP processing; (B) Pin1's regulation of APP processing (adapted from Pastorino *et al.* (2006), *Nature*, 440: 528-534).

Studies by Pastorino *et al.* reveals that Pin1 regulates APP processing (Pastorino et al., 2006). Pin1 can interact with APP phosphorylated at its Thr668-Pro motif on the plasma membrane, thus catalyzing a conformational change of APP from *cis* to *trans*. Interestingly, the *cis* conformation of APP favors amyloidogenic APP processing, and the combination of β- and γ-secretase cleavage generates β-APPs and Aβ. The *trans* conformation undergo non-amyloidogenic APP processing, with the combination of α- and γ-secretase generating α-APPs and p3. By catalyzing the conformational change from *cis* to *trans*, Pin1 thus favors non-amyloidogenic APP processing and reduces Aβ formation (Figure 1-3). In AD's brains, Pin1 is depleted and / or inhibited by oxidative damage in the neurons. Without the proper function of Pin1, the *cis* pThr668-Pro motif would not be isomerized to *trans* in a timely manner. Hence, amyloidogenic APP processing is favored leading to accumulation of secreted Aβ to form neuritic plaques.

1.8 The structural basis of Pin1 function

On a structural perspective, a number of crystal and NMR structures of human Pin1 as well as some of its homologues, together with their biochemical analyses, have furthered our understanding of the structure-function relationship of Pin1.

1.8.1 The X-ray structure of human Pin1

Pin1 and its homologues are characterized by an N-terminal WW domain and a C-terminal PPIase catalytic domain (Ranganathan et al., 1997; Zhou et al., 2000; Yaffe et al., 1997). The three-dimensional crystal structure of human Pin1 was first

determined in 1997. The WW domain of Pin1 (residues 1-39) is made up of a compact anti-parallel three-stranded β-sheet, while the PPIase domain (residues 45-163) folds into a flattened half β-barrel, which consists of a four-stranded anti-parallel β-sheet, surrounded by four α-helices (Figure 1-4) (Lu et al., 2002b; Ranganathan et al., 1997).

In the crystal structures, the two structural domains are organized around a concave hydrophobic cavity and are tethered. There are three hydrophobic patches on the molecular surface: the concave inter-domain cavity, the catalytic site surrounding Cys-113, and the shallow cleft composing of Ile-96, Phe-103, Met-146, and Leu-160 (β3 strand and helix α4). These three hydrophobic surfaces constitute a continuous hydrophobic patch on the Pin1 molecular surface. In NMR studies in solutions, interaction between the two domains was abolished when full length Pin1 is cleaved at the flexible linker. Hence, although a large interface has been observed in the crystal structures, weak interaction between the two domains has been speculated (Bayer et al., 2003; Jacobs et al., 2003). Through differential chemical shift mapping between the two domains, an inter-domain interaction surface as in the X-ray structures is also discernible—the hydrophobic cavity comprising the concave surface of the WW domain (β3' strand, and β1'/β2' and β2'/β3' loops) and the shallow cleft of the PPIase domain (Jacobs et al., 2003).

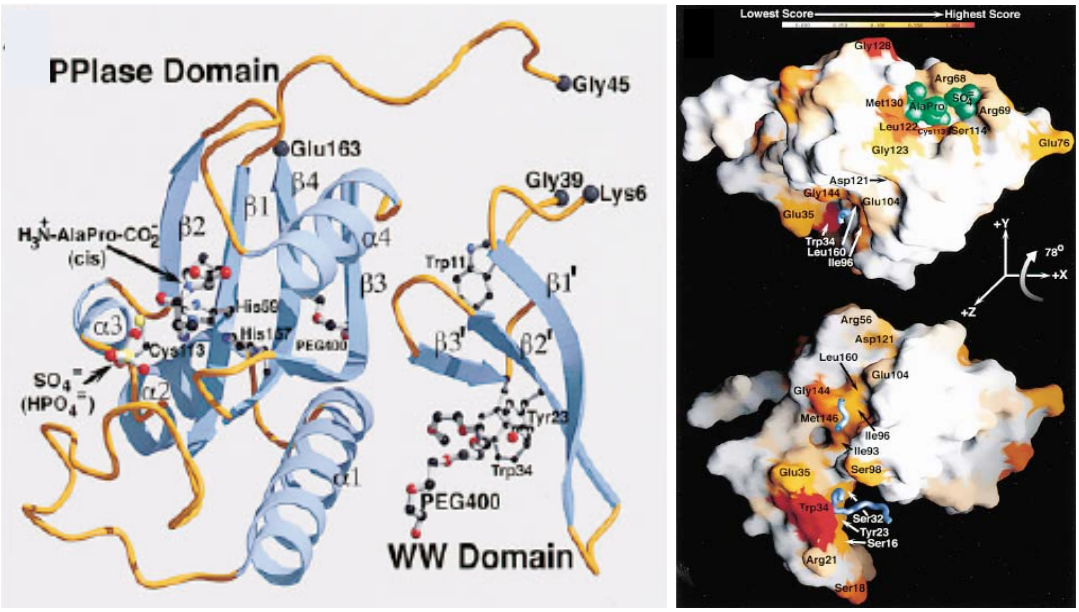

Figure 1-4: Pin1 crystal structure (PDB code: 1PIN). (Left) Cartoon representation of Pin1 structure. (Right) Pin1 surface properties. The figure shows a colour-coded representation of the distribution of a calculated parameter α that describes the degree of conserved, solvent-exposed hydrophobicity. A values range from 0 (white) to 1 (red), where the highest values are scored by identical, fully exposed hudrophobic residues. (Adopted from Ranganathan *et al.* (1997), *Cell*, 89(6):875-886)

1.8.2 The WW domain and its ligand specificity

In general, WW domains behave like Src homology 3 (SH3) domains as they recognize Pro-rich sequences. SH3 domains are modular binding domains found in many signaling proteins that mediate their assembly with specific proteins via binding to proline-rich stretches in their respective binding partners (Macias et al., 2002). Likewise, WW domains work as universal protein modules for binding Pro-rich ligands in many signaling proteins, including Nedd4, Rsp5, Smurf1, and YAP65, to target these to their substrates. The Pin1 WW domain is classified as a Group IV WW domain, which shows substrate preference towards Ser/Thr-Pro-containing peptides in a phosphorylation-dependent manner when assayed alone apart from PPIase domain

(Kato et al., 2002; Kato et al., 2004). On the other hand, mNedd4, Rsp5, Smurf1 and YAP65 contain the Group I WW domains, which recognizes the Pro-Pro-Xaa-Tyr (PY motif, Xaa denotes any amino acid), and the reported NMR structure of the isolated YAP65 WW domain exhibits a similar fold with Pin1 WW domain (Ranganathan et al., 1997). This indicates that WW domains are well conserved. Several groups, through mutational studies, have shown that the Pin1 WW domain is critical for its substrate recognition by acting as a pSer-Pro or pThr-Pro binding module. For example, mutation at Pin1 catalytic site diminishes its PPIase activity but its binding affinity towards its substrate is not compromised (Shen et al., 1998). The WW domains of both human Pin1 and its yeast homologue Ptf1/Ess1 are indispensable for function. Under normal expression conditions, both domains are required to rescue the yeast *ptf1/ess1* mutant. However, when overexpressed, only the PPIase domain, but not the WW domain, can rescue the lethality of Ptf1/Ess1 deletion (Lu et al., 1999b; Lu et al., 2002a; Zhou et al., 2000). Thus, these observations provided evidence that the WW domain confers substrate specificity and target Pin1 to its substrates, whereas the PPIase domain is both sufficient and necessary to induce the conformational changes and to carry out the essential catalytic function of the enzyme. Interestingly, the plant Pin1 homologue, Pin1at, lacks an N-terminal WW domain but still exhibits specific pSer/Thr prolyl *cis*/*trans* isomerase activity (Landrieu et al., 2002).

It remains as a challenge to identify a consensus sequence recognized by Pin1.

However, in general, Pin1 prefers a pSer/Thr-Pro motif that is surrounded by multiple upstream hydrophobic residues such as leucine, isoleucine, valine, tyrosine and/or phenylalanine, and a downstream arginine or lysine residue (see Table 1-2) (Lu et al., 1999b; Yaffe et al., 1997; Wulf et al., 2005).

Table 1-2: Pin1 substrate sequences.

Substrate	Position	Sequence
p73	Ser412-Pro	LQPPSYGPVL**SP**MNKVHGGMN
	Thr442-Pro	GQPPPHSSAA**TP**NLGPVGPGM
	Thr482-Pro	AQSMVSGSHC**TP**PPPYHADPS
β-catenin	Thr81-Pro	PRVAPAPAAP**TP**AAPAPAPSW
	Ser315-Pro	KRALPNNTSS**SP**QPKKKPLDG
	Ser246-Pro	GIPALVKMLG**SP**VDSVLFYAI
Cdc25	Thr48-Pro, Thr67-Pro	SVTFSPEQPL**TP**VTDLAVGFSNLSTFSGE**TP**KRCLDLSNL
Cyclin D1	Thr286-Pro	EVEEEAGLAC**TP**TDVRDVDI
p53	Ser33-Pro, Ser46-Pro	WKLLPENNVL**SP**LPSQAMDDLML**SP**DDIEQWFTE
Tau	Thr212-Pro, Thr231-Pro	SPGTPGSRSR**TP**SLPTPPTREPKKVAVVR**TP**PKSPSSAKS
c-Jun	Ser63-Pro, Ser73-Pro	LRAKNSDLLT**SP**DVGLLKLA**SP**ELERLIIQS
CTD	Repeated sequence	Y**SP**T**SP**SY**SP**T**SP**SY**SP**T**SP**S
c-Myc	Thr58-Pro	SEDIWKKFELLP**TP**PL**SP**SRRSGLCSPSYVAVTP
RARalpha	Ser77-Pro	EEIVPSPP**SP**PPLPRIYKPCFV
Tis21	Ser147-Pro	QVLLGRS**SP**SKNYVMAVSS
NFκB p65/RelA	Thr254-Pro	HRQVAIVFR**TP**PYADPSLQAPVRVSM
Cyclin E	* Ser384	ASPLPSGLLTPPQ**S**GKKQSS

** denotes non pSer/Thr-Pro motif*

The function of Pin1 WW domain in targeting Pin1 to its substrates is further supported by structural analyses of Pin1 and its WW domain complexed with peptides. In these studies, the pSer/Thr-Pro peptides bound to the WW domain in the *trans* conformation, with multiple sequence-specific interactions contributing to the binding specificity. Pin1 structure complex with a doubly phosphorylated peptide (Tyr-**pSer2'-Pro**-Thr-**pSer5'-Pro**-Ser) derived from the C-terminal repeated domain

(CTD) of RNA polymerase II reveals a concave binding site in the WW domain, comprising of Phe-25, Arg-14, Ser-16, Arg-17, Tyr-23, and Trp-34 (see Figure 1-5) (Verdecia et al., 2000). Solution NMR studies of Pin1 WW domain complexed with another two monophosphate peptide substrates derived from *Xenopus laevis* Cdc25 (Glu-Gln-Pro-Leu-**pThr-Pro**-Val-Thr-Asp-Leu) and from human tau protein (Lys-Val-Ser-Val-Val-Arg-**pThr-Pro**-Pro-Lys-Ser-Pro-Ser), respectively, reveal the same extended binding site around residues Ser-16, Arg-17, Tyr-23, and Trp-34 (Wintjens et al., 2001). The Pin1-CTD complex structure displays two positively charged residues which may be important for the phosphopeptide binding, namely Arg-14 and Arg-17. Arg-14 recognizes Pro-3'of the ligand peptide, whereas Arg-17 interacts with the phosphate group of pSer-5'. These two arginine residues on the ligand-binding site may therefore determine the ligand specificity of Pin1 WW domains. However, some WW domains of Pin1 homologues, such as *Aspergillus nidulans* PinA and *Neurospora crassa* SspI, do not have residues at position equivalent to Arg-17, but residue Arg-14 is conserved in these two homologues. When compared across the subfamilies in WW domain family, Group I WW domains of mNedd4, Rsp5 also has a conserve Arg-14 but dystrophin and hYAP65 do not. Moreover, between these two subgroups of Group I WW domain, there is little relationship between charge distribution and ligand specificity. This suggests that the residue Arg-14 in Pin1 may not be important for its substrate specificity in pSer/Thr-Pro motifs binding. Indeed, mutation studies also verified that Arg-14 is less critical for peptide binding than residues Ser-16, Arg-17, Tyr-23, and Trp-34, which

also reside at the binding interface of Pin1 with CTD peptide (Verdecia et al., 2000; Kato et al., 2002).

Structures of several Proline-rich sequence binding modules, analyzed together with Pin1 WW domains, have revealed a model of Pin1 substrate recognition specificity. In the surface of SH3 and WW domain of both dystrophin and Pin1, a series of parallel aromatic residues comprise a groove against which polyproline II (PPII) helix formed by proline-rich sequences packs. These grooves recognize a pair of residues of the sequence Xaa-Pro (where Xaa is any amino acid). In SH3 domains, two successive X-P grooves are formed by the conserved Trp, Tyr, and Phe residues to recognize the consensus sequence Xaa-Pro-Xaa-Pro-Xaa in proline-rich sequences. However, there is only a single X-P groove in Group I and IV WW domains formed by the conserved Tyr and Trp residues to recognize the Pro-Pro-Xaa-Tyr and pSer/Thr-Pro motifs. Hence, such an X-P groove confers the proline binding specificity (Zarrinpar and Lim, 2000).

On the other hand, individual binding module exhibits sequence specificity conferred by the variable loops and neighboring domains. In WW domains, sequences between β1’ and β2’, and between β2’ and β3’ are called loop I and loop II, respectively. Loop I directly abuts on the X-P groove whereas loop II lies at the opposite end of the interaction surface. In Group I WW domains, such as dystrophin and mNedd4, loop II forms a hydrophobic pocket, and Tyr residue within the Pro-Pro-Xaa-Tyr motif in their ligands fits into the pocket. Loop II is thus called the

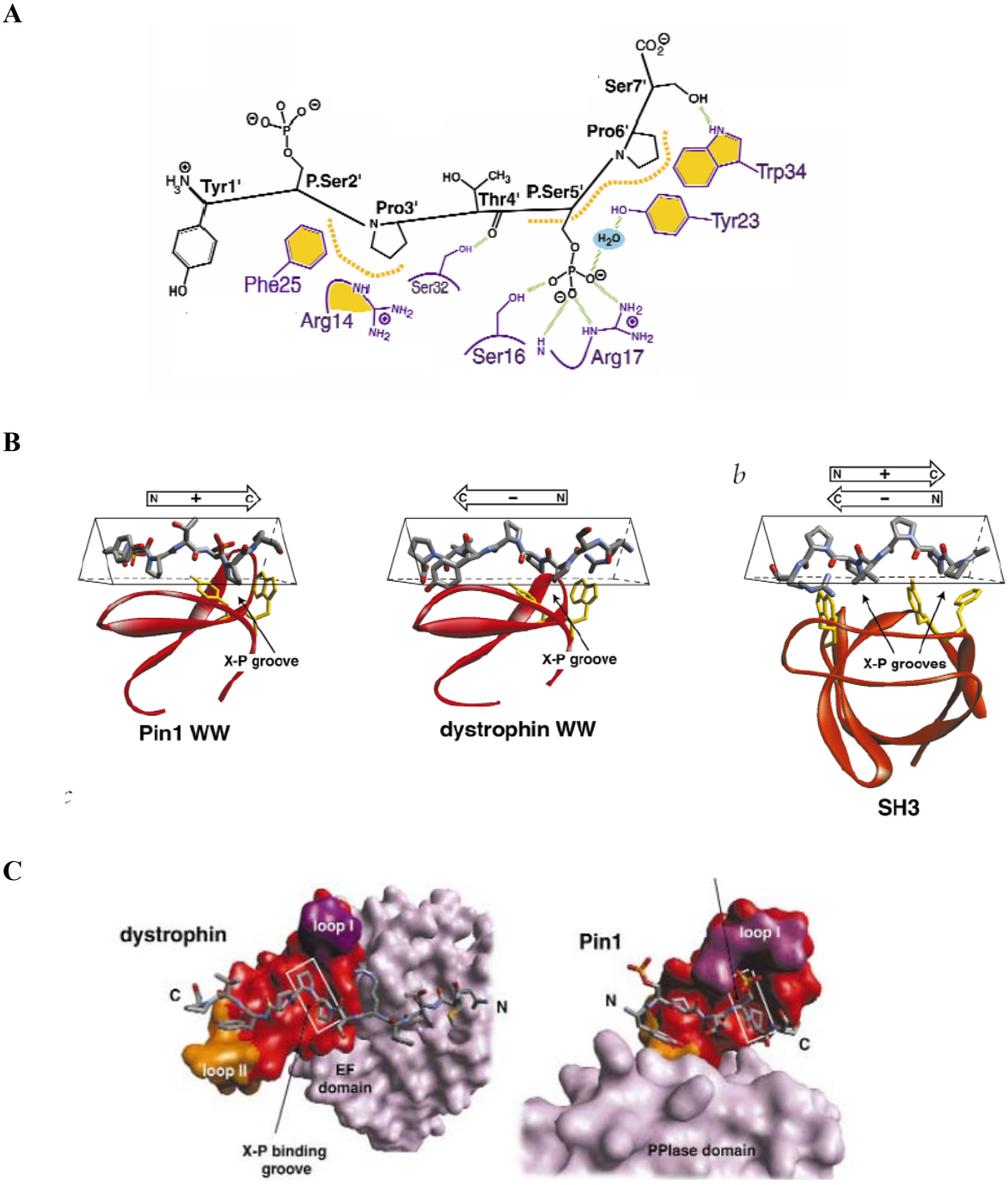

Figure 1-5. Substrate binding of Pin1. (A) Schematic presentation of Pin1 WW domain in complex with the doubly phosphorylated CTD peptide (Tyr-**pSer2'-Pro**-Thr-**pSer5'-Pro**-Ser) (adapted from Verdecia *et al.* (2000), *Nat. Struct. Biol.*, 7: 639-643). (B) Peptide binding orientation to Pin1 and dystrophin WW domain, and SH3 (adapted from Zarrinpar (2000), *Nat. Struct. Biol.*, 7: 611-613). (C) Surface depiction of the Pin1 and dystrophin WW domain in complex with peptides. X-P binding groove (white box) is flanked by multiple specificity elements, including residues in loop I (purple), residues in loop II (orange), and neighbouring domains (lavender).

Tyr binding loop, and it is responsible for the substrate specificity of Group I WW domain. In contrast, loop I accounts for the determination of substrate specificity of Group IV WW domains (Zarrinpar and Lim, 2000; Kato et al., 2002; Kato et al., 2004). As observed in the structure of Pin1 WW domain complexed with CTD phosphopeptide, pSer5' in the pSer-Pro motif was accommodated into loop I specifically and avidly in contact with the backbone amide of Arg-17, and with the side chain of Ser-16, Arg-17, and Tyr-23. The most energetically favoured interaction in this contact being the electrostatic interaction between the pSer5' and the side chain ε-guanido group of Arg-17. Hence, Arg-17 is indeed important in substrate recognition, although it is not conserved in all the Pin1 homologues. In PinA and SspI, Arg-17 is replaced with Asn or Gln, respectively. According to modeled structures, Asn/Gln-17 can form hydrogen bonds with pSer5'. Moreover, Lys-19 can also contribute to the substrate binding through an electrostatic interaction, compensating for the absence of Arg-17. Arg/Asn/Gln-17 seems to be an extra insertion to the loop I region when compared to the Group I WW domain. Hence, recognition of pSer/Thr-Pro motifs is unique to the Group IV WW domains and loop I (or called p-patch) plays a key role in Pin1's substrate specificity (Kato et al., 2002).

Neighboring domains of WW domains may confer substrate specificity too. Evidence is seen when dystrophin WW domain alone cannot bind the dystroglycan ligand. An adjacent EF domain is essential in binding, with at least half of the ligand sequence entering into close interaction (Huang et al., 2000; Zarrinpar and Lim, 2000).

Likewise, in Pin1, the adjacent PPIase domain may also contribute to the substrate binding and specificity. However, the evidence is not conclusive. In the Pin1-CTD crystal structure, peptide binding is mainly contributed by the residues on the concave surface of the WW domain (Phe-25, Arg-14, Ser-32, Ser-16, Arg-17, Tyr-23, Trp-34), but not the PPIase domain, although the peptide is apparently in significant contact with the latter. Site-directed mutagenesis experiments demonstrate that Pin1 binds phosphoproteins mainly through its WW domain and that the interaction is mainly contributed by the aromatic rings of Tyr-23 and Trp-34. Studies with WW or PPIase domain alone showed that the Pin1 WW domain can bind to the peptides derived from Pin1's substrates but Pin1 PPIase domain binds either weakly or not at all (Verdecia et al., 2000; Lu et al., 1999b). PPIase is therefore apparently not responsible for substrate binding. Yet, in most cases, the binding of the WW domain is enhanced by a factor of 1.5-2 in the presence of the PPIase domain (Verdecia et al., 2000). More studies are needed to investigate the role of PPIase domain in substrate specificity and binding.

CTD, Cdc25, and tau are the peptides studied so far for Pin1 binding on a structural basis. All three peptides bind to the Pin1 WW domain in the same orientation from the N- to the C-terminal, as shown in Figure 1-5. A reverse peptide orientation will not fit into the binding surface. Interestingly, the β-dystroglycan peptide binding to dystrophin WW domain adopts a reversed peptide binding orientation compared to that of the Pin1 WW domain, whereas the SH3 domain could

bind to its peptide substrates in either orientation (Huang et al., 2000; Zarrinpar and Lim, 2000). Thus, substrate specificity again arises, with different orientation requirement for the different peptide sequences. Furthermore, the pThr-Pro peptide bonds in the three peptide ligands bound to Pin1 WW domain are in the *trans* conformation. This is consistent with the functional studies of Cdc25 and Tau, where Pin1 catalyzes their conformational change from *cis* to *trans*, makes them substrates for PP2A and/or PP1 dephosphorylation. PP2A is known to dephosphorylate only the *trans* pSer/Thr-Pro motif. Furthermore, in studies with APP peptide using NMR, it was revealed that Pin1 binds to both *cis* and *trans* conformations with comparable affinity although Pin1 catalyzes the *cis* to *trans* conformational switch. Thus, it has been proposed that Pin1 WW domain binding to either *cis* or *trans* conformation is sequence-specific (Pastorino et al., 2006). Moreover, it is the intrinsic catalytic mechanism of Pin1, rather than binding affinity, that routes its isomerization activity from *cis* to *trans* conformation.

Together, these studies suggest a unique binding scheme for the Pin1 WW domain to multiple substrates, although more Pin1 structures complexed with other substrates are useful to further validate this rather unique binding scheme.

1.8.3 The PPIase domain's catalytic mechanism and substrate specificity

The Pin1 PPIase domain catalyzes peptidyl-prolyl isomerization in the pSer/Thr-Pro motifs between the *cis* and *trans* conformations. Such a conformational

change is often demonstrated using biochemical assays, such as by a shift in recognition by the conformation specific MPM-2 antibody and susceptibility to the protease chymotrypsin. Moreover, such a conformation change has been visualized at atomic resolution, as shown by Pastorino *et al.* using NMR spectroscopy (Pastorino et al., 2006). In this study, APP-derived phosphopeptide exhibited two distinct sets of ^{1}H peaks, each corresponding to *cis* and *trans* conformations, respectively. The set of diagonal peaks would diminish and another set of exchange peaks would grow over the incubation time upon the addition of catalytic amounts of Pin1. However, the exchange peaks were absent when either no Pin1 or a catalytically inactive Pin1 mutant was added. Thus, Pin1 indeed causes a conformational change in the phosphopeptide.

1.8.3.1 Pin1 PPIase structure in comparison with FKBP

Despite a lack of primary sequence similarity, the core β sheet and the α4 helix of Pin1 PPIase domain fold in a globally similar fashion to FKBP-like PPIases, in spite of some structural deviations between the two families. On one hand, this indicates that this structural motif is well conserved; on the other hand, the structural deviations explain the different substrate specificity and catalytic mechanisms between these two families of PPIases. The main deviation comes from the segment linking β1 and β2. In Pin1, this segment is comprised of the β1/α1 loop, α1, the α1/α2 loop, α2, the α2/α3 loop, and α3. However, in FKBP, the corresponding region is considerably shorter, spanning a total of 12 residues that form an additional β strand. This deviation from

FKBP has conferred Pin1-type PPIases the unique organization of their catalytic site with the substrate specificity towards pSer/Thr-Pro bonds. In this structural inclusion that is unique to the Pin1 subfamily, the α1 helix provides much of the composite hydrophobic surface shared with the WW domain and the residues from the α1/α2 loop and α2 comprise part of the conserved second polyethylene glycol (PEG) binding site. Most importantly, the catalytic site with the multivalent anion binding site consisting of Lys-63, Arg-68, and Arg-69, and the active site Cys-113 crucial for efficient catalysis in Pin1, reside in this region as well.

In the crystal structure solved by Ranganathan *et al*. (Ranganathan et al., 1997), a dipeptide of Ala-Pro and a sulphate ion are sequestered to the catalytic site. The sulphate ion in close proximity to the β-methyl group of the alanine residue in the dipeptide is sequestered to the basic patch formed by the side chains of conserved Lys-63, Arg-68 and Arg-69 residues, whereas the proline residue is held by a hydrophobic pocket formed by Leu-122, Met-130, and Phe-134 at the catalytic site. Thus at the structural bases, these positions suggested that a pSer/Thr-Pro motif is a preferred substrate for Pin1. The pSer/Thr and proline anchor to the basic patch and the hydrophobic binding pocket, respectively, thus orientating the peptidyl-prolyl bond undergoing catalyzed *cis*/*trans* isomerization near the active site Cys-113 and to be surrounded by the side chains of Cys-113, His-59, His-157, and Ser-154. Hence, the basic patch serves as a selectivity filter to confer Pin1 phosphorylation specificity, whereas the active site grants efficient peptidyl-prolyl *cis*/*trans* isomerization.

Mutation studies support this notion, in which Arg-68 and Arg-69 completely abolishes the phosphorylation-specificity but has little effect on the basic enzymatic activity. Moreover, Cys-113, His-59, His-157, and Ser-154 are absolutely conserved in Pin1 homologues, while the basic patch is present merely in Pin1 homologues, and not in any other known PPIases. In FKBP, instead of a basic patch, hydrophobic residues Ile-90, Ile-91, and Phe-36 are found at a spatially analogous position. This observation has explained its preference for hydrophobic residues N-terminal to proline in its peptide substrates. On the other hand, there isn't any analogous structural motif in cyclophilin, explaining the lack of any specificity at a residue N-terminal to proline when acting upon tetrapeptide substrates by the cyclophilin family of PPIases (Harrison and Stein, 1990). Hence, the basic patch in Pin1 is indeed a signature patch of the Pin1-type PPIases that is critical for the substrate selection. Taken together, these observations imply the unique and conserved catalytic specificity, and mechanism of function of Pin1 in various species.

1.8.3.2 Proposed catalytic mechanism of Pin1

Two catalytic models for Pin1 have been proposed. In the first model, a covalent catalytic mechanism of peptidyl-prolyl isomerization unique to Pin1-type of PPIases has been elaborated based on the spatial arrangement of Cys-113, His-59, His-157, and Ser-154 relative to the isomerized peptide bond, and according to the crystal structure of Pin1 in complex with Ala-Pro dipeptide (PDB code: 1PIN) (Ranganathan et al., 1997). In this model, the first step involves a partial bond rotation by the

favorable energetic forces (substrate in *cis* configuration). A proton from Cys-113 is then extracted by the deprotonated imidazole nitrogen of His-59, followed by a nucleophilic attack on the carbonyl carbon of the substrate's peptide bond by the newly formed thiolate side chain (step 2), thus leading to the formation of a high-energy covalent tetrahedral intermediate between the substrate and enzyme (step 3). The resulting negative charge on the former carbonyl oxygen is then stabilized through electrostatic interactions with a protonated His-157 (step 3). This high-energy intermediate then relaxes back to either *cis* or *trans* ground states of the peptide bond (stage 1 or 4, respectively) (Figure 1-6) (Ranganathan et al., 1997).

In contrast to other PPIase structural classes, Pin1 appears to exhibit the additional properties of covalent catalysis. The catalytic model, with catalysis occurring through the summed energetic contributions of distinct structural units, is supported by several lines of evidence (Ranganathan et al., 1997). Firstly, Pin1 indeed demonstrates a proton concentration dependency with a bell-shaped titration curve, with its activity increasing from zero to maximal with an apparent pKa of 7.5. This is consistent with the reaction scheme which implies pH sensitivity of Pin1 activity, as seen in the deprotonation of His-59 and the protonation of His-157. Moreover, the calculated pKa is well within the expected range for neighboring histidines in a protein environment (Ranganathan et al., 1997). Second, mutation of Cys-113 to alanine or serine resulted in a decrease in Pin1 catalytic activity with a 123-fold or 20-fold decrease in K_{cat}/K_m, respectively (Ranganathan et al., 1997). Finally, a Pin1

triple mutant, G155A-H157A-I159A, failed to complement the yeast *ess1*$^{-}$ mutation *in vivo* and lacked a detectable PPIase activity against the standard PPIase substrate, succinyl-AlaAlaProPhe-pNA, *in vitro*. This has supported a role for His-157 in the catalytic mechanism of Pin1 (Lu et al., 1996b).

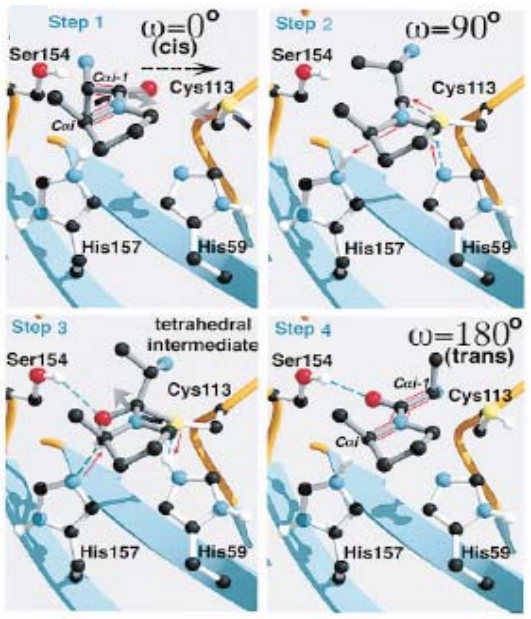

Figure 1-6: Proposed covalent catalytic mechanism of Pin1-nucleophilic catalysis model. (Adopted from Ranganathan *et al.* (1997), *Cell*, 89(6): 875-886)

Based on the first model of nucleophilic attack, replacement of residue Cys-113 with negatively charged residue Asp should result in a much poorer nucleophile. However, mutant C113D did not experience significant loss in Pin1 function. Hence, a second model of non-covalent catalytic mechanism has been proposed, as is the case with other peptidyl-prolyl isomerases (Behrsin et al., 2006). In this second model, the local environment around Cys-113, particularly Ser-111, Ser-115 and water-1005 (from PDB code 1PIN) would maintain Cys-113 in a state such that it would present a partial or full negative charge to the carbonyl oxygen atom of the substrate when it is

bound initially in the *cis* conformation. The negative charge in the immediate environment of the carbonyl oxygen would weaken the double bond character of the substrate pSer-Pro peptide bond, allowing a rotation from the *cis* towards the transition state for catalysis (Behrsin et al., 2006).

1.8.4 Dynamic interactions between Pin1 WW and PPIase domains

From the crystal structures, Pin1 WW domain and PPIase domain appeared to exhibit rigid interaction with other. In contrast, weak interaction between the two functional domains is observed by NMR studies in solution. When full length Pin1 is dissected into two separate domains through the flexible linker, the interaction between the two domains is abolished (Bayer et al., 2003; Jacobs et al., 2003). Since NMR reflects the properties of molecules in solution, it may be a better indication of the native state of Pin1 in solution.

It is important to further understand how the two flexible domains work with each other to achieve Pin1 specificity and *cis*/*trans* isomerization of substrate proteins. *Jacobs et al*. (Jacobs et al., 2003), through several NMR methods, had observed an enhancement of inter-domain interactions upon peptide binding, although there are no substantial conformational changes in the small and compact structures of both functional domains. In the context of Pin1's interaction with Cdc25 (EQPLpTPVTDL), CTD (YpSPTpSPS), and Pintide (WFYpSPR), inter-domain flexibility is reduced upon peptide binding in their *trans* conformation in the order of Cdc25 < CTD < Pintide (i.e. with Pintide most significantly restricts the flexibility of

the two domains). In another words, interaction between the WW and PPIase domains is most enhanced upon Pintide binding. Compared to the other two peptides, Pintide has the highest N-terminal hydrophobicity. This N-terminal hydrophobicity preference suits the N to C peptide binding orientation (as described earlier) well, in which the hydrophobic N-terminus is orientated toward the hydrophobic parts of the inter-domain interaction surface. Note that Pintide is the optimal sequence selected from a peptide scan and which binds to Pin1 with the highest affinity. These observations implied that the two functional domains may indeed interact upon preferable peptide binding. Meanwhile, it is also possible that the two domains interact to form a floppy hydrophobic cleft which accommodates molecules of a limited size upon peptide binding, and larger peptides may disrupt such inter-domain interactions. The sizes for Cdc25, CTD, and Pintide are 10mers, 7mers, and 6mers, respectively, and it cannot be excluded that the observed trend of inter-domain interactions is predominantly a steric hindrance effect. Moreover, in considering that short peptides may not exploit the complete binding site, it remains speculative to what extent the findings are applicable to Pin1 full-length substrates. Nevertheless, these studies have shed some light on the possible substrate specificity and mechanism of Pin1 function.

It is noteworthy that the Pin1 homologue in *Candida albicans*, Ca-Ess1, exhibits a rigid juxtaposition of the WW and PPIase domains, with an orientation that is different from that observed in human Pin1 (Figure 1-7) (Li et al., 2005). Moreover,

the two functional domains are believed to be fixed in a more permanent functional conformation, in contrast to the domain flexibility observed for human Pin1. These attributes are mainly contributed by a linker which is 11 residues longer than that of human Pin1, and the extensive interaction between the two functional domains and the linker. The linker contains a long α-helix which is highly structured. This helix and its interaction with nearby residues are believed to constrain the WW domain against the PPIase catalytic domain. Extensive interaction was observed between the N-terminal β1 of the WW domain and the loop connecting α5 (corresponds to α4 of Pin1) and β6 of the PPIase domain, and between the loops linking β2 and β3 of the WW domain and the C-terminus of α2 of the PPIase domain. Moreover, through such an extensive inter-domain interaction, the hydrophobic pocket between the domains that was implicated as the substrate binding site is eliminated. Thus, these differences suggest different mechanisms of substrate interaction and catalysis among the Pin1 homologues (Table 1-3).

Some Pin1 homologues such as the homologues in bacteria and plants do not have the WW domains at the N-terminus, although these too have the same specificity for pSer/Thr-Pro motifs. NMR studies revealed that the *Arabidopsis thaliana* Pin1 homologue, At-Pin1at, has a similar overall folded structure with Pin1's PPIase domain, except that it has an additional 19-residue flexible loop between β1 and α1 (Figure 1-7) (Landrieu et al., 2002). Its interaction site with phosphor-Cdc25 peptide was mapped in the loops between α4 and β3, between β3 and β4, in α3, and in

theβ1/α1 loop. The Arg-21 and Arg-22 residues which are located in the β1/α1 loop are analogous to Arg-68 and Arg-69 in the human Pin1, which is responsible for the substrate specificity. Besides these two acidic residues which are unique among the plant Pin1 homologues, no other structural elements likely to participate in substrate binding are known. Metzner *et al.* (Landrieu et al., 2002; Metzner et al., 2001) had proposed that another Pin1 homologue in plant, DIPar13, apparently overcomes the absence of the WW domain by improving the substrate affinity, based on its higher K_{cat}/K_m compared to human Pin1.

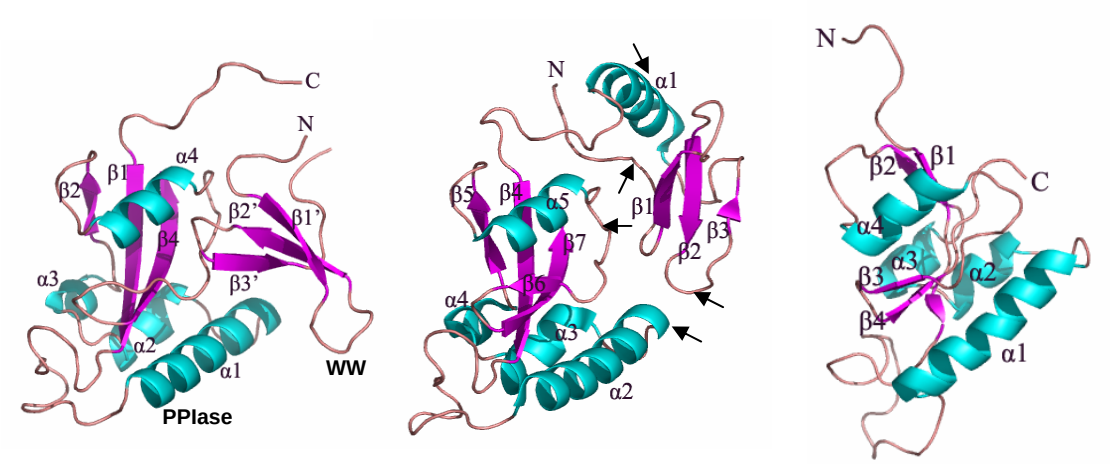

Figure 1-7: Structural comparison of human Pin1 (left), Ca-ESS1 (middle) and At-Pin1at (right). Pin1 homologue in Candida albicans, Ca-ESS1 (PDB code: 1YW5), has an extra linker (α1) which is 11 residues longer than that of human Pin1 (PDB code: 1PIN). While Pin1's WW and PPIase domains are loosely interact with each other in solution, functional domains of Ca-ESS1 have a rigid interaction, contributed by extensive interaction between the N-terminal β1 and the α5/β6 loop, and between the β2/β3 loop and the C-terminal α2 (as indicated as arrows). These interactions abolish the hydrophobic pocket between WW and PPIase domains compared to human Pin1. Pin1 homologue in Arabidopsis thaliana, At-Pin1at (PDB code: 1J6Y), has an identical PPIase domain with human Pin1 although it lacks a WW domain.

Table 1-3: Pin1 homologue abbreviations and their functional domains.

Sequence	Origin		Functional Domains	Reference
h-Pin1	*Homo sapiens*	Animal	WW, Rotamase	(Maleszka et al., 1996)
m-Pin1	*Mus musculus*		WW, Rotamase	(Fujimori et al., 1999)
x-Pin1	*Xenopus laevis*		WW, Rotamase	(Winkler et al., 2000)
Dm-dodo	*Drosophila melanogaster*	Fruit Fly	WW, Rotamase	(Maleszka et al., 1996)
Nc-ssp1	*Neurospora crassa*	Fungi	WW, Rotamase	(Kops et al., 1998)
Ca-Ess1	*Candida albicans*		WW, Rotamase	(Li et al., 2005)
En-Pin1	*Emerucella nidulans*		WW, Rotamase	(Crenshaw et al., 1998)
Cn-ESS1/PTF1	*Cryptococcus neoformans var. neoformans*		WW, Rotamase	Unpublished
Md-Pin1	*Malus×domestica (cultivated apple)*	Plant	Rotamase	Unpublished
At-Pin1at	*Arabidopsis thaliana (thale cress)*		Rotamase	(Landrieu et al., 2002)
Dl-*Dl*Par13	*Digitalis lanata*		Rotamase	(Metzner et al., 2001)
Sc-ESS1/PTF1	*Saccharomyces cerevisiae*	Yeast	WW, Rotamase	(Hani et al., 1995)
Pin1p	*Schizosaccharomyces pombe*		WW, Rotamase	(Huang et al., 2001)
Ec-Parv	*Escherichia coli*	Bacteria	Rotamase	(Rahfeld et al., 1994a)

1.8.5 Pin1's mechanism of action

The current understanding on Pin1's mechanism of action is as follows. Although the *trans* conformation is favorably generated by protein kinases in response to growth factor stimulation (Brown et al., 1999; Weiwad et al., 2000), the actual conformation adapted (either *cis* or *trans*) depends on individual pSer/Thr-Pro motifs with their surrounding residues in a native protein. This is influenced by the local structural constraints after phosphorylation, such as hydrogen-bond formation, which might lock certain pSer/Thr-Pro motifs in the *cis* conformation (Wulf et al., 2005).

These structural constraints determine which direction Pin1 tilts the dynamic equilibrium between *cis* and *trans* isomers to significantly affect the local (or even the global) tertiary structure of the specific target protein, thus regulating their biological functions. For example, under the condition in which the peptidyl-prolyl bond is locked in a *cis* conformation, Pin1 may be needed to catalyze the *cis* to *trans* conversion for subsequent post-translational modifications. Indeed, proteases such as trypsin and chymotrypsin can cleave their target peptide bonds only when the proline is in the *trans* conformation. Phosphatases such as PP2A dephosphorylate only the *trans* pSer/Thr-Pro motifs, and Pin1-dependent prolyl isomerization promotes the dephosphorylation of a large number of proteins including Cdc25, Tau, c-Myc, and Raf-1 (Dougherty et al., 2005; Lu et al., 1999a; Zhou et al., 2000; Yeh et al., 2004; Stukenberg and Kirschner, 2001; Smet et al., 2004). Moreover, recent X-ray structural studies reveal that the F-box proteins, which target ubiquitin-mediated proteolysis in a phosphorylation-dependent manner, target specific pSer/Thr-Pro motifs in the *trans* conformation only (Wulf et al., 2005; Orlicky et al., 2003). This may explain the role of Pin1 in promoting protein turnover in the cases of Btk, Cyclin E, c-Myc, SRC-3, Cf-2, and RARalpha. On the other hand, when there is no local structural constraint, Pin1 may bind to specific *trans* pSer/Thr-Pro motifs and catalyzes its conversion to *cis* conformation. Thus, the resulting cis conformation is protected from dephosphorylation and ubiquitin-mediated proteolysis. This may explain the case of NFAT in which active Pin1 inhibits its dephosphorylation by calcineurin, although it is not yet known whether the action of calcineurin is conformation-specific. In the

cases of Cyclin D1, p53, IRF3, p73, BIMEL, and β-catenin, the presence of Pin1 promotes protein stability. Pin1 might also use similar mechanisms to prevent Pin1 substrates from being inhibited and translocated to another subcellular compartment as in the case of the interaction between β-catenin and APC, p53 and Mdm2, and NFκB and IκB (Wulf et al., 2005).

1.8.6 Proposed regulatory mechanism models of Pin1

As reviewed above, structural studies have shown that both the two functional domains of Pin1 exhibit peptide binding sites with a specificity for pSer/Thr-Pro motifs in phosphopeptides. However, it remains unclear as to exactly how the two domains, respectively, bind to and isomerize the substrates. There is indirect evidence showing that these domains might act in close temporal order on the same pSer-Pro motif. For example, the optimal binding peptide, Pintide, binds both WW domain and PPIase domain with high affinity, with dissociation constants (Kd) of 1.2 μM and 11.0 μM, respectively. It is also the best available substrate for the PPIase activity of Pin1 (Yaffe et al., 1997; Schutkowski et al., 1998; Lu et al., 1999b). Moreover, WW domain binding site appears crucial for regulating the phosphorylation site, and mutating them abolishes the effects of Pin1 on its substrates. However, the possibility of the two domains acting on separate pSer-Pro motifs cannot be excluded. In the case of c-Myc, Pin1 has been shown to bind to one pThr-Pro motif while promoting dephosphorylation of another motif in the same protein. Indeed, many Pin1 substrates have multiple Pin1 binding sites, such as Cdc25, p73, β-catenin, p53, Tau,

c-Jun, and CTD. It remains to be determined how these multiple Pin1 binding sites relate themselves to the Pin1 catalytic action. On the other hand, many other Pin1 substrates have only one recognized pSer/Thr-Pro motif. In the early scenario, the WW domain has to dissociate from, before the catalytic domain engages and isomerizes, the same pSer/Thr-Pro. Alternatively the catalytic domain could act on another pSer/Thr-Pro in the same protein molecule. It may be informative to consider the continuous hydrophobic path on the Pin1 molecular surface constituted with the two peptide binding sites at WW and PPIase domains and the hydrophobic path on the backside of Pin1. This suggests that Pin1 may interact with its substrates using an extended recognition surface (Ranganathan et al., 1997). Thus, structural studies with longer substrate peptides will be needed to further delineate Pin1's mechanism of action.

Despite the limitations of the current knowledge, several models of how Pin1 regulates the activities of mitotic phosphoproteins have been proposed. In all of the proposed models, phosphorylation of the Ser/Thr-Pro motif is a prerequisite for Pin1 targeting and *cis*/*trans* isomerization. The first model is the sequential action model, in which the WW domain first targets the pSer/Thr-Pro motif and the PPIase domain catalyzes the *cis*/*trans* isomerization of the peptidyl prolyl bond of the same pSer/Thr-Pro motif (Jacobs et al., 2003; Zhou et al., 1999; Wintjens et al., 2001). These two events can occur sequentially and independently, and thus the inter-domain flexibility is not crucial. This proposal is supported by the findings that at high

cellular concentrations, the Pin1 PPIase domain is itself sufficient to carry out the essential function of Pin1 (Zhou et al., 2000). The Pin1 WW domain may specifically target *trans* pSer/Thr-Pro motifs, and in doing so increase the local concentration of the target. Full-length Pin1 therefore gives higher catalytic activity compared to the PPIase domain alone. In another scenario, the catalytic domain could induce a conformational transition from *cis* to *trans* of the pSer/Thr-Pro motif prior to WW domain binding. Before a return to the *cis*/*trans* equilibrium state, the WW domain could then immediately engage the pSer/Thr in the *trans* conformation, thereby stabilizing this conformation and simultaneously increasing the local concentration of Pin1. For substrates with repetitive targeting motifs such as Cdc25, Tau, and CTD, initial binding and isomerization may trigger a succession of alternating binding and isomerization, each one revealing a further site to be isomerized. Thus, Pin1 "jumps" from one motif to another. Moreover, in this model, inter-domain contacts may serve as an extended recognition surface to control the accessibility of different substrates. However, two functionally separate domains are not mandatory for this sequential model, because the WW domain needs to dissociate in order for the PPIase domain to then bind and isomerize the pSer/Thr-Pro peptide substrate.

The second model is "tag and twist" model in which kinases "tag" the substrates via phosphorylation and Pin1 subsequently isomerizes ("twist") the pSer/Thr-Pro imide bond, and in this model inter-domain flexibility is crucial (Jacobs et al., 2003; Lu et al., 2002a; Wintjens et al., 2001). For substrates with repetitive targeting motifs,

the WW domain could target Pin1 to the specific pSer/Thr-Pro motifs, followed by isomerization of neighbouring pSer/Thr-Pro amide bonds through the PPIase domain. In another scenario in which Pin1 functions in a multienzyme complex with a kinase or phosphatase, Pin1 is recruited to the multienzyme complex through its WW domain interacting with a pSer/Thr-Pro motif, and PPIase domains isomerizes a pSer/Thr-Pro on another protein in the complex. For CTD, which exists in a dynamic equilibrium between hypophosphorylated and hyperphosphoryated forms resulting from antagonistic actions of specific kinases and phosphatases, this model suits well. Pin1 WW domain may also bind to phosphorylated Plk I to provide a complex that first phosphorylates Cdc25 and subsequently activates this substrate by *cis*/*trans* isomerization (Jacobs et al., 2003). Indeed, many kinases and phosphatases have pSer/Thr-Pro motifs themselves. In view of the substrate diversity of Pin1, Pin1 can be recruited and catalytically active in multitude different target protein complexes only when its inter-domain interaction is very flexible. As reported by Jacobs *et al*. (Jacobs et al., 2003), Pin1 alone in solution tends towards a state with non-interacting domains. Upon addition of substrates, the equilibrium is shifted towards the complexed form of Pin1, with the two domains interacting with each other. Pin1 could thus fit into multienzyme complexes to isomerize and active its substrates. These scenarios could also explain the higher catalytic activity of full-length Pin1 in comparison with Pin1 PPIase domain alone.

The third model is “induced-fit” model which is based on the two crystal

structures of Pin1 (Ranganathan et al., 1997; Verdecia et al., 2000), involving the opened and closed conformations at the α1/β1 loop with a tripartite basic cluster (Lys-63, Arg-68, and Arg-69). With no peptide binding, Arg-68 and Arg-69, which confer preferential binding of phosphorylated substrates to the Pin1 PPIase domain, reside outside of the proline ring binding pocket, adopting an opened conformation. Upon Ala-Pro dipeptide binding, these residues cluster in the lower portion of the active site Cys-113, changing Pin1 into its closed conformation. Hence the orientation of the α1/β1 loop might serve as an additional substrate selectivity filter in addition to the substrate preference of anionic charge at peptide N-terminus as conferred by the tripartite basic cluster. In contrast, Pin1 structure in solution appears to demonstrate that no such structural rearrangement occurs and the loop is in its closed conformation under both conditions. Furthermore, based on the structure of Pin1 homologue in *Candida albicans* Ca-Ess1, the conformation of this loop resembles the closed conformation, despite the fact that there are no ligands present in the active site (even though the crystallization buffer does contain 50 mM phosphate). Thus, these data suggest that the movement of the loop may not be important for substrate binding and catalytic activity.

1.9 Unresolved questions and challenges in investigations on Pin1 structure and function

Pin1 is apparently involved in many essential cellular processes and it is indeed the only PPIase identified so far that is essential for cell growth. However, it remains

to be investigated why the *Pin1* gene is essential in some systems but not in others (Lu et al., 2002a). Moreover, Pin1 function is very likely depended on the cell type and the specific signaling cascades that determine the fate of these cells (Wulf et al., 2005). Thus, one prominent challenge would be to further define the specificity of Pin1 function in different cell types or systems. A number of crystal and NMR structures have been solved for human Pin1 as well as for some of its homologues. Together with biochemical studies, substantial information on the enzymatic specificity and its catalytic mechanism has been gathered. However, there are still a lot of uncertainties on Pin1's mechanism of action and how exactly Pin1 does exert an action towards such a broad spectrum of substrates. This uncertainty has been largely due to the lack of available structural information on Pin1's phosphorylated substrates (Wulf et al., 2005). Furthermore, it is still also a challenge for researchers to come up with a consensus sequence recognized by Pin1. Major challenges in the Pin1 field would also include defining the structural and functional differences of the *cis* and *trans* phosphorylated proteins, and to further develop tools to visualize Pin1-catalyzed conformational changes and to study their biological and pathological significance (Wulf et al., 2005).

CHAPTER 2: OBJECTIVES

Pin1 is essential in a diverse array of cellular processes for regulating the function of a large number of critical proteins through catalysis of *cis/trans*-isomerization of the peptide bond preceding proline, in the sequence of pSer/Thr-Pro, thus inducing a conformational change in these substrate proteins. Through extensive studies on Pin1, more than 50 biological substrates of Pin1 have been identified so far. The first crystal structure of Pin1 has been reported in 1997, and this was followed by another crystallographic analysis and several NMR structural determinations along with the short peptide substrate complex (2 to 7 residues). However, much remains to be learned about Pin1's catalytic mechanism and its interaction with biological substrates. In this project, we focused on the structural and functional studies on Pin1 mutants in order to better understand Pin1's mechanism of action, and how exactly Pin1 exerts its action to its substrates.

Mutants for this study were selected based on functionally important amino acid residues in Pin1 according to the literature. These residues include those that are involved in the peptide binding groove in the WW domains: Arg-14, Ser-16, Arg-17, Tyr-23, Phe-25, Ser-32, and Trp-34 (Verdecia et al., 2000), and those that are involved in substrate specificity and catalytic activity in the PPIase domain: His-59, Lys-63, Arg-68, Arg-69, Cys-113, Leu-122, Met-130, Phe-134, Ser-154, and His-157 (Ranganathan et al., 1997). An alanine screening for these residues was performed by first substituting them with alanine. Besides, double mutant R68A/R69A was made

because Arg-68 and Arg-69 are twin residues involving in phosphate binding and acting as a selectivity filter at the WW domain (Ranganathan et al., 1997). Ser-16 was also substituted with Glu which is a negatively charged residue. Substitution of Ser with Glu mimics phosphorylation at this side and would provide us structural and functional details of how phosphorylation at this side would abolish Pin1's ability to interact with its substrates (as reviewed in section 1.6). These were summarized in Table 2-1.

Table 2-1. Functionally important amino acid residues selected for Pin1 mutation studies.

Functional domain	Pin1 mutant	Description
WW domain	R14A	Peptide binding groove
	S16A/S16E	
	R17A	
	S32A	
	F25A	
	W34A	
PPIase domain	K63A	Positively charged residues involved in phosphate binding
	R68/69A	
	C113A	Catalytic active site
	H59A	Together with C113, involved in covalent catalytic mechanism of peptide bond isomerization
	H157A	
	S154A	
	L122A	Proline binding pocket
	M130A	

The techniques involved in this project included the basic molecular cloning, site-directed mutagenesis, mammalian cell culture, and protein expression and purification. The particular methods in structural biology included circular dichroism (CD) and X-ray crystallography. Purified mutant proteins were subjected to thermo-stability testing by CD analysis. Pin1 mutant crystals were grown for X-ray

crystallographic analyses. We successfully solved seven mutant Pin1 structures: R14A, F25A, S32A, W34A, K63A, C113A, and M130A, while crystals for the rest of the mutants were failed to be obtained. Mutants' crystal structures and *in vitro* peptide binding assay combined with functional studies in mammalian cells was planned. Together, these studies would provide a deeper understanding of Pin1's mechanism of action and perhaps eventually lead to effective Pin1-based drug design.

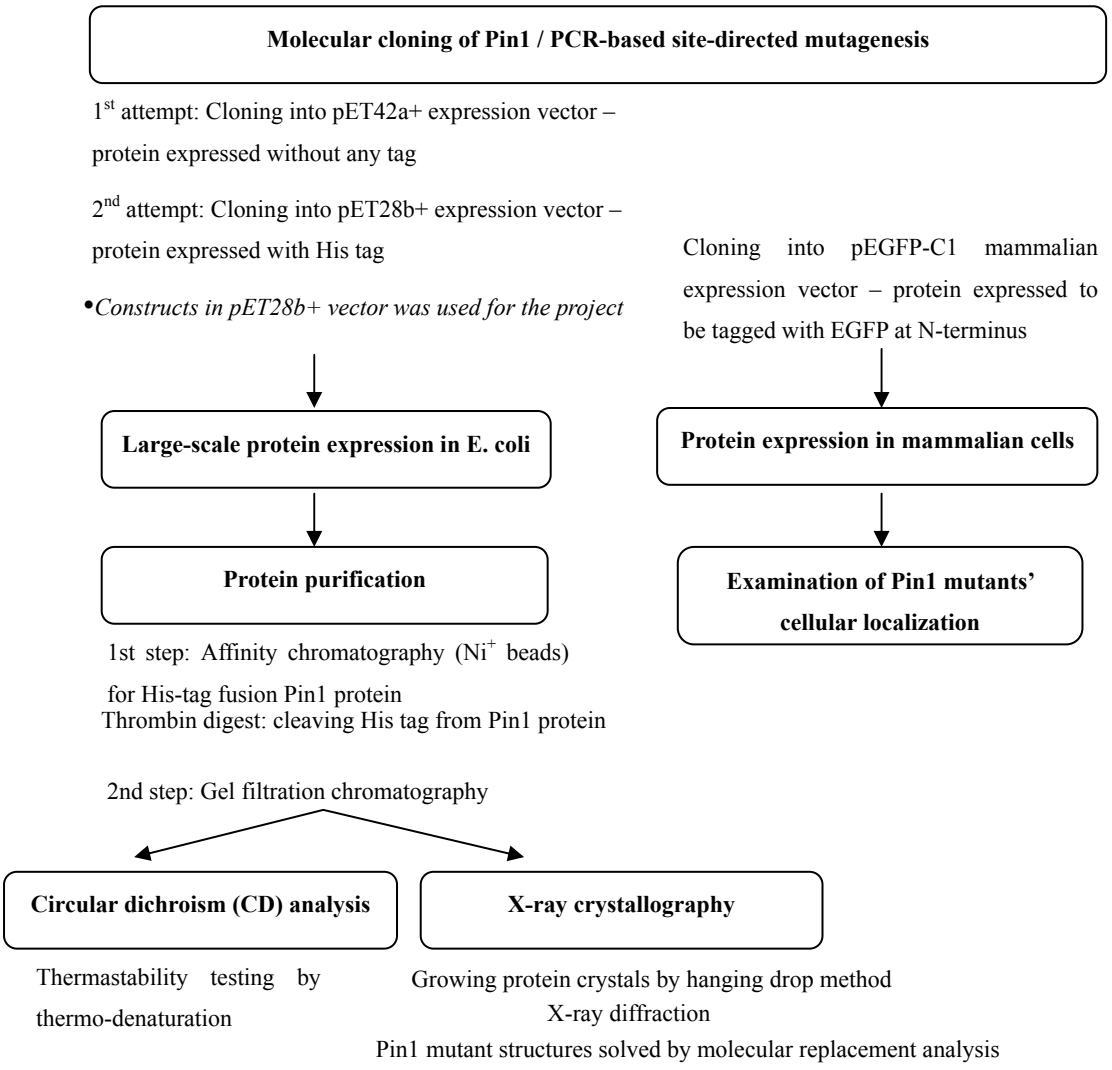

Figure 2-1: Project work flow chart

CHAPTER 3: MATERIALS AND METHODS

3.1 Materials

3.1.1 cDNA constructs, expression vectors and primers

Pin1 cDNA was reported previously (Gene bank accession number NM_006221) and the wild-type, W34A, K63A, S16A, and S16E mutant cDNA constructs were kindly provided by Prof. Kun Ping Lu. pET42a+ and pET28b+ vectors were purchased from Novagen (Madison, WI) whereas pEGFP-C1 vector was from BD Biosciences Clontech (Palo Alto, CA, USA). PCR and sequencing primers were purchased from either Sigma-Proligo (Singapore) or 1^{ST} Base Pte Ltd (Singapore).

3.1.2 Enzymes and proteases

Most restriction enzymes were purchased from Promega Corporation (Madison, WI) except Dpn I was from New England Biolabs (Beverly, MA, USA). T4 DNA ligase and Taq DNA polymerase were from Promega Corporation (Madison, WI), whereas PfuTurbo® DNA polymerase and thrombin was purchased from Stratagene (La Jolla, CA, USA) and Sigma-Aldrich (Singapore), respectively.

3.1.3 Bacterial culture media and other reagents

Luria Bertani broth (LB) and terrific broth (TB) were purchased from AMRESCO (USA) and Amersham Biosciences (Buckinghamshire, UK), respectively. Antibiotics kanamycin was from USB Corporation (Cleveland, OH, USA).

3.1.4 Mammalian cell lines, cell culture media and other reagents

Human cervical cancer cells line HeLa and Chinese hamster ovary (CHO) cells were purchased from the American Type Culture Collection (ATCC), (Manassas, VA, USA). Dulbeco's Minimum Eagles Medium (DMEM) and fetal bovine serum (FBS) were from Hyclone (Logan, UT). The antibiotics penicillin and streptomycin were from Invitrogen Pte. Ltd. Lipofectamine 2000 and Effectene transfection reagents were purchased from Invitrogen Pte Ltd (Carlsbad, CA, USA), and Qiagen GmbH, (Hilden, Germany), respectively. Tissue culture flasks, culture dish, 12-well plates and other disposables were either from Nunc (Roskilde, Denmark) or Falcon (Oxnard, CA, USA). Cell cycle drugs nacodazole, hydroxyurea and thymidine were all purchased from Sigma-Aldrich (Singapore).

3.1.5 Western blot reagents

Pin1 antibody was generated as described previously (Lu *et al*., 1999). Anti His-tag (sc-8036), anti β-tubulin (sc-5274), anti GFP (sc-8334), and goat anti-mouse (sc-2005) or anti-rabbit (HRP conjugated) (sc-2004) antibodies were purchased from Santa Cruz Biotechnology (CA, USA). Derivatized polyvinylidene difluoride (PVDF) membrane was purchased from Amersham Biosciences (Buckinghamshire, UK). SuperSignal West Pico Chemiluminescent Substrate was from Pierce Chemical Co. (Rockford IL, USA).

3.1.6 DNA cleanup, plasmid DNA preparation, and DNA cycle sequencing kits

QIAquick gel extraction kit, QIAquick PCR purification kit, and mini-plasmid

preparation kit were all purchased from Qiagen GmbH (Hilden, Germany). The ABI PRISM BigDye terminator cycle sequencing ready reaction kit and Hi-Di formamide were from Applied Biosystems (Foster City, CA, USA).

3.1.7 Protein purification and crystallization-related materials and reagents

Ni-NTA agarose was purchase from Qiagen Gmb H (Hilden, Germany). UNO ion exchange and Bio-Scale ceramic hydroxyapatite Type I (CHT-I) columns were from Bio-Rad (CA, USA) whereas HiPrep 26/60 Sephacryl S-200 High Resolution and HiLoad 16/60 Superdex 75 Prep Grade gel filtration columns were from Amersham Biosciences (Buckinghamshire, UK). Amicon Ultra-15 and Amicon Ultra-4 centrifugal filter units were from Millipore (Bedford, MA, USA). Crystallization plates (EasyXtal Tool X-seal) were from Qiagen GmbH (Hilden, Germany) whereas the other crystallization tools were from Hampton Research (CA, USA).

3.2 Methods

3.2.1 Molecular cloning

In general, DNA fragment (see Figure 3-1) to be cloned into a specific vector was amplified by polymerase chain reaction (PCR) in a 50μl reaction mix (3.2 pmol forward and reverse primers, 10mM dNTP, and 1 U DNA polymerase) with 35 thermal cycles (95^{o} C 1 min, 58ºC 1 min, and 72ºC 1 min; final extension at 72ºC for 5 min). The sequence of the primers includes the sequence recognized by specific restriction enzymes selected for the cloning. To clone Pin1 or mutant cDNAs into pET42a+ expression vector at NdeI and Sal I cloning sites, forward and reverse

primers were designed as 5’ GTA GTA CAT ATG GCG GAC GAG GAG AAG CTG 3’ (the NdeI recognition sequence is underlined), and 5’ GTA GTA GTC GAC TCA CTC AGT GCG GAG GAT GAT GTG 3’ (the Sal I recognition sequence is underlined), respectively (Figure 3-1). The same set of primers were used to clone Pin1 or mutants cDNA into pET28b+ expression vector at Nde I and Sal I cloning sites so that the Pin1 protein expressed would have a 6X His-tag at its N-terminus partitioned by a thrombin cutting site (Figure 3-2). To clone Pin1 or mutant cDNAs into pEGFP-C1 mammalian expression vector, Bgl II and Sal I were used as the cloning sites with the forward and reverse primers designed as 5’ GTA GTA AGA TCT ATG GCG GAC GAG GAG AAG CTG 3’ (underlined is Bgl II recognition sequence) and 5’ GTA GTA GTC GAC TCA CTC AGT GCG GAG GAT GAT GTG 3’ (underlined is Sal I recognition sequence), respectively. Proteins expressed would have an enhanced green fluorescent protein (EGFP) fused to its N-terminus (Figure 3-3).

After DNA amplication by PCR, the PCR product was subjected to agarose gel electrophoresis and the amplified DNA fragment was purified by gel extraction kit according to the manufacturer’s instruction. In brief, the DNA band was cut out from the agarose gel and incubated with gel extraction buffer (100μl per 0.1 gram of cut-out gel) at 50 ºC until the gel was dissolved. The dissolved gel solution was then applied to a spin column and centrifuged at 13, 000 rpm for 1 min to let the solution flowed through the spin column membrane while DNA fragments remained bound to

the membrane. To wash the bound DNA, 750 µl of wash solution was added to the column and spin column was subjected to centrifugation again. This washing step was repeated once, followed by DNA elution with 50 µl of DNase-free water (autoclaved distilled water). It was then followed by digestion overnight at 37ºC by appropriate restriction enzymes.

After digestion, the insert DNA was purified with PCR extraction kit according to the manufacturer's instruction. Briefly, 3 volumes of Buffer PE was added to the DNA digestion mixture followed by applying the mixture into the spin column, and spin column was processed as above.

On the other hand, vectors were digested at 37ºC for 4 hr by appropriate restriction enzymes and purified by the gel extraction kit as described. Ligation was performed by incubating insert DNA fragment and vector with T4 DNA ligase overnight at 16ºC. The ligation mixture was then incubated with *E. coli* BL21 (DE3) competent cells for transformation and the recombinant plasmid was verified by automated DNA sequencing.

3.2.2 PCR-based site-directed mutagenesis

Wild type Pin1 recombinant plasmid was used as template for mutagenesis. Template-specific mutagenic primers (see Table 3-1) were designed for the PCR-based site-directed mutagenesis (with reference to Stratagene's QuikChange® Site-Directed Mutagenesis Kit). Briefly, a 50 µl reaction system containing 5-50ng

A

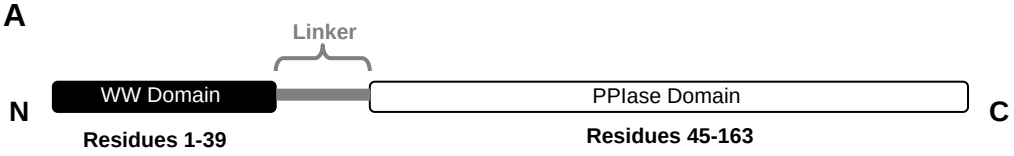

B

1 *ATGGCGGACG AGGAGAAGCT GCCGCCCGGC TGGGAGAAGC GCATGAGCCG CAGCTCAGGC CGAGTGTACT 70*

*71 ACTTCAACCA CATCACTAAC GCCAGCCAGT GGGAGCGGCC CAGCGGC***AAC AGCAGCAGTG GT**GGCAAAAA 140

141 CGGGCAGGGG GAGCCTGCCA GGGTCCGCTG CTCGCACCTG CTGGTGAAGC ACAGCCAGTC ACGGCGGCCC 210

211 TCGTCCTGGC GGCAGGAGAA GATCACCCGG ACCAAGGAGG AGGCCCTGGA GCTGATCAAC GGCTACATCC 280

281 AGAAGATCAA GTCGGGAGAG GAGGACTTTG AGTCTCTGGC CTCACAGTTC AGCGACTGCA GCTCAGCCAA 350

351 GGCCAGGGGA GACCTGGGTG CCTTCAGCAG AGGTCAGATG CAGAAGCCAT TTGAAGACGC CTCGTTTGCG 420

421 CTGCGGACGG GGGAGATGAG CGGGCCCGTG TTCACGGATT CCGGCATCCA CATCATCCTC CGCACTGAGT 490

491 GA 492

C

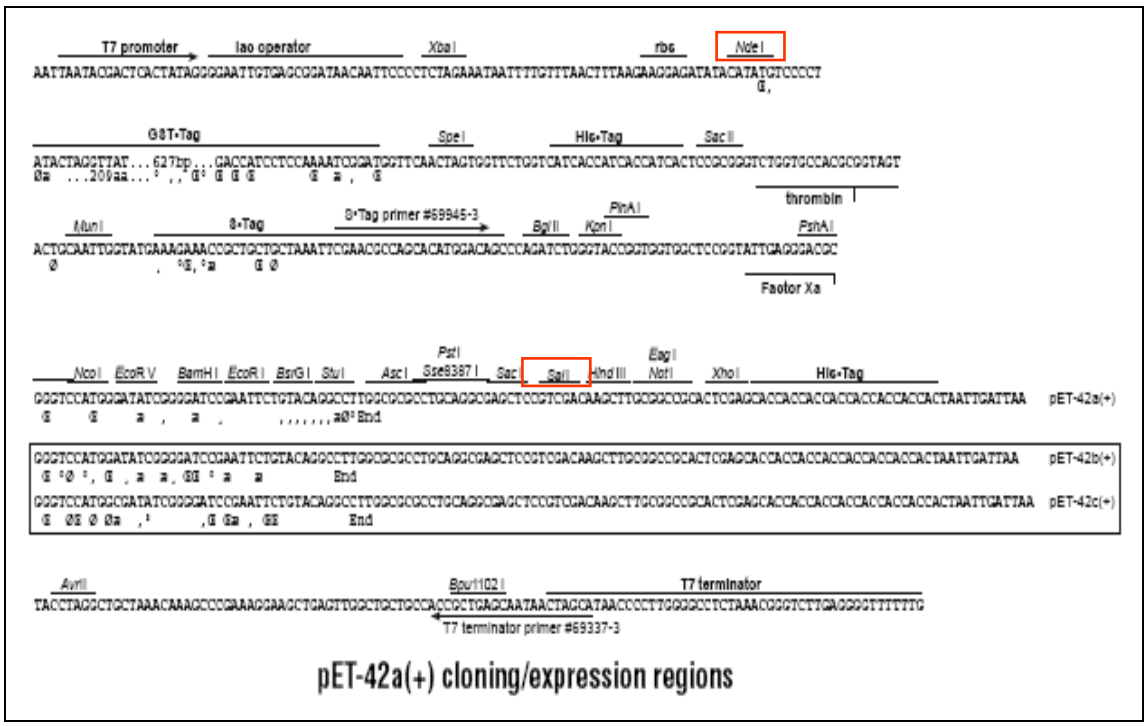

Figure 3-1: Cloning of Pin1-WT and its mutants into pET42b+ vector. (A) Schematic diagram of Pin1 protein. (B) Full-length cDNA sequence of hPin1. Nucleotides 1-117 encode WW domain (in *Italic*). Nucleotides 118-132 are linker regions (in bold), whereas the nucleotides 133-492 are PPIase domain region. Sequences of WW domain and PPIase Underlined are the primers' positions. (C) Cloning and expression regions of pET42 series vector. Cloning sites were boxed in red.

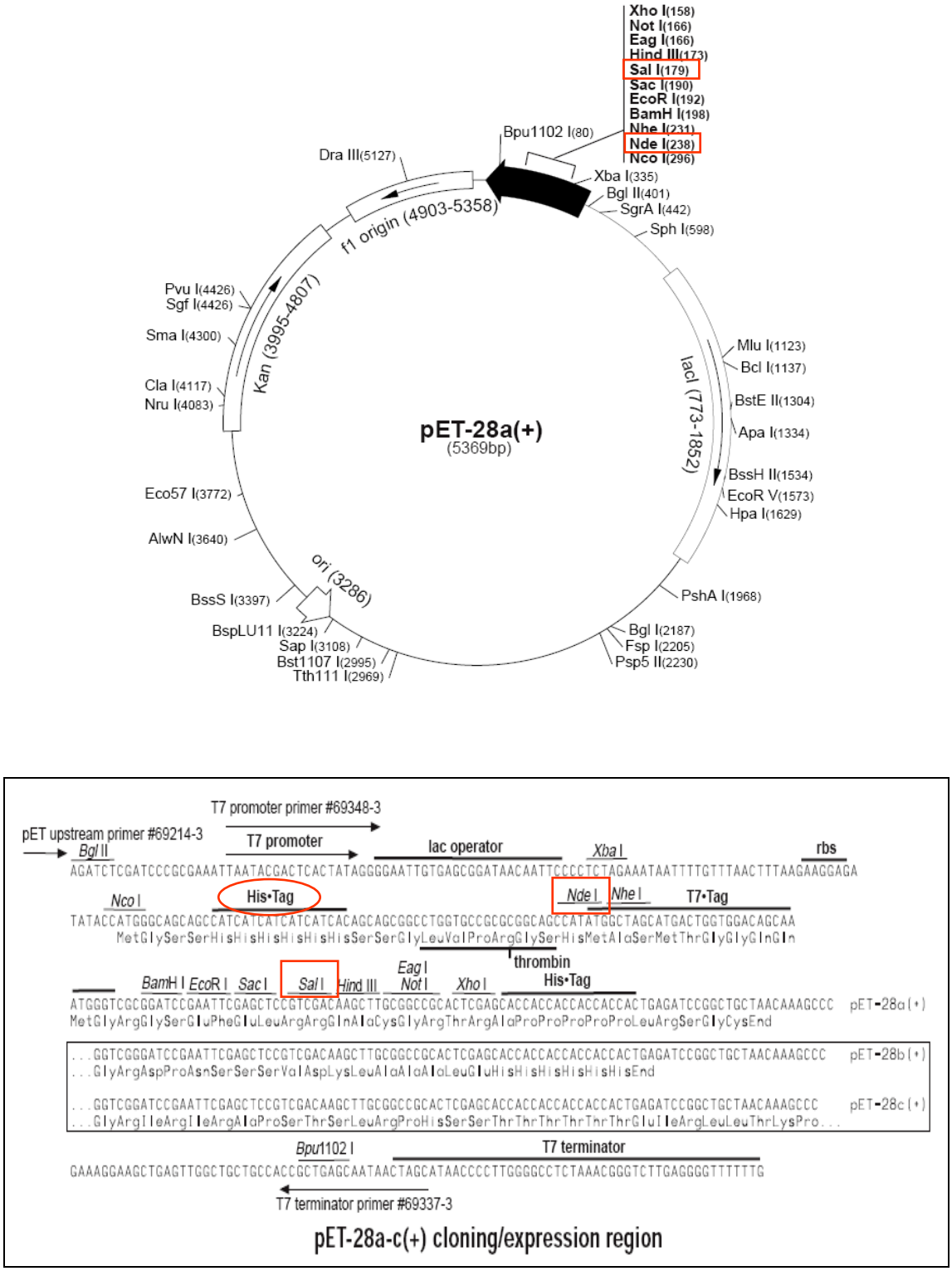

Figure 3-2: Cloning of Pin1-WT and its mutants into pET28b+ vector. Schematic diagram of pET28b+ vector (upper panel) and its multiple cloning site (lower panel). Cloning sites, which are Nde I and Sal I, were boxed in red. The protein expressed was His tagged fusion protein.

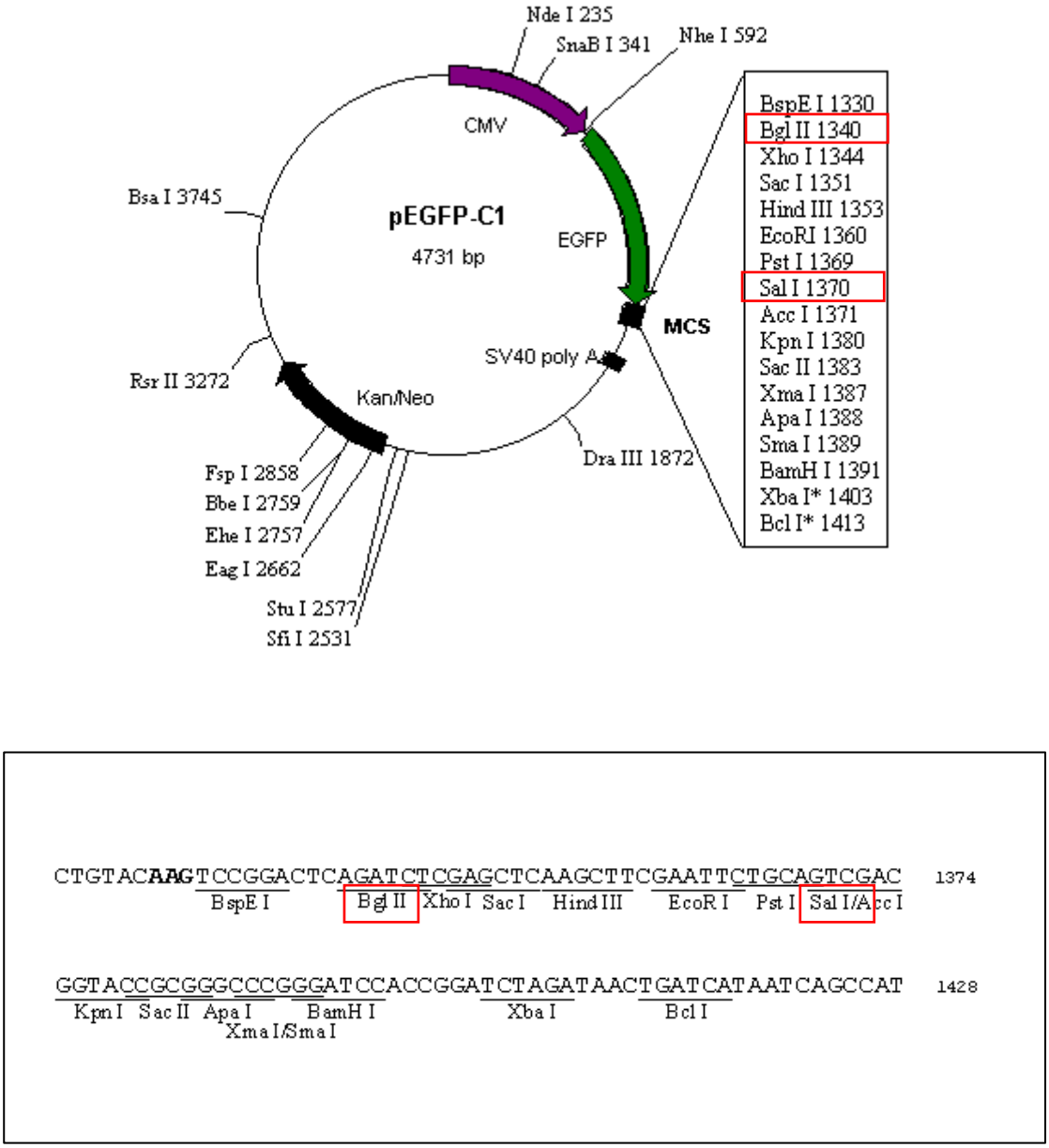

Figure 3-3: Cloning of Pin1-WT and its mutants into pEGFP-C1 vector. Schematic diagram of pEGFP-C1 vector (upper panel) and its multiple cloning site (lower panel). Cloning sites, which is Bgl II and Sal I, were boxed in red. The protein expressed was EGFP tagged fusion protein.

Pin1 wild-type plasmid, 0.25 μM of sense and antisense mutagenic primers respectively, 0.2 μM dNTPs, and 2.5 U of PfuTurbo® DNA polymerase was subjected to 16 thermal cycles (95 °C 1 min, 55 °C 1 min, and 72 °C 6 min; final extension at 72 °C for 20 min). 15 μl of the PCR products were then treated for 2 hr with 5 U of Dpn I at 37 °C for the digestion of the methylated, non-mutated parental DNA template. The mixture was then incubated with 100 μl of *E. coli* BL21 (DE3) competent cells for the transformation of the remaining undigested mutated plasmids into the bacteria. The mutant sequences were verified by automated DNA sequencing.

Table 3-1: Mutagenic Primers

Pin1 mutants	Primer Sequence	
S32A	Sense	5' CCA CAT CAC TAA CGC C**GC A**CA GTG GGA GCG GCC 3'
	Antisense	5' GGC CGC TCC CAC TG**T GC**G GCG TTA GTG ATG TGG 3'
F25A	Sense	5'TCA GGC CGA GTG TAC TAC **GCA** AAC CAC ATC ACT AAC GCC 3'
	Antisense	5' GGC GTT AGT GAT GTG GTT **TGC** GTA GTA CAC TCG GCC TGA 3'
C113A	Sense	5' CCT CAC AGT TCA GCG AC**G CA**A GCT CAG CCA AGG CC 3'
	Antisense	5' GGC CTT GGC TGA GCT **TGC** GTC GCT GAA CTG TGA GG 3'
H59A	Sense	5' GGG TCC GCT GCT CG**G CA**C TGC TGG TGA AGC ACA 3'
	Antisense	5' TGT GCT TCA CCA GCA G**TG C**CG AGC AGC GGA CCC 3'
H157A	Sense	5' CAC GGA TTC CGG CAT C**GC A**AT CAT CCT CCG CAC TG 3'
	Antisense	5' CAG TGC GGA GGA TGA T**TG C**GA TGC CGG AAT CCG TG 3'
S154A	Sense	5' CCC GTG TTC ACG GAT **GCA** GGC ATC CAC ATC ATC 3'
	Antisense	5' GAT GAT GTG GAT GCC **TGC** ATC CGT GAA CAC GGG 3'
L122A	Sense	5' AGG CCA GGG GAG AC**G CA**G GTG CCT TCA GCA GAG 3'
	Antisense	5' CTC TGC TGA AGG CAC C**TG C**GT CTC CCC TGG CCT 3'
M130A	Sense	5' CCT TCA GCA GAG GTC AG**G CA**C AGA AGC CAT TTG AAG ACG 3'
	Antisense	5' CGT CTT CAA ATG GCT TCT G**TG C**CT GAC CTC TGC TGA AGG 3'
R14A	Sense	5' CCC GGC TGG GAG AAG **GCA** ATG AGC CGC AGC TCA 3'
	Antisense	5' TGA GCT GCG GCT CAT **TGC** CTT CTC CCA GCC GGG 3'
R17A	Sense	5' GAG AAG CGC ATG AGC **GCA** AGC TCA GGC CGA GTG 3'
	Antisense	5' CAC TCG GCC TGA GCT **TGC** GCT CAT GCG CTT CTC 3'

* Nucleotides in bold and underlined denote sites for point mutations

3.2.3 Preparation of competent cells

To prepare *E. coli* BL21 (DE3) competent cells, BL21 (DE3) bacteria strain was inoculated in 50 ml LB broth at 37 °C until cell density reached an optical density at 600 nm (OD_{600}) of 0.6. The cells were then chilled on ice for 10 min followed by centrifugation at 2,500 rpm at 4 °C for 10 min. The bacterial pellet was resuspended gently in 17 ml CCMB buffer (80 mM $CaCl_2$, 20 mM $MnCl_2$, 10 mM $MgCl_2$, 10 mM KOAc, 10 % (v/v) glycerol, and adjusted with HCl to pH 6.4) and incubated on ice for 20 min. After centrifugation at 3,000 rpm at 4 °C for 10 min, the cell pellet was resuspended again in 4 ml CCMB buffer and stored at -80 °C in small aliquots.

3.2.4 Transformation

Transformation was performed using the conventional heat-shock method (Seidman et al., 1997). In brief, ligation mixture or recombinant plasmids were gently mixed with 100 µl of *E.coli* BL21 (DE3) competent cells and the mixtures were placed on ice for 30 min prior to heat-shock. The mixtures were then subjected to 42 ºC for 90 s for heat-shock and quickly placed on ice for 5 min. The mixtures were then incubated for 1 hr with LB for recovery and subsequently plated onto agar plates supplemented with 50 µg/ml antibiotic kanamycin. Plates were incubated overnight at 37 ºC. Transformant colonies were obtained the next day and the presence of inserts was verified by PCR and restriction digestion. Colonies were picked and allowed to grow overnight into liquid culture followed by plasmid extraction and purification using Miniprep DNA purification kit. The plasmid sequences were then verified by

automated DNA sequencing.

3.2.5 Mini-plasmid preparation

Recombinant plasmid DNA was extracted from liquid bacterial culture at room temperature using Mini-plasmid preparation kit according to the manufacturer's instruction (Qiagen GmbH (Hilden, Germany). In brief, 1-5 ml of bacteria liquid culture was harvested by centrifuging at 13, 000 rpm for 1 min. The bacteria pellet was resuspended in 250 µl of resuspension buffer (50 mM Tris-HCl (pH 8.0), 10 mM EDTA, 100 µg/ml RNase A) followed by adding of 250 µl of lysis buffer (200 mM NaOH, 1 % SDS (w/v)). After gentle and thorough mixing for 5 min, 350 µl of neutralization buffer was added, followed by centrifuging at 13, 000 rpm for 15 min. The supernatant, which contained the plasmid DNA, was then applied to a spin column and centrifuged at 13, 000 rpm for 1 min to let the solution flowed through the spin column membrane while the plasmid DNA remained adsorbed to the membrane. To wash the bound plasmid, 750 µl of wash solution was added to the column and spin column was subjected to centrifugation again. This washing step was repeated once, followed by plasmid elution with 50 µl of DNase-free water (autoclaved distilled water).

3.2.6 Automated DNA sequencing

The ABI PRISM® BigDye terminator cycle sequencing ready reaction kit (Applied Biosystems) was used for automated cycle sequencing. Recombinant plasmid DNA was first extracted from liquid bacterial culture using Miniprep DNA

purification kit as described earlier. Subsequently, a reaction system of 20 µl consisting of 2 µl BigDye terminators, 3.2 pmol of either forward or reverse sequencing primer, 2 µl of purified plasmid DNA template, and 3 µl of 5X reaction buffer (400 mM Tris-HCl (pH 9.0), 10 mM $MgCl_2$) was subjected to 35 thermal cycles (95 °C 1 min, 58 °C 1 min, and 72 °C 1 min; final extension at 72 °C for 5 min). The extension products were then precipitated with 80 µl of ethanol-sodium acetate solution (consisting of 3 µl of 3 M sodium acetate, pH 4.6, 62.5 µl of non-denatured 95 % (v/v) ethanol, and 14.5 µl of deionized water) for 15 min at room temperature. After centrifugation at 13,000 rpm for 20 min, the DNA pellet was wash twice with 70 % (v/v) ethanol, with an incubation time of 5-15 min each time, followed by centrifugation at 13,000 rpm for 10 min. The DNA pellet was allowed to dry and was resuspended in 170 µl of Hi-Di Formamide. The resuspended DNA was heated at 95 ºC for 2 min to denature the DNA strands and was then immediately placed on ice. 10 µl of the DNA was dispensed into a 96-well microtiter place and sent to ABI PRISM® 3100 DNA Sequencer for automated DNA sequencing. The sequencing results were viewed and analyzed by the software Vector NTI (Invitrogen, CA, USA).

3.2.7 Small-scale protein expression

1.5 ml overnight inoculated *E. coli* BL21 (DE3) containing Pin1 plasmid (or mutants) was added to 8.5 ml fresh LB supplemented with 50 µg/ml kanamycin and was grown at 37 °C with shaking at 250 rpm until the optical density at 600nm reached 1.0. The recombinant Pin1 proteins were then induced with 0.8 mM isopropyl

β-D-1-thiogalactopyranoside (IPTG) for 4 hr. 1 ml of *E. coli* culture was sampled for harvest by centrifugation at 13,000 rpm for 1 min and the cells were resuspended in 50 µl *E.coli* lysis buffer (1 % glycerol, 50 mM Tris-HCl (pH8.0), 0.15 M NaCl, 1 % Triton-X100, 1 mM DTT, and 2 mM EDTA) followed by 3 freeze-thaw cycles using liquid nitrogen to ensure complete lysis. After centrifugation at 13,000 rpm for 20 min at 4 ºC, the supernatant and pellet were separated and the protein expression was examined by SDS-PAGE.

3.2.8 Large-scale protein expression

E. coli cells were grown in 2 L terrific broth supplemented with 50 µg/ml kanamycin at 37 °C with shaking at 250 rpm until the optical density at 600nm reached 1.0. The recombinant Pin1 proteins were then induced with 0.4 mM IPTG for 4 hr. *E. coli* were harvested by centrifugation at 4600×g for 30 min and resuspended in 30 ml cold sonication buffer (25 mM Tris-HCl (pH8.0), 0.5 M NaCl, 10mM β-mercaptoethanol, and 1% (v/v) Tween-20). The cells were sonicated on ice for 10 min at 30 s burst cycles at 300 W with a 30 s cooling period between each burst. The cleared lysate were obtained by ultra-centrifugation at 18,000×g for 30 min followed by an additional step of filtering through 0.45 µm syringe filters. The cleared lysate was then ready for protein purification.

3.2.9 Protein purification

3.2.9.1 Gel filtration (HiPrep 26/60 Sephacryl S-200 High Resolution)

Bacterial crude lysate was loaded onto a HiPrep 26/60 Sephacryl S-200 High

Resolution column equilibrated in an elution buffer containing10 mM HEPES-Na^+ (pH 7.5), 100 mM NaCl, and 1 mM DTT, with a flow rate of 1.3 ml/min controlled by a peristaltic pump. Fractions of 6 ml were collected and the protein content was monitored by a spectrophotometer at 280 nm. Pin1-containing fractions were identified by SDS-PAGE and Western blot. The positive fractions were pooled together for the second step of purification.

3.2.9.2 Ion-exchange chromatography

Pin1-containing fractions from gel filtration described above were subjected to UNO ion exchange S-6 column (column volume = 6 mL) equilibrated in Buffer A (10 mM HEPES-Na+ (pH 7.5), 100 mM NaCl) with a flow rate of 1 ml/min in a fast performance liquid chromatography (FPLC) system (Biologic DuoFlow™ 40 System, Bio-Rad, CA, USA). After injection of sample, 4 column volume of 24 mL of Buffer A was allowed to flow isocratically for the binding of proteins unto the cation ion-exchanger. Salt gradient from 0 % to 100 % Buffer B (10 mM HEPES-Na^+ (pH 7.5), 1 M NaCl) in 60 ml was performed for protein elution and fractions of 2 ml were collected. The fractions were analyzed for Pin1 by SDS-PAGE and Western blot. To optimize the protein purification, pH or ionic strength of Buffer A and B were varied.

To complement the ion-exchange chromatography, CHT-I column was employed. Protein sample after gel filtration was loaded onto the column equilibrated with Buffer C (10 mM sodium phosphate (pH 6.8)) with a flow rate of 1 ml/min. After injection of sample, 3 column volume of Buffer C was allowed to flow isocratically

for the binding of proteins onto the column matrix. Salt gradient from 0 % to 100 % Buffer D (500 mM sodium phosphate (pH 6.8) in 60 ml was performed for protein elution and 2 ml fractions were collected. The fractions were analyzed for Pin1 by SDS-PAGE and Western Blot.

3.2.9.3 His-tag fusion protein purification and gel filtration (HiLoad 16/60 Superdex 75 Prep Grade column)

Bacterial crude lysate was incubated with 2.5 ml Ni-NTA agarose bead slurry (Qiagen, Hilden, Germany) with gentle shaking at 4 °C for 3 hr and loaded into an empty glass Econo-Column column (2.5 cm × 10 cm, Bio-Rad, CA, USA). The recombinant proteins were eluted with 10 ml elution buffer (sonication buffer minus Tween-20 and supplemented with 250 mM imidazole) after washing with 20 ml wash buffer (sonication buffer minus Tween-20 and supplemented with 5 mM imidazole). To cleave 6X His-tag from the fusion protein, the eluted protein was incubated with thrombin (5U per mg protein) (Sigma, St. Louis, MO, USA) at 4 °C for 18 hr. To further purify, the cleaved fraction was fractionated by a HiLoad 16/60 Superdex 75 Prep Grade gel filtration column (Pharmacia, New Jersey, USA) equilibrated in elution buffer containing 5mM HEPES-Na^+ (pH 7.5), 100 mM NaCl, and 1 mM DTT with a flow rate of 1 ml/min. Fractions of 1 ml were collected. Pin1-containing fractions were pooled and concentrated to at least 100 mg/ml with an Amicon Ultra-15 centrifugal unit (Millipore, Bedford, MA) with a molecular mass cutoff at 5 kDa. The purified Pin1 protein was stored at -80 °C for further application.

3.2.10 Protein concentration assay

Pin1 protein concentrations were quantified using the Bradford method (Bradford, 1976). Bovine serum albumin (BSA) was used as the protein standard, ranging from 0-10 μg/ml. 800 μl of the protein standards or protein samples was mixed with 200 μl of the Bradford protein assay reagent from Bio-Rad (CA,USA), and incubated at room temperature for 10 min. The absorbance was then read at wavelength of 595 nm and the protein concentration in the samples was determined by comparing to the BSA standard curve.

3.2.11 Agarose gel electrophoresis

Agarose gels were cast with the Bio-Rad gel casting system. Typically, for most Pin1 clones, the gels contain 1 % (w/v) agarose in TAE buffer (40 mM Tris base, 20 mM acetic acid, 1mM EDTA pH 8.0) supplemented with 0.5 μg/ml ethidium bromide. DNA samples were mixed with 6X sample buffer (10 mM Tris-HCl (pH 7.6), 0.03 % (w/v) bromophenol blue, 0.03 % (w/v) xylene cyanol, 60 % (v/v) glycerol, and 60 mM EDTA) and loaded onto the gels. Gel electrophoresis was typically carried out in TAE buffer at a constant voltage of 100 V for 40 min.

3.2.12 Sodium dodecyl sulphate polyacrylamide gel electrophoresis (SDS-PAGE)

SDS-PAGE gels were cast with the Bio-Rad miniprotein III gel casting system. The resolving gel contains 10 % of acrylamide/bisacrylamide mixture (30% with a ratio of 29:1) in 0.375 M Tris-HCl (pH 8.8) and 0.1 % SDS. The stacking gel contains 4 % acrylamide/bisacrylamide in 0.125 M Tris-HCl (pH 6.8) and 0.1 % SDS.

Polymerization was induced by the addition of 1 % ammonium persulphate (APS) and N,N,N,N,-Tetramethyl-Ethylenediamine (TEMED). Protein samples were mixed with 2X SDS sample buffer (100 mM Tris-HCl (pH 6.8), 4 % (w/v) SDS, 200mM dithiothreitol (DTT), 20 % (v/v) glycerol and 0.2 % (w/v) bromophenol blue) and heated at 95 ºC for 5 min before loading onto the gel. Gel electrophoresis was typically carried out in Tris-Glycine buffer (25 mM Tris-base, 192 mM Glycine and 0.1 % (w/v) SDS) at a constant voltage of 120 V for 2 h.

3.2.13 Coomassie blue staining and destaining of SDS-PAGE gel

The SDS-PAGE gel is stained in Coomassie Brilliant Blue staining solution (0.25 % (w/v) Coomassie Blue R-250 in 50 % methanol and 10 % acetic acid) at room temperature with shaking for 30 min. The gel is then destained with destaining buffer (30 % methanol and 10 % acetic acid) until the background staining was cleared.

3.2.14 Western blot analysis

After SDS-PAGE, the separated proteins were transferred onto a PVDF membrane. The transfer was carried out in transfer buffer (0.3 % (w/v) Tris-base, 1.4 % (w/v) glycine and 20% (v/v) methanol) with a Bio-Rad semi-dry transfer apparatus at constant current of 180 mA for 45 min (typically for Pin1 protein). The membrane was then blocked overnight with 5 % skim milk plus 1 % BSA in TBST (25mM Tris-base (pH 7.4), 137 mM NaCl, 0.05 % (v/v) Tween-20) at 4ºC followed by incubations with specific primary antibodies for 1 hr and appropriate secondary antibodies conjugated with horse radish peroxidase (HRP) for 1 hr. All the antibodies

were diluted in TBST. Membranes were washed three times with TBST after each antibody incubation step. Immunoreactive signals were visualized using a chemiluminescent substrate (Supersignal West Pico Chemiluminescence Substrate, Pierce) and X-ray films (Fuji SuperRX Film, Fuji, Japan), which were developed using a Kodak X-ray film processor.

3.2.15 Mass spectrometry (MS)

Protein bands were excised from Coomassie Blue-stained SDS-PAGE gel and sent to Protein and Proteomic Center (PPC) (Department of Biological Sciences, National University of Singapore) for mass spectrometry analysis.

3.2.16 Circular dichroism (CD)

CD measurements were conducted using a Jasco J-810 spectropolarimeter (Tokyo, Japan) equipped with a Neslab RIE-111 water-circulated thermal controller using 1 mm path-length cuvettes with a 0.1 nm spectral resolution. The samples with a protein concentration of 0.5 mg/ml were prepared in 5mM HEPES-Na^+ (pH7.5) with or without supplementing 10mM phosphate. For wavelength scans in the far UV regions (260-190 nm), each spectrum was obtained at 20 °C by averaging three successive accumulations with a wavelength step of 0.2 nm at a rate of 20 nm/min, response time 1 s, and band width 1 nm. All spectra were corrected for buffer contributions and converted to mean residue ellipticity ([Θ]) using the following equation:

$$[\Theta] = (MRW.\theta_\lambda)/10.l.c$$

where MRW is the mean residue weight (a value of 111.3 was used for the WT), θ_λ is the measured ellipticity in degree at wavelength λ, l is the cuvette path length (0.1 cm), and c is the protein concentration in mg/ml. The secondary structure analysis was performed using the K2d programme, which provides an interactive web site server allowing the deconvolution of data from CD spectroscopy experiments (www.embl-heidelberg.de/~andrade/k2d/).

Thermal stability of proteins were analyzed by monitoring the changes in ellipticity at 202 nm continuously at the temperature range between 20 °C and 90 °C, with heating rates of 1.5 K/min. The temperature at which half of the protein molecules were unfolded was recorded as the melting temperature (Tm).

3.2.17 Protein crystallization and data collection

Protein crystals were obtained by hanging drop vapor diffusion method (McPerson, 1982) at either room temperature or 4 °C by mixing 1µl of concentrated Pin1 mutant with 1 µl of a reservoir solution. A series of conditions were screened by varying protein concentration (ranging from 20 to 200 mg/ml), temperature (room temperature or 4°C) and the reservoir solution. Conditions of the reservoir solutions are summarized in Table 3-2. These conditions were modified from crystallization conditions of wild type Pin1 or Pin1 homologue published by Ranganathan *et al*., Verdecia *et al.* and Li *et al*. (Li et al., 2005; Ranganathan et al., 1997; Verdecia et al., 2000).

Table 3-2: Conditions of the crystallization reservoir solutions.

100 mM HEPES-Na^+ (pH7.5) 2.0 M $(NH_4)_2SO_4$ 1% PEG400 1 mM DTT	100 mM MOPS-Na^+ (pH7.0) 28% PEG8000 2 mM DTT	100 mM HEPES-Na^+ (pH7.5) 20% PEG8000 2 mM DTT
100 mM HEPES-Na^+ (pH7.5) 2.2 M $(NH_4)_2SO_4$ 1% PEG400 1 mM DTT	100 mM MOPS-Na^+ (pH7.0) 30% PEG8000 2 mM DTT	100 mM HEPES-Na^+ (pH7.5) 22% PEG8000 2 mM DTT
100 mM HEPES-Na^+ (pH7.5) 2.5 M $(NH_4)_2SO_4$ 1% PEG400 1 mM DTT	50 mM KH_2PO_4 (pH7.5) 10% PEG8000 0.2 M Ammonium acetate	100 mM HEPES-Na^+ (pH7.5) 24% PEG8000 2 mM DTT
100 mM HEPES-Na^+ (pH7.5) 2.0 M $(NH_4)_2SO_4$ 1% PEG400 1 mM DTT	50 mM KH_2PO_4 (pH7.5) 12% PEG8000 0.2 M Ammonium acetate	100 mM HEPES-Na^+ (pH7.5) 26% PEG8000 2 mM DTT
100 mM MOPSO-Na^+ (pH7.0) 20% PEG8000 2 mM DTT	50 mM KH_2PO_4 (pH7.5) 14% PEG8000 0.2 M Ammonium acetate	100 mM HEPES-Na^+ (pH7.5) 28% PEG8000 2 mM DTT
100 mM MOPSO-Na^+ (pH7.0) 22% PEG8000 2 mM DTT	50 mM KH_2PO_4 (pH7.5) 16% PEG8000 0.2 M Ammonium acetate	100 mM HEPES-Na^+ (pH7.5) 30% PEG8000 2 mM DTT
100 mM MOPSO-Na^+ (pH7.0) 24% PEG8000 2 mM DTT	50 mM KH_2PO_4 (pH7.5) 18% PEG8000 0.2 M Ammonium acetate	100 mM MOPS-Na^+ (pH7.0) 2.0 M $(NH_4)_2SO_4$ 1% PEG400 1 mM DTT
100 mM MOPSO-Na^+ (pH7.0) 26% PEG8000 2 mM DTT	50 mM KH_2PO_4 (pH7.5) 20% PEG8000 0.2 M Ammonium acetate	100 mM MOPS-Na^+ (pH7.0) 2.2 M $(NH_4)_2SO_4$ 1% PEG400 1 mM DTT
100 mM MOPSO-Na^+ (pH7.0) 28% PEG8000 2 mM DTT	100 mM HEPES-Na^+ (pH7.5) 2.0 M $(NH_4)_2SO_4$ 1% PEG400 2 mM DTT	100 mM MOPS-Na^+ (pH7.0) 2.5 M $(NH_4)_2SO_4$ 1% PEG400 1 mM DTT
100 mM MOPSO-Na^+ (pH7.0) 30% PEG8000 2 mM DTT	100 mM HEPES-Na^+ (pH7.5) 2.5 M $(NH_4)_2SO_4$ 1% PEG400 2 mM DTT	100 mM MOPSO-Na^+ (pH7.0) 2.0 M $(NH_4)_2SO_4$ 1% PEG400 1 mM DTT
100 mM MOPS-Na^+ (pH7.0) 20% PEG8000	100 mM HEPES-Na^+ (pH7.5) 2.0 M $(NH_4)_2SO_4$	100 mM MOPSO-Na^+ (pH7.0) 2.2 M $(NH_4)_2SO_4$

2 mM DTT	2% PEG400 1 mM DTT	1% PEG400 1 mM DTT
100 mM MOPS-Na^+ (pH7.0) 22% PEG8000 2 mM DTT	100 mM HEPES-Na^+ (pH7.5) 2.5 M $(NH_4)_2SO_4$ 2% PEG400 1 mM DTT	100 mM MOPSO-Na^+ (pH7.0) 2.5 M $(NH_4)_2SO_4$ 1% PEG400 1 mM DTT
100 mM MOPS-Na^+ (pH7.0) 24% PEG8000 2 mM DTT	100 mM HEPES-Na^+ (pH7.5) 2.0 M $(NH_4)_2SO_4$ 2% PEG400 2 mM DTT	
100 mM MOPS-Na^+ (pH7.0) 26% PEG8000 2 mM DTT	100 mM HEPES-Na^+ (pH7.5) 2.5 M $(NH_4)_2SO_4$ 2% PEG400 2 mM DTT	

The optimal crystallization condition for wild-type Pin1 and its mutants (R14A, S16E, F25A, S32A, W34A, K63A, C113A, M130A) was at 4 °C by mixing 1μl of 100-200 mg/ml concentrated protein with 1 μl of a reservoir solution consisting of 2.5 M ammonium sulfate, 100 mM HEPES-Na^+ (pH 7.5), 2 % PEG400 (Sigma), and 2 mM DTT. Protein crystals appeared within 1 week and further grew into appropriate sizes of ~0.1 mm within 3 weeks. Crystals were cryoprotected in 40 % (v/v) PEG400, 50mM HEPES-Na^+ (pH 7.5), and 1mM DTT and frozen in a stream of 100K nitrogen gas (Oxford Cryosystems, Oxford, UK). X-ray diffraction data were collected using an R-axis IV++ image plate detector mounted on a RU-H3RHB rotating anode generator (Rigaku Corp., Tokyo, Japan). Synchrotron data was collected at beamline X25, National Synchrotron Light Source, Brookhaven National Laboratory using a Q315 CCD detector (Area Detector Systems Corp., Poway, CA, USA). All diffraction images were integrated and scaled by using the program HKL2000 (Otwinowski and Minor, 1997). The Pin1 mutant structures were solved by the molecular replacement analysis, using the program MOLREP (Vagin and Teplyakov, 1997) from the CCP4

program package (Collaborative Computational Project Number 4, 1994), with the structure of Pin1 WT as the search model [PDB code: 1PIN]. All stages of crystallographic refinement were carried out with the program CNS (Brunger et al., 1998) and model building was performed with the program O (Jones et al., 1991). Molecular figures were generated in PyMOL (DeLano, 2002) or MOLMOL (Koradi et al., 1996).

3.2.16 Cell Culture

HeLa and CHO mammalian cell lines were maintained in Dulbeco's Minimum Eagles Medium (DMEM) supplemented with 10% fetal bovine serum (FBS) and 1% antibiotics penicillin and streptomycin at 37 ºC under 5% CO_2 and saturated moisture.

3.2.17 Transient transfection and cell cycle synchronization

The EGFP-Pin1 constructs (in mammalian expression vector pEGFP-C1) were transfected into HeLa and CHO cells. Cells were plated onto cover slips in 12-well plates and grown for 24 hr to a confluency of 50-60%. Lipofectamine 2000 (Invitrogen Pte Ltd, Carlsbad, CA, USA) and Effectene Invitrogen Pte Ltd, Carlsbad, CA, USA) were used as transfection reagents for HeLa cells and CHO cells, respectively, according to the manufacturers' instructions. Cells were harvested for microscopic examination 20 hr after transfection or were treated with drugs 12 hr after transfection. To arrest cells at G_0 phase, cells were starved in serum-free DMEM for 40 hr. To arrest cells at early S phase, cells were treated with 2mM thymidine for 16 hr. Cells were then released to grow for 9 hr followed by 2mM thymidine

treatment for another 15 hr. To arrest cells at S phase, cells were treated with 4mM hydroxyurea for 40 hr. To arrest cells at G2/M phase, cells were treated with 2mM thymidine for 24 hr and released to grow for 3 hr followed by treatment with 100ng/ml nocodazole for 12 hr.

3.2.18 Immunofluorescence staining and fluorescence microscopy

Cells grown on cover slips were fixed in 4% paraformaldehyde for 20 min at room temperature. Cells were then rinsed three times with PBS and stained with DAPI for 20 min followed by washing with PBS for three times. The cells were then analyzed by fluorescent microscopy for EGFP-Pin1 cellular localization. For colocalization of EGFP-Pin1 with centrosome, cells were fixed with 4% paraformaldehyde for 15 min at room temperature and then with cold pure methanol for 10 min. After washing with three times PBS, cells were then stained for centrosomes with anti γ-tubulin antibodies (dilution 1:200) (Sigma) and were stained for nucleus with DAPI followed by imaging under a fluorescent microscope (Zeiss Inverted Microscope, Jena, Germany) (Suizu et al., 2006).

CHAPTER 4: RESULTS AND DISCUSSION

4.1 Molecular cloning and protein expression/purification using the pET42a+ expression vector system

4.1.1 Protein purification strategy I

Pin1 protein was generally expressed as His-tagged fusion protein in large-scale protein preparation system for structural studies purposes (Bayer et al., 2003; Ranganathan et al., 1997; Verdecia et al., 2000). We first attempted to express Pin1 without any tag, with the following reasonings. First, Pin1 is a relatively small molecule with a molecular weight of 18,000 Dalton and it is highly soluble. In past experience, Pin1 protein was easily expressed in *E. coli*. Second, it would be preferable to use the native protein without any additional sequences to ensure that the protein structure is not locally or globally affected. Thus, the first purification strategy was to express the proteins in *E. coli* BL21 (DE3) strain, followed by purification using gel filtration and ion-exchange chromatography (Figure 4-1).

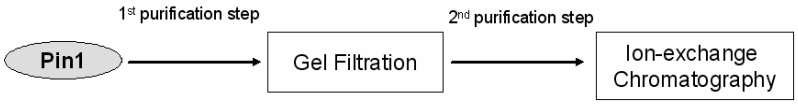

Figure 4-1: Protein purification strategy I.

4.1.2 Molecular cloning of Pin1

Pin1 cDNA was cloned into the pET42a+ expression vector at the cloning sites, Nde I and Sal I, as described in the "Materials and methods" session. First, Pin1 wild type and various mutant cDNAs S16A, S16E, W34A, K63A, as well as the the double

mutant R68A/R69A (generous gifts from Prof. Lu Kun Ping's lab) were used as templates for PCR to generate various inserts flanked with Nde I and Sal I linkers. Various specific bands of approximately 500 bp were obtained (Figure 4-2 A). These were excised from agarose gels, followed by DNA fragment purification and restriction enzyme digestions with Nde I and Sal I. The DNA fragments were then ligated with Nde I- and Sal I-digested pET42a+ vector, followed by transformation into *E. coli* BL21 strain. Most of the transformant colonies selected showed specific bands of approximately 500 bp when analyzed by PCR (Figure 4-2 B&C). Furthermore, restriction digests also retrieved DNA inserts of approximately 500 bp (Figure 4-2 B&C). Thus, these colonies bore the recombinant plasmids. Sequences of these inserts were further confirmed by DNA sequencing and the mutated residues for W34A, K63A, S16A, S16E, and R68A/R69A were thus verified (data not shown).

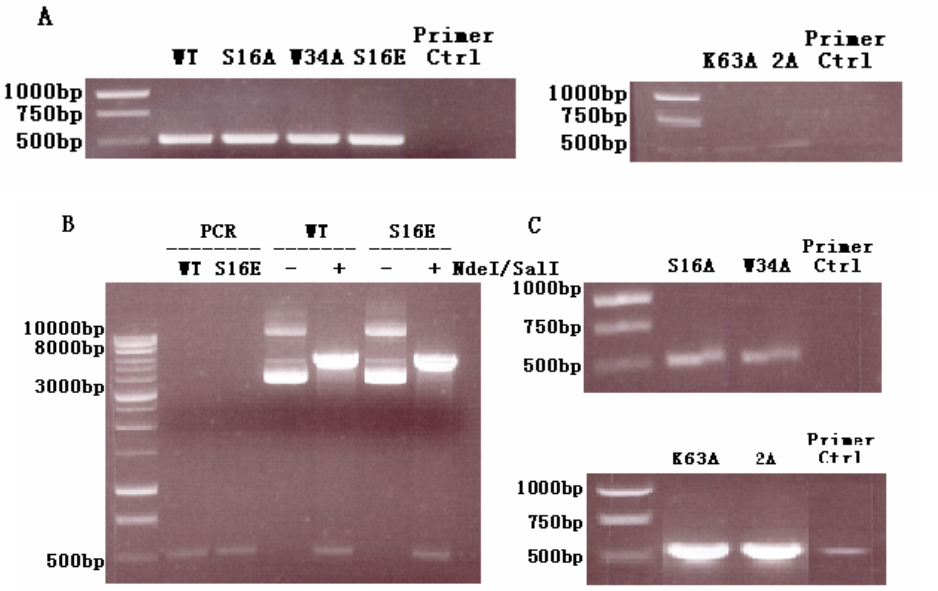

Figure 4-2: Molecular cloning of Pin1-WT and mutants. (A) Pin1-WT and mutants flanked with Nde I and Sal I linkers were obtained via PCR, with an expected size of 513 bp. 2A denotes the double mutant, R68A/R69A. (B) PCR and restriction digest analysis of BL21 colonies transformed with recombinant Pin1 wild-type or S16E constructs. (C) PCR analysis of Pin1 mutants S16A, W34A, K63A, and R68A/R69A.

4.1.3 Site-directed mutagenesis

Other Pin1 mutants besides were generated by site-directed mutagenesis as described in the "materials and methods" session. Figure 4-3 shows representatively the PCR and restriction digestion analysis of the selected transformants. Most of the transformants selected contain Pin1 recombinant plasmid. Mutant constructs of R14A, R17A, S32A, F25A, C113A, H59A, H157A, S154A, L122A, and M130A were all successfully obtained.

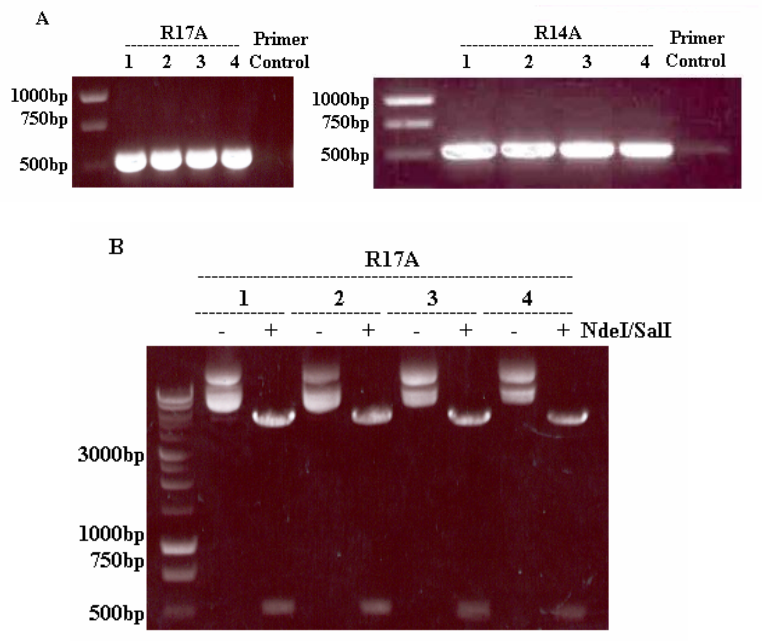

Figure 4-3: Site-directed mutagenesis. (A) PCR analysis of BL21 colonies transformed with Pin1 mutant constructs, R17A and R14A, in site-directed mutagenesis. (B) Restriction digest analysis for R17A. Numbers (1-4) on the top of the lanes denoted different colonies selected for analysis.

4.1.4 Pin1 protein expression

Wild type Pin1 and mutant recombinant proteins were expressed in a small scale (10 ml) as described in the "materials and methods" session. As representatively

shown in Figure 4-4, all the proteins were highly expressed after IPTG induction. Moreover, all the proteins were highly soluble and were found in the lysate supernatant.

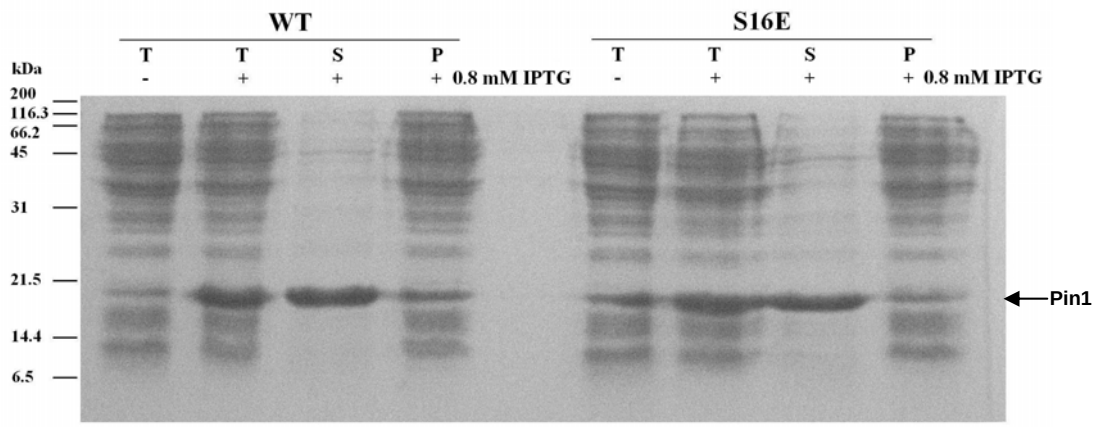

Figure 4-4: Pin1 protein expression. *E.coli* BL21 (DE3) was induced with 0.8 mM IPTG. *E. coli* were then lysed and separated as supernatant and pellet, followed by SDS-PAGE analysis. Coomassie blue staining showed that Pin1 wild type and mutant proteins were highly soluble. T: Total protein; S: Supernatant; P: Pellet.

4.1.5 First step of Pin1 and mutant protein purification—gel filtration chromatography

E. coli lysates prepared in large scales (1 l) were passed through a HiPrep 26/60 Sephacryl S-200 High Resolution gel filtration column with a flow rate of 1.5 ml/min. The elution profile of a typical chromatographic experiment was shown in Figure 4-5. As verified by SDS-PAGE with Coomassie blue staining and Western blot, Pin1 protein was eluted between elution volumes of 180 ml and 210 ml. These fractions were thus pooled together for the second step of purification.

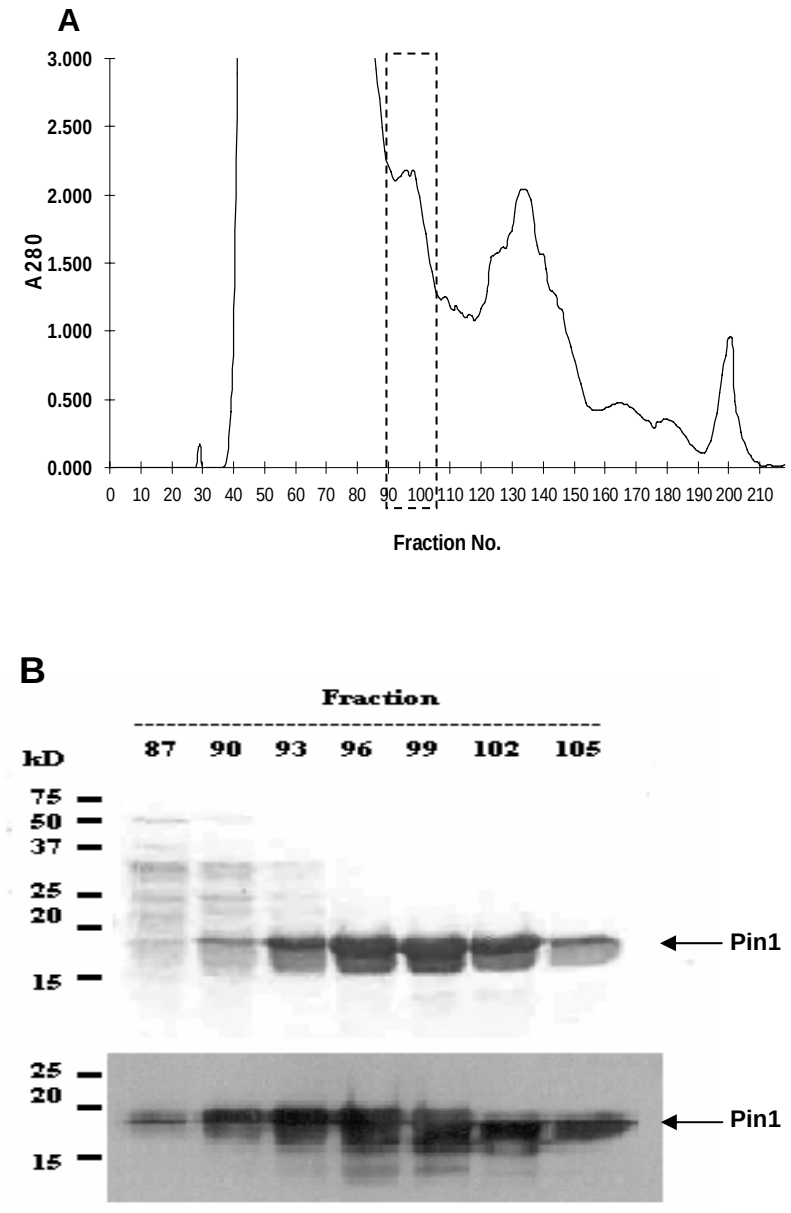

Figure 4-5: Gel filtration chromatography. (A) Elution profile of gel filtration for Pin1-WT. Fractions 90-105 (180-210 ml) contained the Pin1 recombinant protein, as shown by coomassie blue staining (B, upper panel) and western blot (B, lower panel). All Pin1 mutants showed a similar elution profile (not shown). Column used: HiPrep 26/60 Sephacryl S-200 High Resolution; flow rate: 1.5ml/min.

4.1.6 Second step of purification—ion-exchange chromatography

Fractions from the previous step of gel filtration were passed through an S-6 cation-exchange chromatography column. The predicted isoelectric point (pI) of Pin1 is 8.9. In a buffer condition of pH 7.5, Pin1 should be positively charged and bind to a cation-exchanger. However, Pin1 failed to bind to the cation-exchanger at all and was found in the void volume, as detected by SDS-PAGE and Western blot (Figure 4-6 A). Further attempts were made by increasing the solvent buffering capacity from 10 mM to 20 mM HEPES-Na^+ (pH 7.5), and by decreasing the flow rate from 1 ml/min to 0.6 or 0.3 ml/min. In these attempts, a portion of Pin1 bound to cation-exchanger and was eluted out at the early part of a salt gradient. However, there were still a considerable portion of Pin1 (approximately 30%) that had remained unbound in the void volume, as gauge by Western blot (Figure 4-6 B). Further increasing of buffering capacity to 50 mM HEPES-Na^+ slightly improved Pin1 binding to the cation exchanger (data not shown). Attempts were made to further optimize the cation binding efficiency at pH 6.8. With both 10 mM and 50 mM HEPES-Na^+. However, we observed that a considerable portion of Pin1 (approximately 30%) still could not bind to the cation exchanger and was eluted out in the void volume (Figure 4-6 C). Further decreasing the pH to pH 5.5 totally abolished Pin1 binding to the cation exchanger (data not shown).

Interestingly, when the protein eluted in void volume was loaded onto the cation-exchange column again, 60-70% of Pin1 would then bind to the

cation-exchanger (data not shown). When Pin1 was loaded unto a quarternary ammonium Q column, which is an anion-exchange column, a portion of Pin1 also remained unbound in the void volume (data not shown). Nevertheless, the two populations of Pin1 (Pin1 in void volume and Pin1 eluted at the early salt gradient respectively) were both verified as Pin1 protein by mass spectrometry (MS) (data not shown). Furthermore, MS sequencing results showed oxidation of the Pin1 proteins at considerable number of methionine residues. Oxidation of methionine residues could therefore have altered the net charge, thus the pI, of the protein. To attempt to remedy this, *E. coli* cells were lysed with a buffer containing a reducing agent (1mM DTT) to prevent protein oxidation. The lysate was loaded onto the gel filtration column with a mobile phase of 10 mM HEPES-Na^+, pH 7.5, supplemented with 1mM DTT. However, a subpopulation of Pin1 protein still did not bind to the cation-exchange column (data not shown). Thus, oxidation of the protein could not fully explain the poor binding and the existence of the subpopulations of Pin1. Pin1 protein appears therefore to exist in equilibrium between the two populations, which exhibit different surface charges.

The nature of the two populations of Pin1 was not clear and taking either population while ignoring the other would not be desirable. Thus, a ceramide hydroxyapatite (CHT) column was used in place of the ion-exchange column. Pin1 fractions from a HiPrep 26/60 Sephacryl S-200 High Resolution gel filtration column were loaded onto the CHT column as described in the "Materials and methods"

session. As seen in Figure 4-6 D, Pin1 bound tightly to the column and no Pin1 was detected in the void volume (as verified by Western blot). Pin1 was eluted out at the early part of a salt gradient, in fractions 17 to 23. However, in these fractions, three close peaks were observed. In view of the uncertainties observed, we shifted to another purification strategy, as described in the next session.

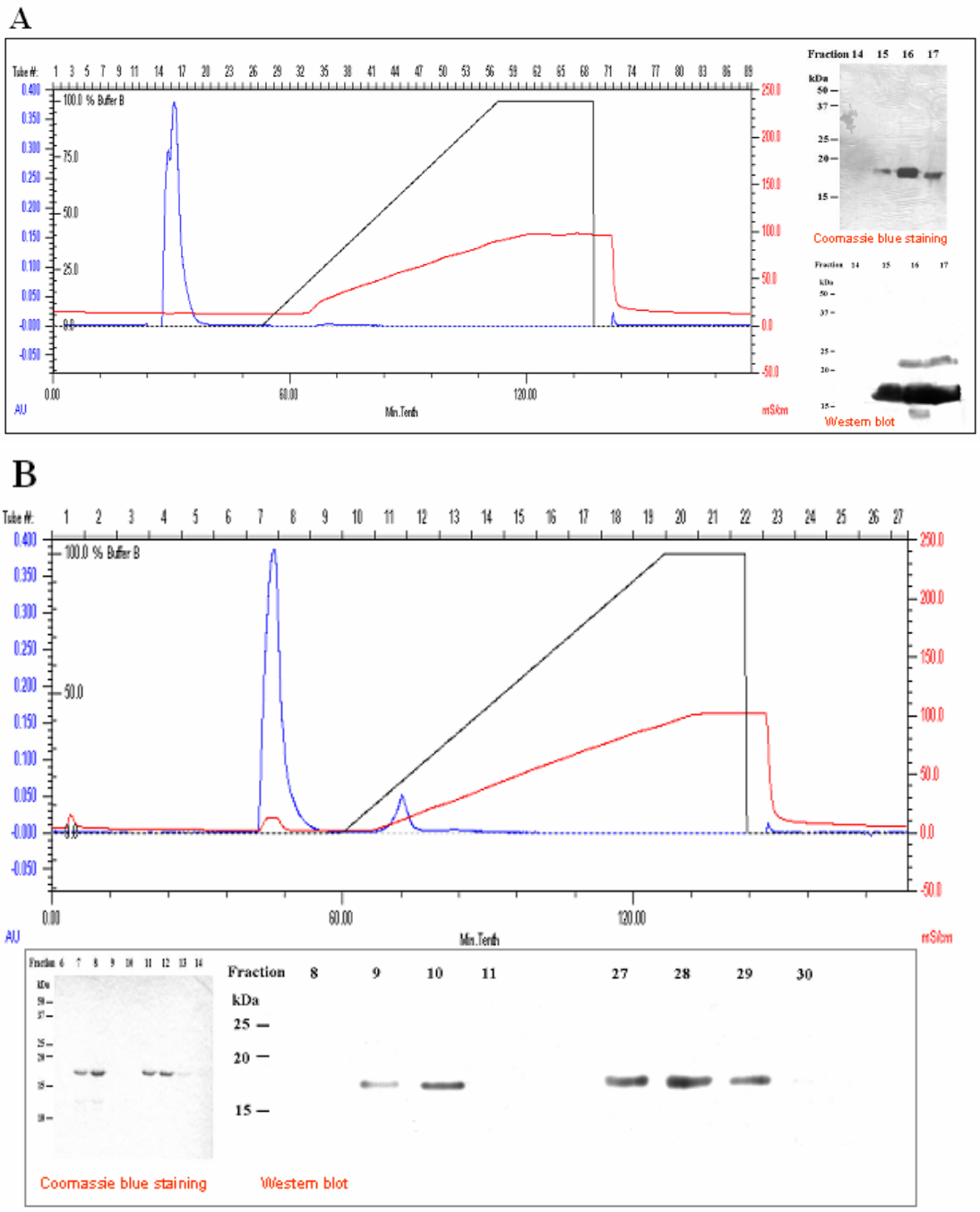

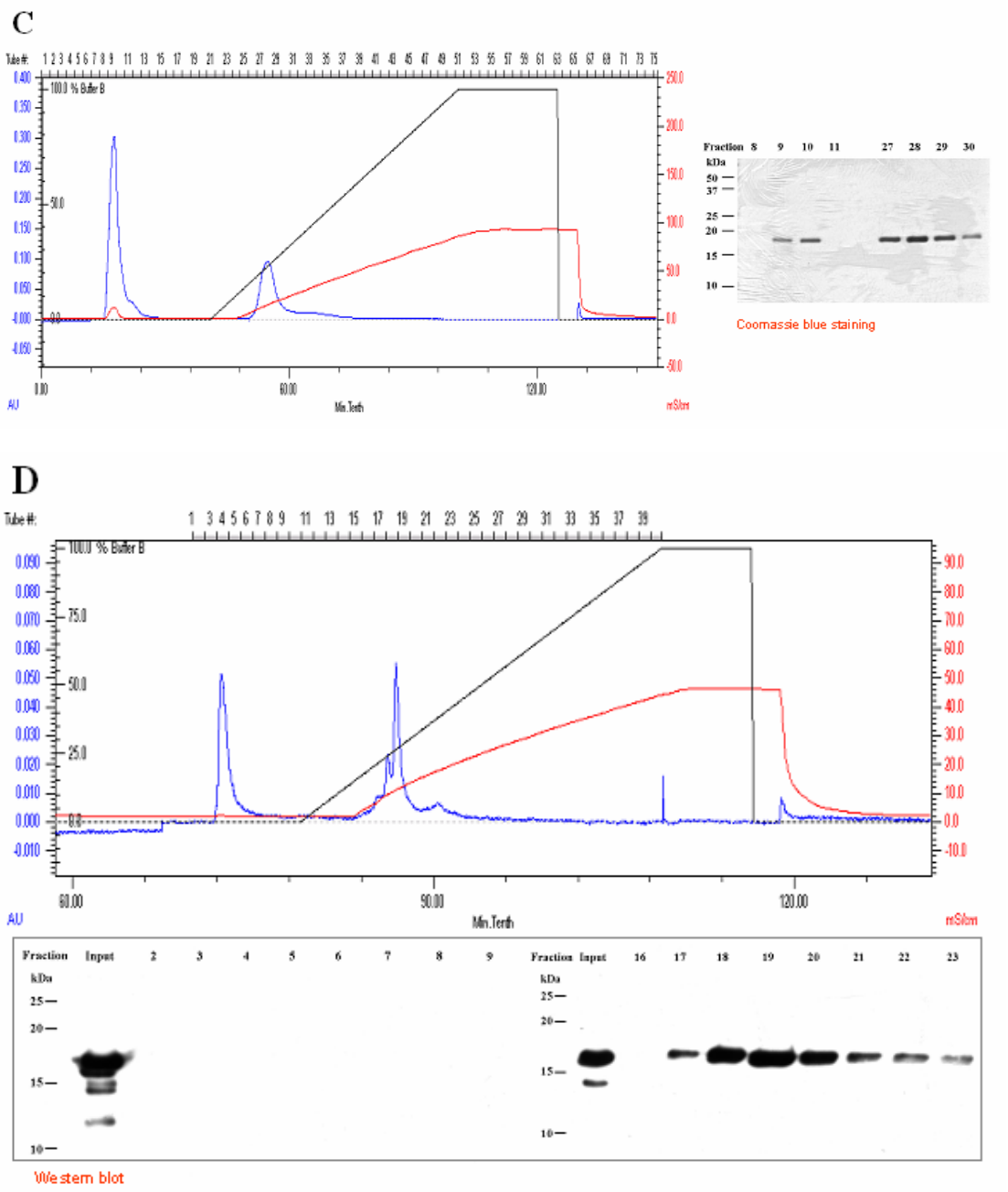

Figure 4-6: Ion exchange chromatography elution profiles and fraction analysis. (A) S-6 column; buffer system: 10 mM Hepes-Na+ pH 7.5; flow rate: 1 ml/min. (B) S-6 column; buffer system: 20 mM Hepes-Na+ pH 7.5; flow rate: 0.6 ml/min. (C) S-6 column; buffer system: 10 mM Hepes-Na+ pH 6.8; flow rate: 0.6 ml/min. (D) CHT column; buffer system: 10 mM sodium phosphate pH 6.8; flow rate: 1 ml/min. Blue lines, red lines, and black lines denote absorbancy at 280 nm, conductivity, and percentage of Buffer B (see "materials and methods"), respectively. All Western blots were blotted with anti-Pin1 antibody. Samples loaded were either of wild type Pin1 or S16E mutant protein.

4.2 Molecular cloning and protein expression/purification using the pET28b+ expression vector system

4.2.1 Protein purification strategy II

In this alternative purification strategy, Pin1 protein was expressed as hexahistidine (His) -tag fusion protein and purified with Ni-NTA affinity chromatography specific for the His-tag. The His-tag was then thrombin-cleaved. The full-length Pin1 protein was further purified by the second step of gel filtration chromatography (Figure 4-7).

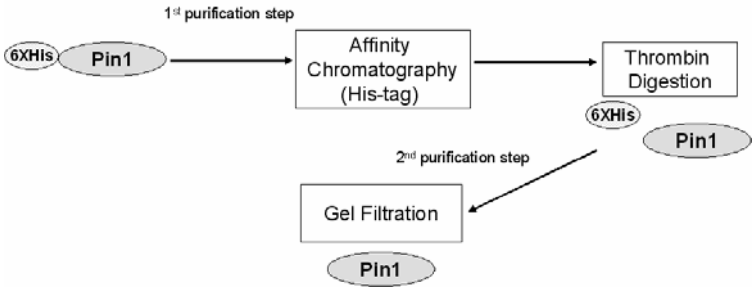

Figure 4-7: Protein purification strategy II.

4.2.2 Molecular cloning of His-Pin1 and protein expression

Pin1 wild type and mutant cDNAs were subcloned from the constructs in pET42a+ vector (from protein purification strategy I) into pET28b+ expression vector at cloning sites Nde I and Sal I, such that proteins expressed from the new constructs would be His-tagged at the N-terminus, partitioned by a thrombin cleavage site, as described in the "Materials and methods" session (cloning data not shown). Wild-type Pin1 as well as all the mutant recombinant proteins were highly expressed when induced with IPTG, as detected by SDS-PAGE and Western blot with specific

anti-Pin1 and anti-His antibodies where the wild type Pin1 recombinant prtein is shown as a representative (Figure 4-8). Moreover, the proteins were soluble and were predominantly found in the supernatant.

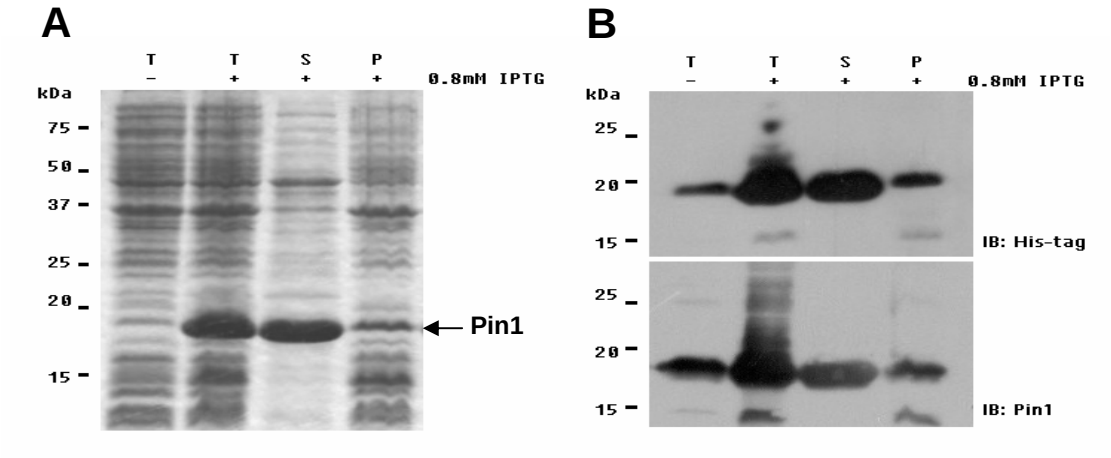

Figure 4-8: Expression of His-Pin1 fusion protein. Wild type Pin1 is shown as a representative. (A) Coomassie blue staining of SDS-PAGE gel. Pin1 protein was found in the supernatant. (B) Western blot analysis. Antibodies used were specific against His-tag (upper panel) or Pin1 (lower panel). T: Total protein; S: Supernatant; P: Pellet.

4.2.3 Protein purification—His-tag affinity chromatography and gel filtration

After induction with IPTG, cleared *E. coli* lysate was incubated with Ni-NTA agarose beads for 4 hours to allow His-tag fusion protein binding to the beads. The bound His-tag fusion protein was eluted with 250 mM imidazole after washing with 10 mM imidazole, as shown in Figure 4-9 A. The His-tag was then cleaved from the fusion protein by incubating with 5 U of thrombin per mg of protein at 4 ºC. Near complete cleavage was achieved after 18 h, as monitored by SDS-PAGE and Coomassie blue staining (Figure 4-9 B).

Thrombin digested Pin1 was then loaded onto a HiLoad Superdex 75 Prep Grade gel filtration column as described in the "Materials and methods". Pin1 was eluted out as a peak between 60 to 80 ml of elution volume (Figure 4-10 A&B). The Pin1 proteins (wild type and all the mutant proteins) were at least 98 % pure as verified by SDS-PAGE (Figure 4-10 C), and were ready for further structural and functional studies.

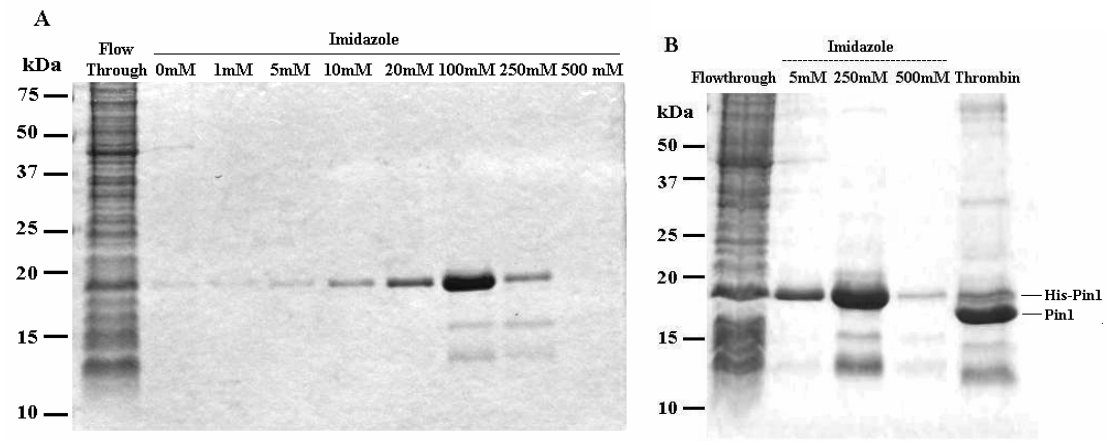

Figure 4-9: His-tag affinity chromatography of Pin1 recombinant protein. Wild type Pin1 is shown as a representative. All Pin1 mutants behave in a similar manner. (A) Elution of His-Pin1 from Ni^{+} beads. Bacterial lysate was incubated with Ni^{+} beads at 4 °C for 4 hours followed by stepwise elution with increasing concentration of imidazole. His-Pin1 started to be eluted out at 5 mM imidazole, as monitored by SDS-PAGE and Coomassie blue staining. (B) Elution of His-Pin1 from Ni+ beads and subsequent thrombin digestion. After washing with 5 mM imidazole, His-Pin1 was eluted with 250 mM imidazole followed by incubation with 5 U/mg of thrombin at 4 °C for 18 hours for the cleavage of His-tag from Pin1.

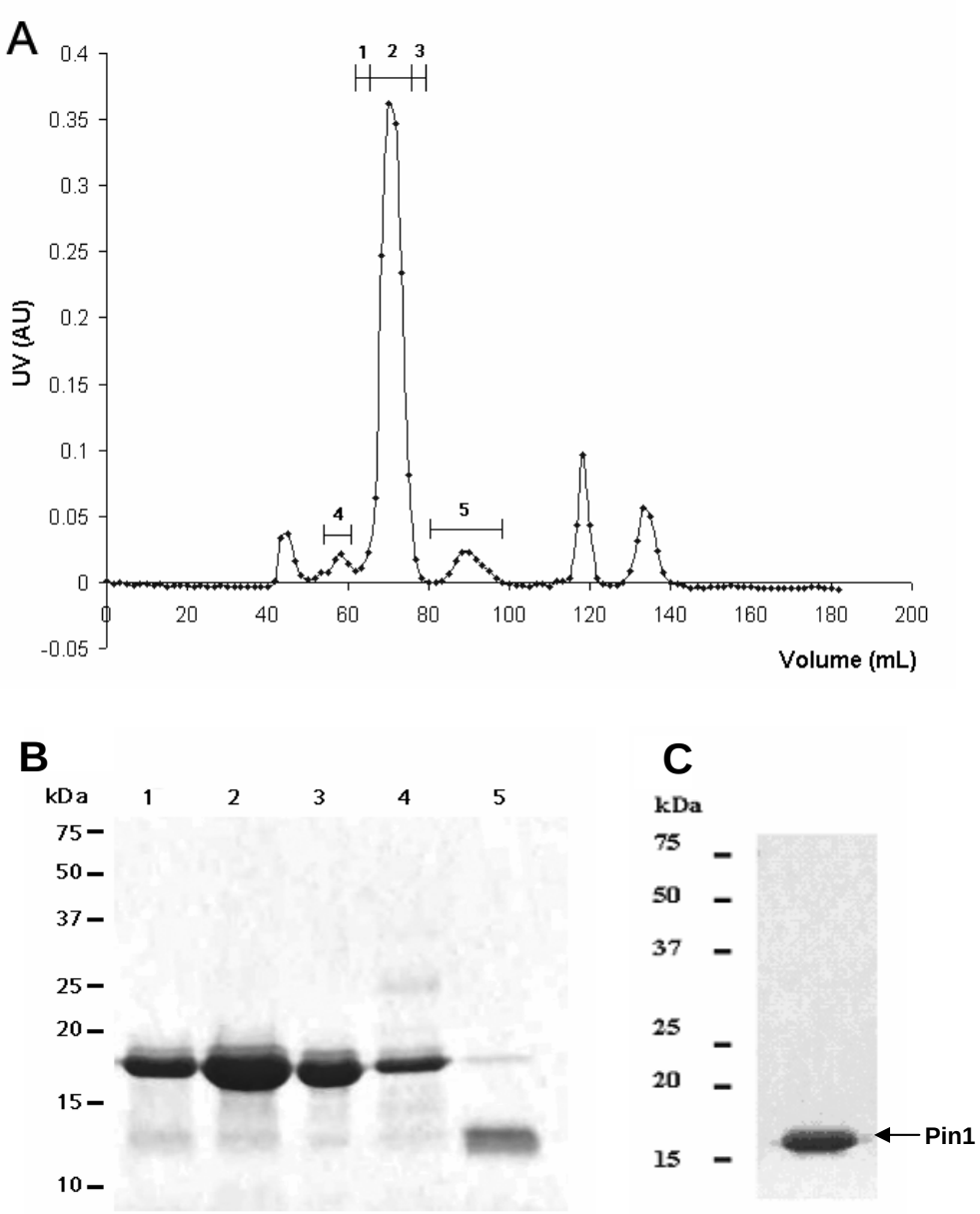

Figure 4-10: Protein purification by gel filtration chromatography. (A) A gel filtration chromatography elution profile. Protein sample was loaded onto a HiLoad Superdex 75 Prep Grade column and fractionated with a flow rate of 1 ml/min. Proteins at various peaks were analyzed by SDS-PAGE and Coomassie blue staining (B). (C) Final purity of the Pin1 protein verified with Coomassie blue staining.

4.3 Secondary structure elements of Pin1 as analyzed by circular dichroism (CD)

Pin1 proteins were first subjected to circular dichroism (CD) analysis to determine whether *E.coli* expressed Pin1s are well-folded. CD spectra of wild type

Pin1 in far-UV range (190-260 nm) exhibited a typical spectrum for a polypeptide with a mixture of α-helix and β-sheet (Figure 4-11). Data analysis using the K2d programme showed that wild type Pin1 contains 15 % and 35 % in the absence, and 7% and 42 % in the presence of phosphate, of α-helix and β-sheet, respectively (Table 4-1). However, both α-helix and β-sheet comprises 22 % respectively in a reported Pin1 crystal structure (PDB code: 1PIN). Thus, the CD analysis had underestimated α-helices but overestimated β-sheets. Indeed all the algorithms used to analyze CD data employ certain reference protein sets to estimate the secondary structure of the input protein. Drawbacks for each method exist. Nevertheless, all the mutants (such as S16A) analyzed showed similar percentage (ranging from 28.5 to 43.7 %) in the β-sheet component, suggesting that these have a similar folded structure with that of the wild type protein. Wild type Pin1 structure does not differ in the presence or absence of phosphate. However, interestingly, the mutants R17A, R68A/R69A, and M130A showed significant change in the percentage of β-sheets when phosphate was added. The R17A mutant had a decrease in the percentage of β-sheets by 10 %, whereas R68A/R69A and M130A had an increase in the percentage by 30 % and 29 %, respectively. From previous studies, the three basic residues Arg-17, Arg-68, and Arg-69 have been shown to be important for phosphate group binding by Pin1 with pSer/Thr-Pro motifs. Residue Arg-17 is involved in the WW domain's interaction with pSer5' in the CTD phosphopeptide (Verdecia et al., 2000), whereas Arg-68 and Arg-69 are residues in the tripartite basic cluster that serve as a selectivity filter for pSer/Thr-Pro motifs (Ranganathan et al., 1997). Hence, the CD data are in agreement

with the important role of these three basic residues in their interactions with the phosphate group in the pSer/Thr-Pro motifs. In addition, the residue Met-130 may also play a role in the phosphate binding in spite of residing in the hydrophobic pocket where the proline residue of the target motif is sequestered (Ranganathan et al., 1997). No studies have previously investigated the role of Met-130 in the regulatory mechanism of Pin1 in detail. Thus, Met-130 may be a new candidate residue important for regulating Pin1's phosphosubstrate recognition.

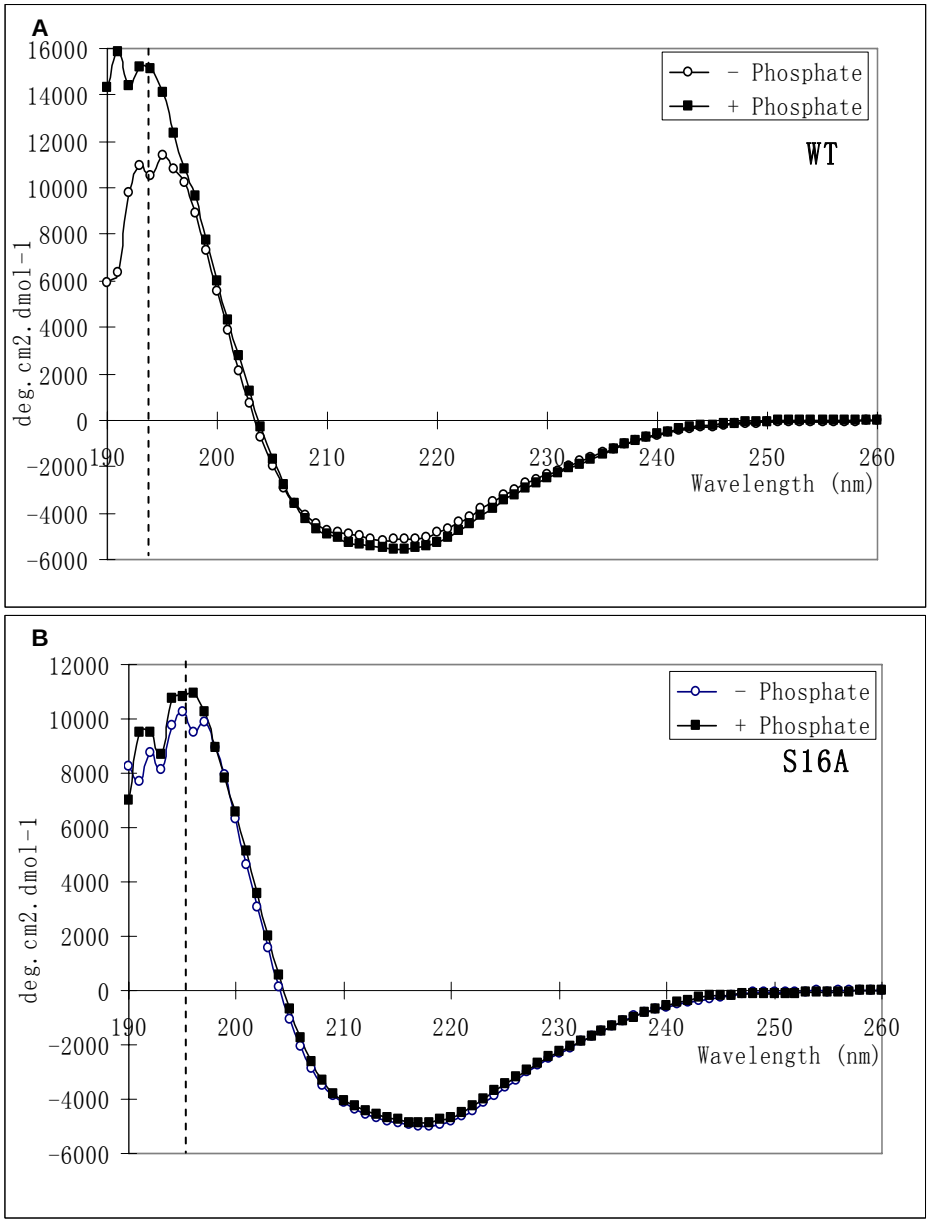

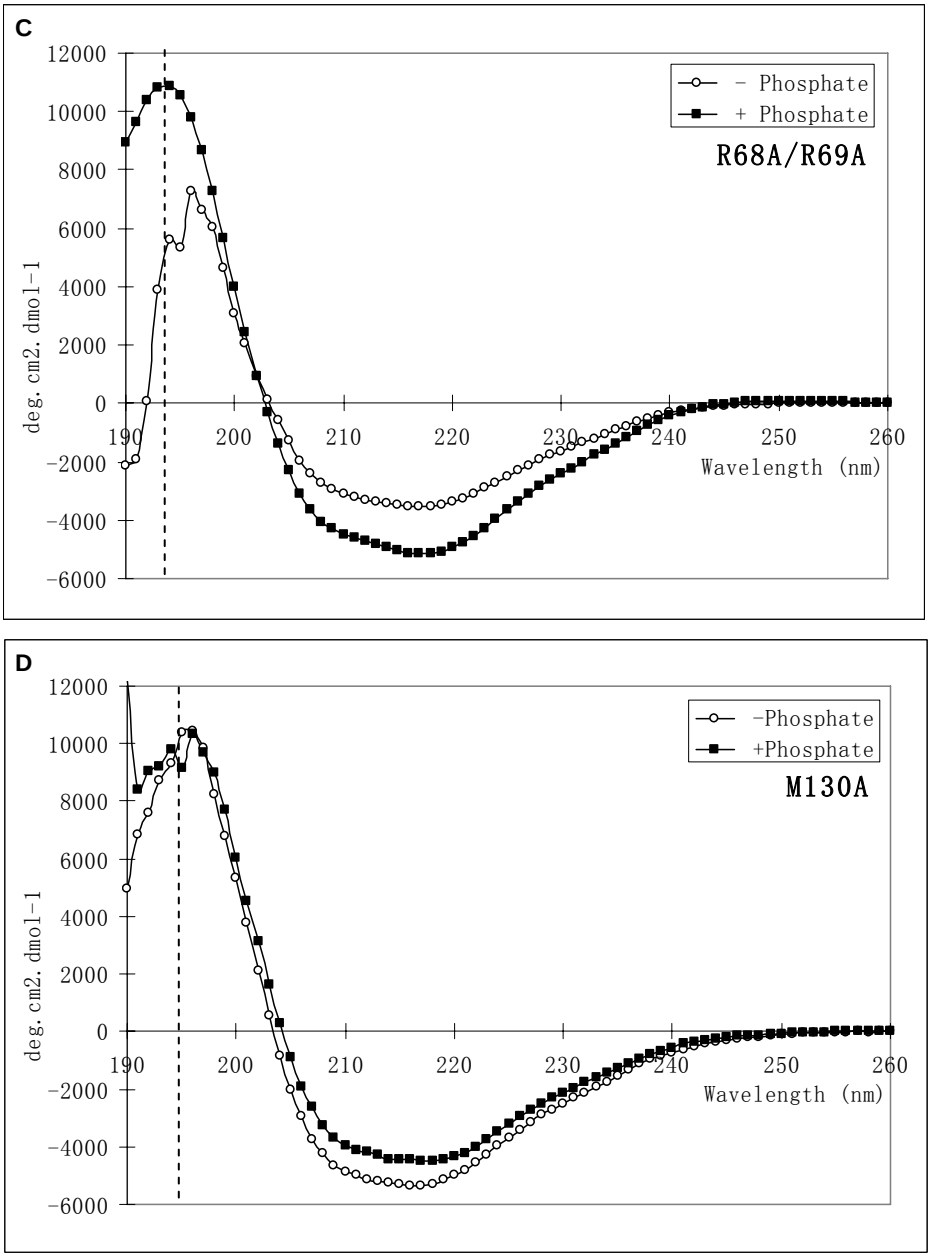

Figure 4-11: CD spectra of Pin1 mutants. Pin1 wild type (A), S16A mutant (B), R68A/R69A (C), and M130A (D) were subjected to CD analysis in far-UV range (190-260 nm) at 20 ºC. R68A/R69A and M130A exhibited a slight shift at the positive peak, implying a conformational change, in the absence and presence of phosphate. Only representative pictures were presented.

Table 4-1: The percentage (%) of the secondary structure elements in Pin1 as analyzed by circular dichroism (CD). Data shown is the average and standard deviation from three independent experiments. Data highlighted in bold represent those with significant change between the absence and presence of phosphate.

IN THE ABSENCE OF Pi					IN THE PRESENCE OF Pi				
	Helix	*Strand*	*Turns*	*Unordered*		*Helix*	*Strand*	*Turns*	*Unordered*
WT	15.0 ± 1.4	35.5 ± 0.7	21.0 ± 0.0	28.0 ± 1.4	*WT*	7.0 ± 1.0	42.0 ± 3.6	21.3 ± 2.1	29.0 ± 1.0
R14A	4.3 ± 1.5	40.0 ± 3.6	19.7 ± 1.5	34.0 ± 3.6	*R14A*	6.7 ± 0.6	35.0 ± 1.0	19.3 ± 2.3	38.3 ± 1.2
S16A	6.7 ± 0.6	39.3 ± 0.6	22.3 ± 2.1	30.7 ± 1.2	*S16A*	7.0 ± 1.4	41.5 ± 2.1	21.0 ± 0.0	30.0 ± 1.4
S16E	4.3 ± 0.6	43.7 ± 0.6	22.0 ± 1.0	28.3 ± 1.5	*S16E*	6.5 ± 0.7	40.5 ± 2.1	21.5 ± 0.7	30.5 ± 0.7
R17A	7.5 ± 0.7	**40.0 ± 0.0**	22.0 ± 0.0	30.0 ± 0.0	*R17A*	16.3 ± 1.2	**36.3 ± 0.6**	20.3 ± 2.1	26.3 ± 1.5
S32A	16.0 ± 0.0	33.0 ± 2.8	22.0 ± 0.0	28.5 ± 2.1	*S32A*	15.5 ± 0.7	32.5 ± 2.1	22.5 ± 0.7	28.5 ± 0.7
F25A	15.0 ± 0.0	33.5 ± 3.5	21.0 ± 1.4	29.0 ± 4.2	*F25A*	17.3 ± 2.3	29.3 ± 4.0	21.7 ± 1.2	32.0 ± 1.7
W34A	17.0 ± 1.4	32.0 ± 0.0	20.5 ± 2.1	31.0 ± 4.2	*W34A*	16.0 ± 1.4	34.0 ± 1.4	21.0 ± 1.4	28.5 ± 0.7
K63A	5.0 ± 0.0	39.0 ± 0.0	22.0 ± 0.0	33.0 ± 0.0	*K63A*	6.0 ± 1.0	41.3 ± 2.5	22.0 ± 1.0	29.0 ± 3.0
R68/69A	20.0 ± 1.4	**28.5 ± 0.7**	19.5 ± 3.5	32.5 ± 2.1	*R68/69A*	6.7 ± 0.6	**41.0 ± 1.7**	23.0 ± 2.0	28.7 ± 2.1
C113A	6.5 ± 0.7	34.5 ± 4.9	22.0 ± 0.0	36.5 ±3.5	*C113A*	6.7 ± 1.2	46.0 ± 3.0	20.7 ± 1.5	26.0 ± 4.4
H59A	6.3 ± 0.6	37.3 ± 2.1	21.7 ± 2.5	34.3 ± 0.6	*H59A*	20.7 ± 2.3	25.7 ± 2.3	19.0 ± 1.7	35.3 ± 3.1
H157A	6.0 ± 1.0	33.3 ± 0.6	19.3 ± 1.2	40.3 ± 2.3	*H157A*	16.0 ± 0.0	29.0 ± 0.0	20.0 ± 0.0	35.5 ± 0.7
S154A	17.0 ± 0.0	33.0 ± 0.0	22.5 ± 0.7	27.5 ± 0.7	*S154A*	17.0 ± 2.6	34.7 ± 3.1	21.7 ± 0.6	26.0 ± 2.0
L122A	7.0 ± 1.0	37.7 ± 2.1	21.7 ± 0.6	32.7 ± 1.5	*L122A*	6.3 ± 1.5	39.0 ± 3.0	22.0 ± 1.7	32.0 ± 3.0
M130A	17.0 ± 2.0	**30.7 ± 4.5**	21.7 ± 0.6	30.3 ± 3.2	*M130A*	5.5 ± 0.7	**43.5 ± 3.5**	21.5 ± 0.7	28.5 ± 2.1

4.4 Thermal stability of Pin1 and its mutants

The thermal stability of Pin1 wild type and mutant proteins was investigated by monitoring changes in the intrinsic ellipticity by CD at 202 nm when these proteins were heated from 20 ºC to 90 ºC. Pin1 appeared fully unfolded when heated to 90 ºC as its CD spectra remained unchanged beyond 90 ºC (data not shown). The wavelength of 202 nm was used because changes in ellipticity were the greatest when Pin1 was heated from 20 ºC to 90 ºC (Figure 4-12). The temperature at which half of the protein molecules were unfolded was defined as melting temperature (Tm). Graphical presentation of the determination of Tm was shown in Figure 4-13, with C113A mutant as a representative.

The Tm values of wild type and the various mutant proteins were shown in Table 4-2 (page 110). Wild type Pin1 had a Tm of 58.4 ºC or 60.7 ºC in the absence or presence of phosphate, respectively. Interestingly, only mutants of the PPIase domain of Pin1, including mutants C113A, H59A, H157A, L122A, and M130A, experienced a left shift or decrease in Tm, indicating a decrease in thermal stability. All mutants of the WW domain had Tm values comparable to the wild type protein (Table 4-2; Figure 4-14). From the reported Pin1 crystal structure in complex with an Ala-Pro dipeptide (Ranganathan et al., 1997), the residues Cys-113, His-59, and His-157 are proposed to participate directly in the catalytic activity of Pin1. On the other hand, residues Leu-122 and Met-130 reside in the hydrophobic pocket that holds the proline residue of the Ala-Pro dipeptide, which is in proximity with the catalytic site.

Although residues Ser-154, Arg-68, Arg-69, and Lys-63 are located in the PPIase domain, mutations of these residues do not appear to destabilize the protein, as shown by their comparable Tm to the wild-type protein. Structurally speaking, these four residues (Ser-154, Arg-68, Arg-69, and Lys-63) reside at a flexible region mainly composed of the loop between α1 and β1, as well as between β3 and β4, which is further from the core region of the PPIase domain involving of the active site (Cys-113). Although residue Ser-154 is proposed to participate in the forming of an enzyme-substrate intermediate during the catalytic reaction, it may be relatively less critical to protein stability due to its structural location in this flexible region (Figure 4-15). Hence, our data suggest that the PPIase domain, particularly the residues that reside in the core region of the catalytic site, is important in the overall stability of the Pin1 protein.

In general, consistent with previous data reported by Bayer *et al.* (Bayer et al., 2003), the presence of phosphate in the protein solution might slightly elevate the Tm values of the wild type and mutant proteins, although this may not be significant as seen in our data. Nevertheless, mutation of residues Arg-14, Lys-63, and Arg-68/Arg-69 to alanine seemed to abolish the stabilization by phosphate (Figure 4-14). Thus, these residues may play an important role in phosphate binding, which is consistent with previously reported studies, as well as the secondary structure element analysis, discussed earlier in section 4.3. Although residues Arg-68, Arg-69, and Lys-63 do not directly contribute to the stability of the molecule, their role in substrate

specificity towards the pSer/Thr-Pro motif is undoubtedly significant, and their locations at the relatively flexible α1/β1 loop region may enable them to fulfill their task as a sort of selectivity filter.

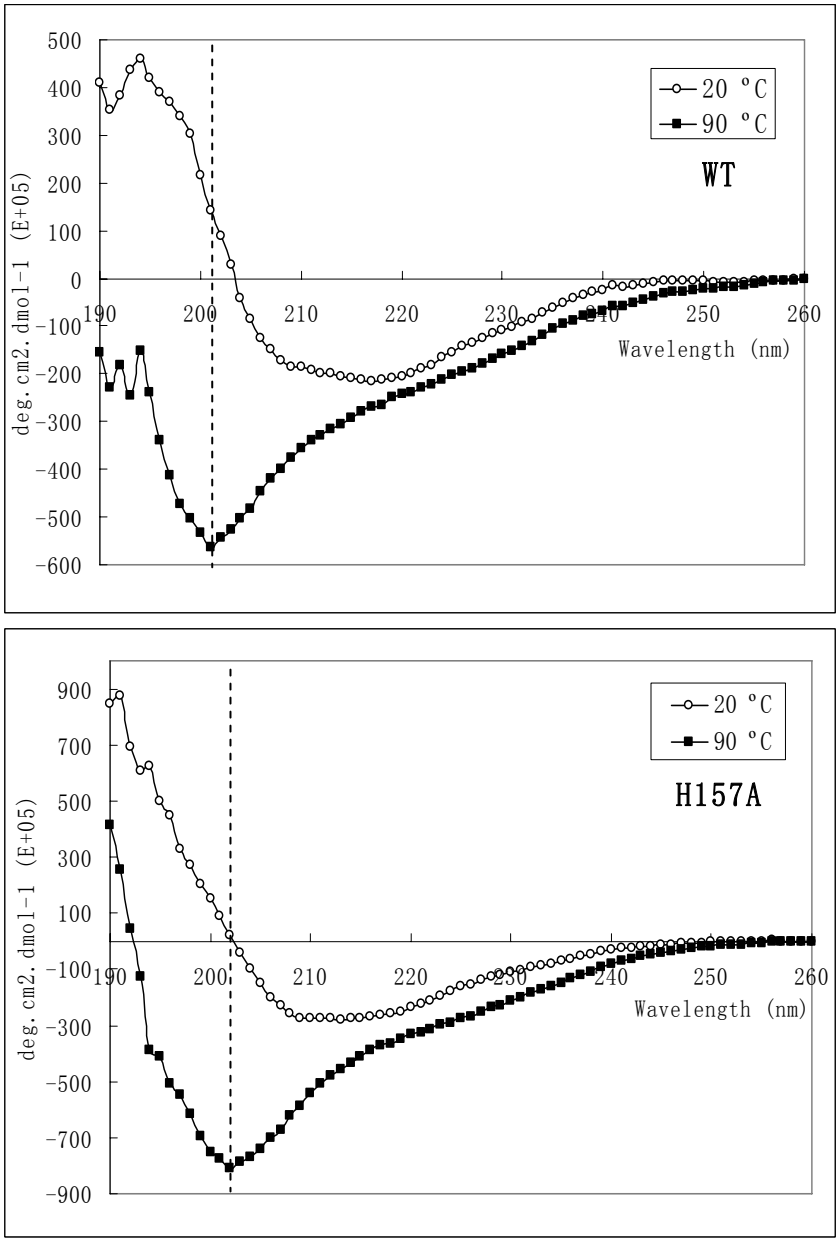

Figure 4-12: Thermal denaturation of Pin1. Pin1 was heated from 20 ºC to 90 ºC with 1 ºC step intervals and the CD spectra was recorded. Ellipticity change was most drastic at the wavelength of 202 nm. Only representative spectra of WT and H157A were shown.

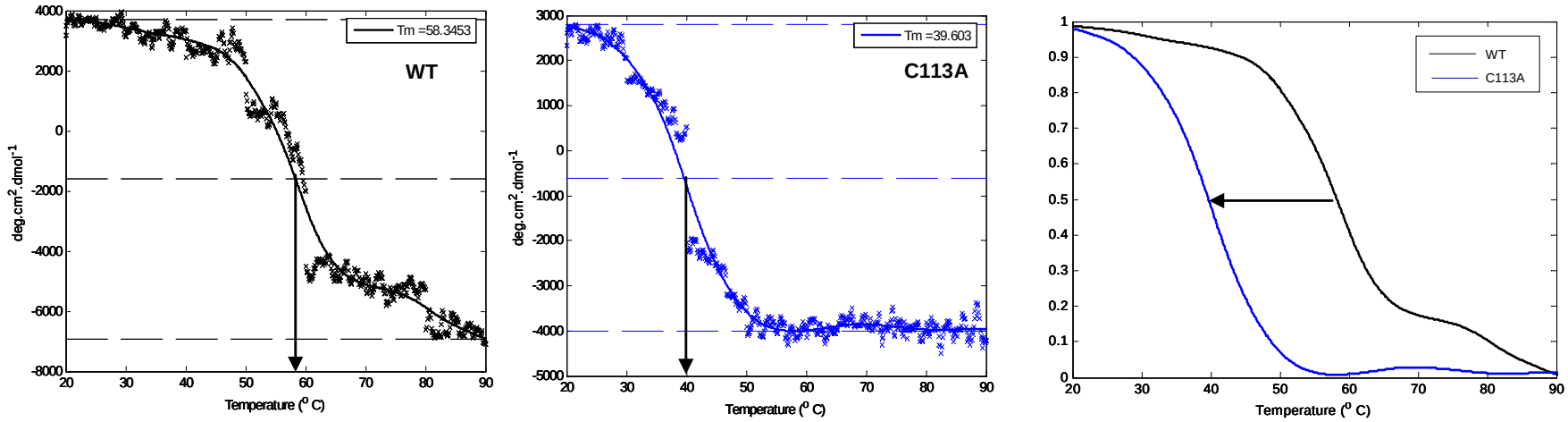

Figure 4-13: Thermo-unfolding of Pin1. Pin1 wild-type (left) or mutant (middle) was heated from 20 ºC to 90 ºC. Melting temperature (Tm) was recorded as the temperature at which half the protein molecules was denatured. Thermo-unfolding curve of the C113A mutant was compared with wild-type (right), revealing a right shift of Tm of C113A mutant.

Table 4-2: Melting temperature (ºC) of Pin1.

	In the absence of Pi	In the presence of Pi
WT	58.4 ± 0.1	60.7 ± 0.7
R14A	58.6 ± 2.7	60.7 ± 1.1
S16A	59.0 ± 0.5	61.4 ± 0.1
S16E	59.3 ± 0.7	62.1 ± 0.2
R17A	59.2 ± 0.1	62.4 ± 0.1
S32A	58.1 ± 0.2	60.2 ± 0.2
F25A	58.7 ± 0.2	61.2 ± 0.0
W34A	59.5 ± 1.2	62.2 ± 0.8
K63A	59.8 ± 0.5	60.0 ± 0.1
R68/69A	60.4 ± 0.2	60.1 ± 0.2
C113A	40.7 ± 1.6	48.8 ± 0.8
H59A	46.0 ± 1.0	49.2 ± 1.6
H157A	46.1 ± 2.4	49.1 ± 0.6
S154A	60.6 ± 03	61.4 ± 0.4
L122A	49.7 ± 0.3	53.0 ± 0.5
M130A	54.2 ± 0.1	58.3 ± 0.4

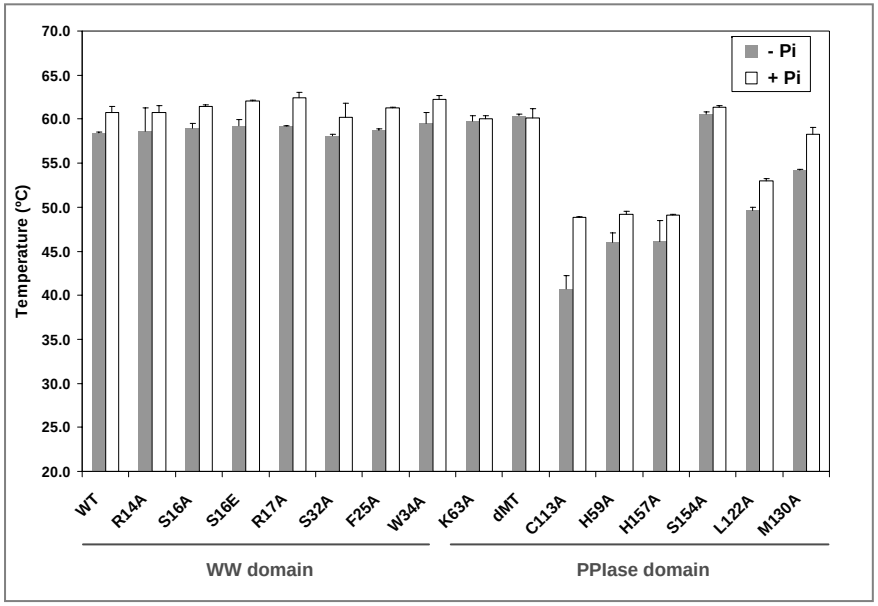

Figure 4-14: Melting temperature (ºC) of Pin1. Measurements were done by circular dichroism (CD) analysis in the presence or absence of 10 μM phosphate. dMT denoted the double mutant R68/69A.

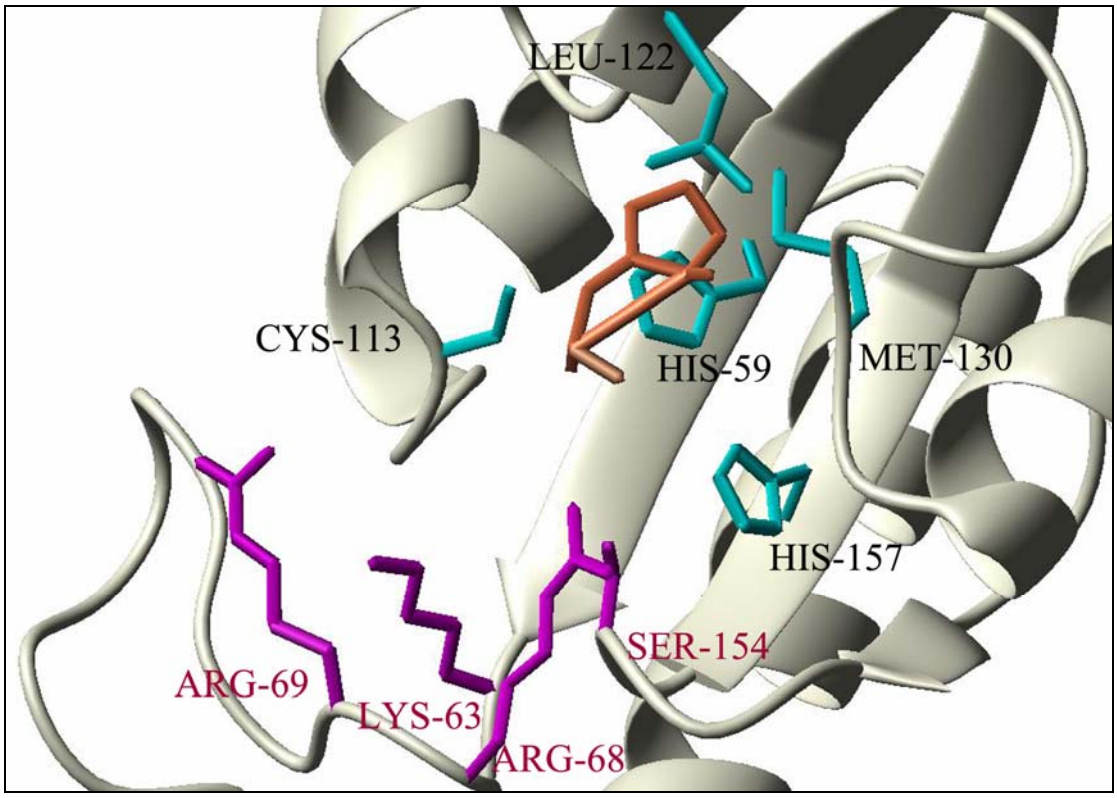

Figure 4-15: Structural analysis of the residues critical for Pin1 stability. Pin1 crystal structure in complex with Ala-Pro dipeptide (PDB code: 1PIN) with the functionally important PPIase domain residues was shown. Residues in cyan denote residues critical for thermal stability of Pin1. Ala-Pro dipeptide was coloured in orange. Figure is generated by the MOLMOL program (http://hugin.ethz.ch/wuthrich/software/molmol/).

4.5 The crystal structures of Pin1 mutants

The Pin1 mutant structures were solved by X-ray crystallography to study the structure-function relationship of Pin1. Together with wild type, seven Pin1 mutants, including R14A, F25A, S32A, W34A, K63A, C113A, and M130A were crystallized，while the other mutants were failed to obtain the crystals. The crystal sizes range from 0.3 × 0.3 mm to 0.3 × 0.8 mm (Figure 4-16). X-ray diffraction data were collected (Figure 4-17) and all mutant structures were solved by molecular replacement analysis and the resolutions were varied for different mutants. C113A and M130A structures were solved with a resolution up to 2.0 Å, whereas S32A and W34A 2.5 Å,

K63A 2.6 Å, F25A 2.7 Å, and R14A 3.4 Å (Table 4-4). The electron density maps of these mutants were clear to position the side chains. Thus the resolution of 2.0 Å to 3.4 Å is sufficient to see the interaction of side chains. Ramachandran plot analyses were performed to check the stereochemical quality of the protein structures (Figure 4-18). Table 4-3 shows a summary of the Ramachandran plot analysis. Percentage of residues that fell into the favored and allowed regions ranges from 79.2 % to 98.7 % and from 93.3 % to 99.3 %, respectively (Table 4-3). These ranges are generally regarded as acceptable. Among the mutants, crystals of R14A, F25A, and K63A belong to P3(1)21 space group, whereas crystals of S32A, W34A, C113A, and M130A belong to P4(3)2(1)2 space group, the same space group as wild type Pin1 (Table 4-4).

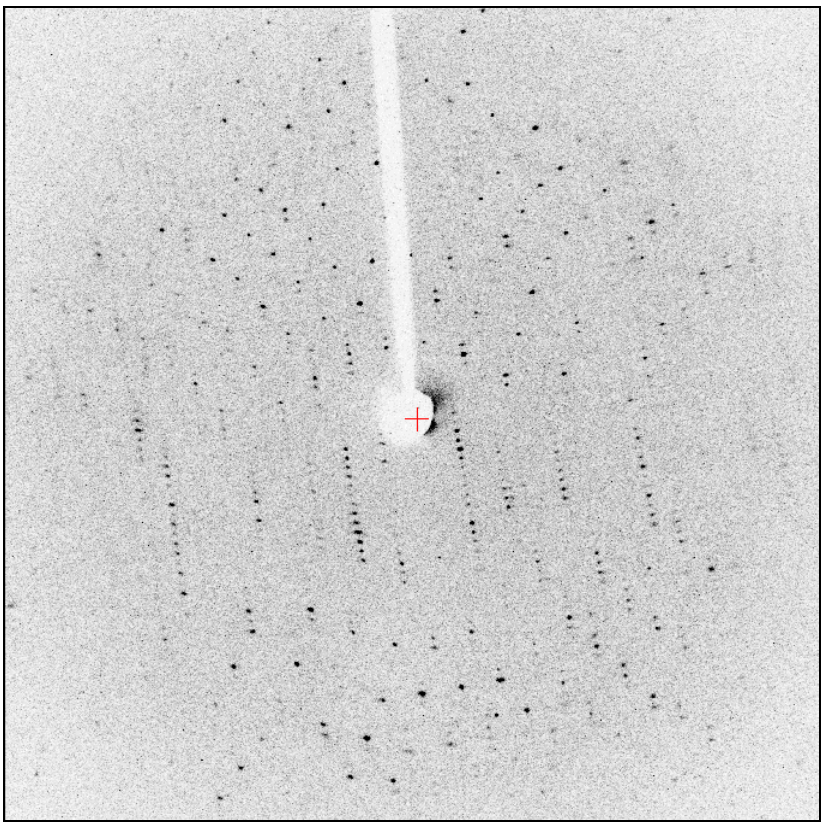

Figure 4-17: A representative X-ray diffraction picture of a Pin1 crystal (W34A).

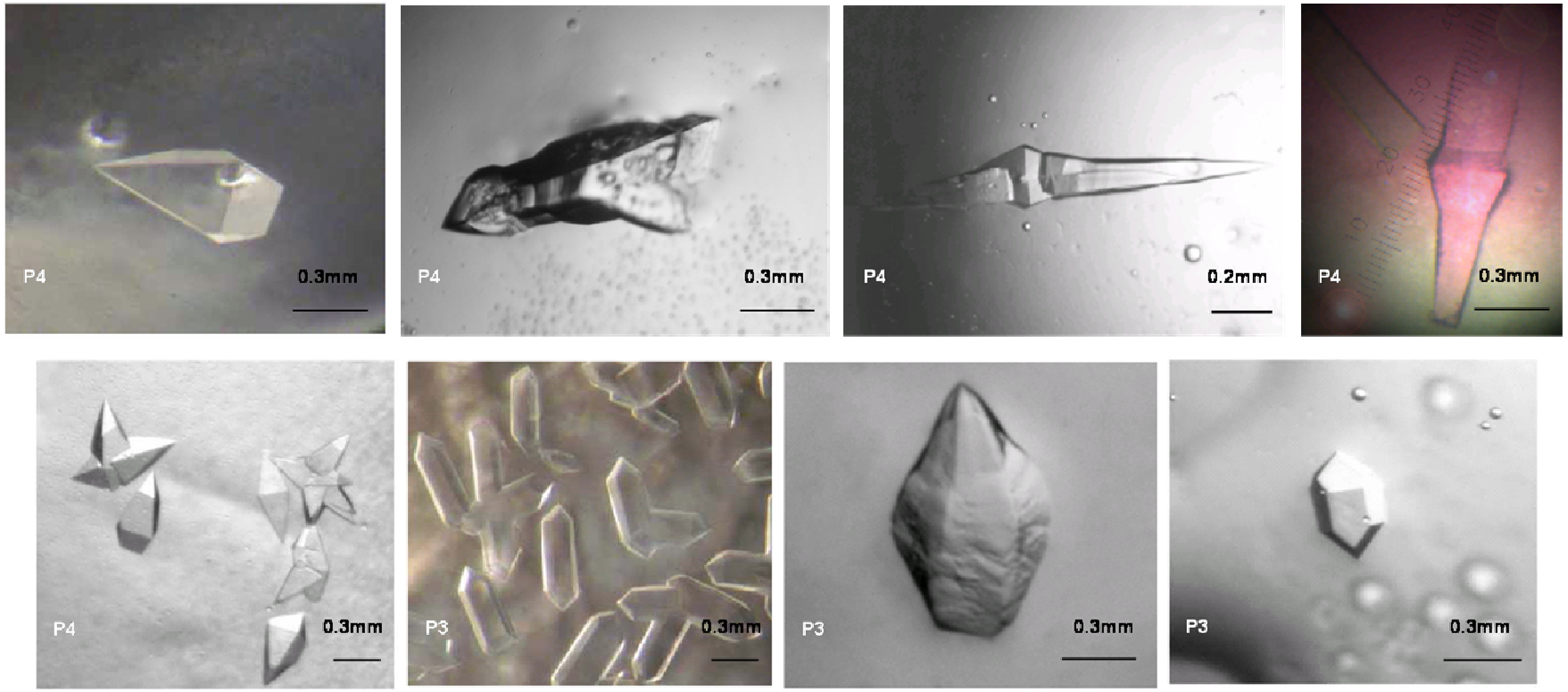

Figure 4-16: Crystals of Pin1 mutants. Top panel (left to right)—wild-type, M130A, S32A, W34A; bottom panel (left to right)—C113A, R14A, F25A, K63A. Space groups of P4 or P3 were indicated at the left bottom corner.

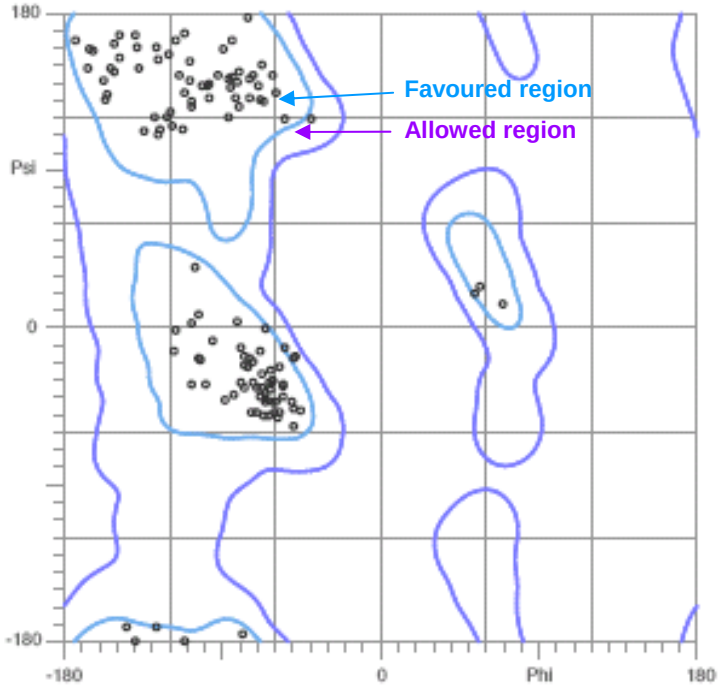

Figure 4-18: Ramachandran plot analysis of W34A mutant. 96.6 % and 99.3 % of residues fall in the favored regions and allowed regions, respectively.

Table 4-3: Summary of Ramachandran plot analysis.

	Residues in favoured regions	Residues in allowed regions	Outliers
R14A	79.2 %	93.3 %	10 (Leu7, Ala14, Ser18, Ser19, Gln49, Arg54, Trp73, Asp112, Arg127, Gly128)
F25A	93.2 %	96.6 %	5 (Leu7, Arg17, Ser18, Lys46, Pro70)
S32A	96.0 %	97.3 %	4 (Leu7, Ser18, Gly20, Pro70)
W34A	96.6 %	99.3 %	1 (Leu7)
K63A	93.3 %	98.0 %	3 (Leu7, Met15, Ser18)
C113A	98.0 %	99.3 %	1 (Leu7)
M130A	98.7 %	99.3 %	1 (Leu7)

Table 4-4: Crystallographic data and refinement statistics.

Data set	**R14A**	**F25A**	**S32A**	**W34A**	**K63A**	**C113A**	**M130A**
Data collection							
Wavelength (Å)	1.1	1.5418	1.1	1.5418	1.5418	1.1	1.1
Resolution Range (Å)	25.0-2.5	50.0-2.5	50.0-1.49	25.0-2.4	50.0-2.6	50.0-1.9	50.0-1.46
Observation	28934	70855	378612	75174	38459	158858	372911
Unique Reflections	7329	7431	52496	6722	6504	13863	29859
Completeness (%)	94.9	95.6	99.8	95.5	92.6	99.8	98.7
(working + test)							
R_{sym}	9.5	8.6	6.2	8.2	8.3	7.3	6.0
I/σ	15.8	22.8	15.0	14.9	16.8	8.4	11.7
Space group	P3(1)21	P3(1)21	P4(3)2(1)2	P4(3)2(1)2	P3(1)21	P4(3)2(1)2	P4(3)2(1)2
	a=67.980	a=68.309	a=48.547	a=49.011	a=68.646	a=48.758	a=48.966
	b=67.980	b=68.309	b=48.547	b=49.011	b=68.646	b=48.758	b=48.966
	c=79.434	c=79.359	c=139.631	c=136.796	c=79.412	c=137.980	c=138.091
	α=β=90,	α=β=90,	α=β=γ=90	α=β=γ=90	α=β=90,	α=β=γ=90	α=β=γ=90
	γ=120	γ=120			γ=120		
Refinement							
Resolution Range (Å)	20.0-3.4	20.0-2.7	25.0-2.5	15.0-2.5	15.0-2.6	25.0-2.0	20.0-2.0
R factor	22.5	24.5	24.9	21.7	23.5	23.9	25.5
R_{free}	32.2	30.6	33.2	29.0	29.5	28.3	28.7
Protein atoms	1207	1209	1207	1204	1209	1212	1210
Water molecules	59	205	126	158	125	129	181
R.m.s.d. of Bonds (Å)	0.0070	0.0083	0.0153	0.0060	0.0081	0.0049	0.0050
R.m.s.d. of Angles (°)	1.41	1.44	1.74	1.34	1.35	1.24	1.31
Average B-factors	25.85	39.66	28.893	35.082	44.31	31.76	19.535

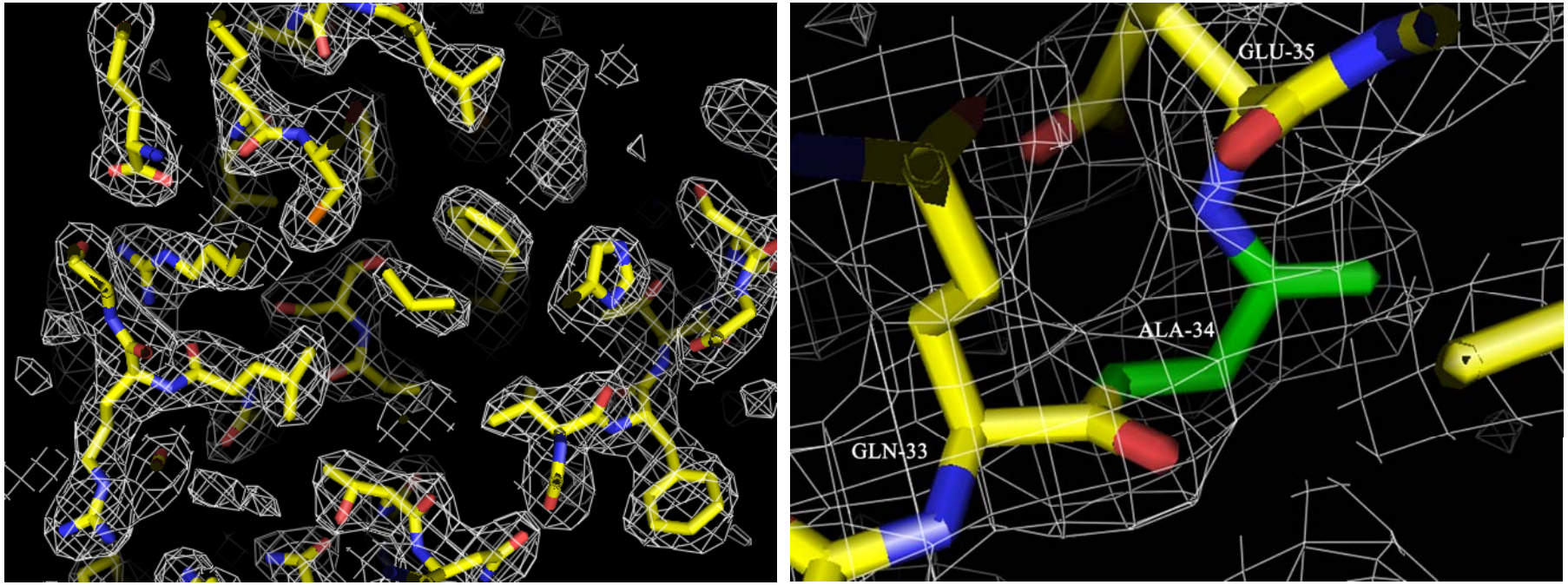

Figure 4-19: Electron density maps of the Pin1 mutant W34A. Figures were generated by PyMOL (http://pymol.sourceforge.net/).

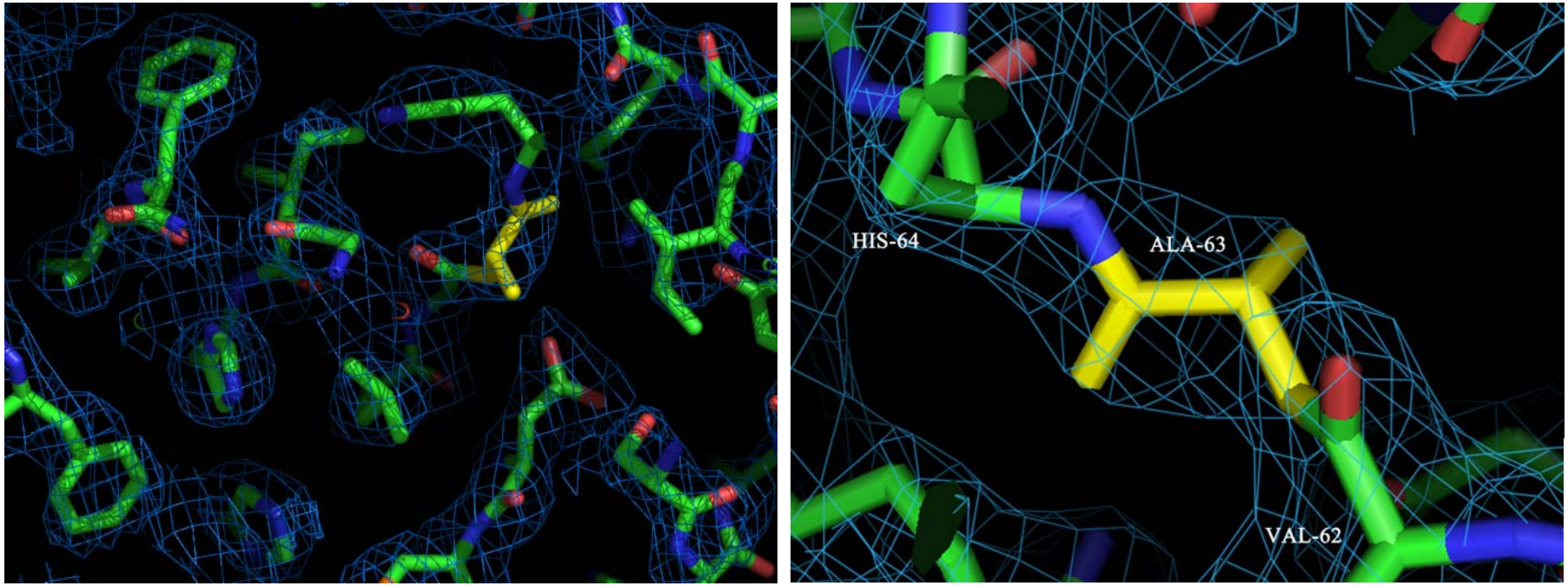

Figure 4-20: Electron density maps of the Pin1 mutant K63A. Figures were generated by PyMOL.

4.6 Comparison of Pin1 mutant structures with the wild type structure

All mutant structures were essentially grossly identical to the wild type structure (PDB code: 1PIN), with backbone R.M.S.D. values ranging from 0.272 Å to 0.642 Å (Figure 4-21). However, some side chain shifts were observed. Side chain shifts greater than the respective structure's resolution were regarded as significant. These are shown in Figures 4-22 to 4-25 and summarized in Table 4-5. In the mutant R14A with a resolution of 3.4 Å, residues His-27, Gln-66, and Lys-117 exhibited significant side chain shift (Figure 4-22). Likewise, residues Arg-14, Arg-17, Arg-21, His-27, and Arg-68 for the F25A mutant (resolution of 2.7 Å) (Figure 4-23), as well as residues Arg-14, Arg-21, and His-27 for the S32A mutant (resolution of 2.5 Å) (Figure 4-24) also exhibited significant side chain shifts. Thus, besides those residues previously reported as important in substrate binding or catalytic activity of Pin1 (Arg-14, Arg-17, and Arg-68), side chain shifts in some other residues, such as Arg-21, His-27, Gln-66, and Lys-117, were observed as well. On the other hand, no other significant side chain shifts were observed in the Pin1 mutants W34A, K63A, C113A, and M130A, except for the respective mutated residues (Figure 4-25).

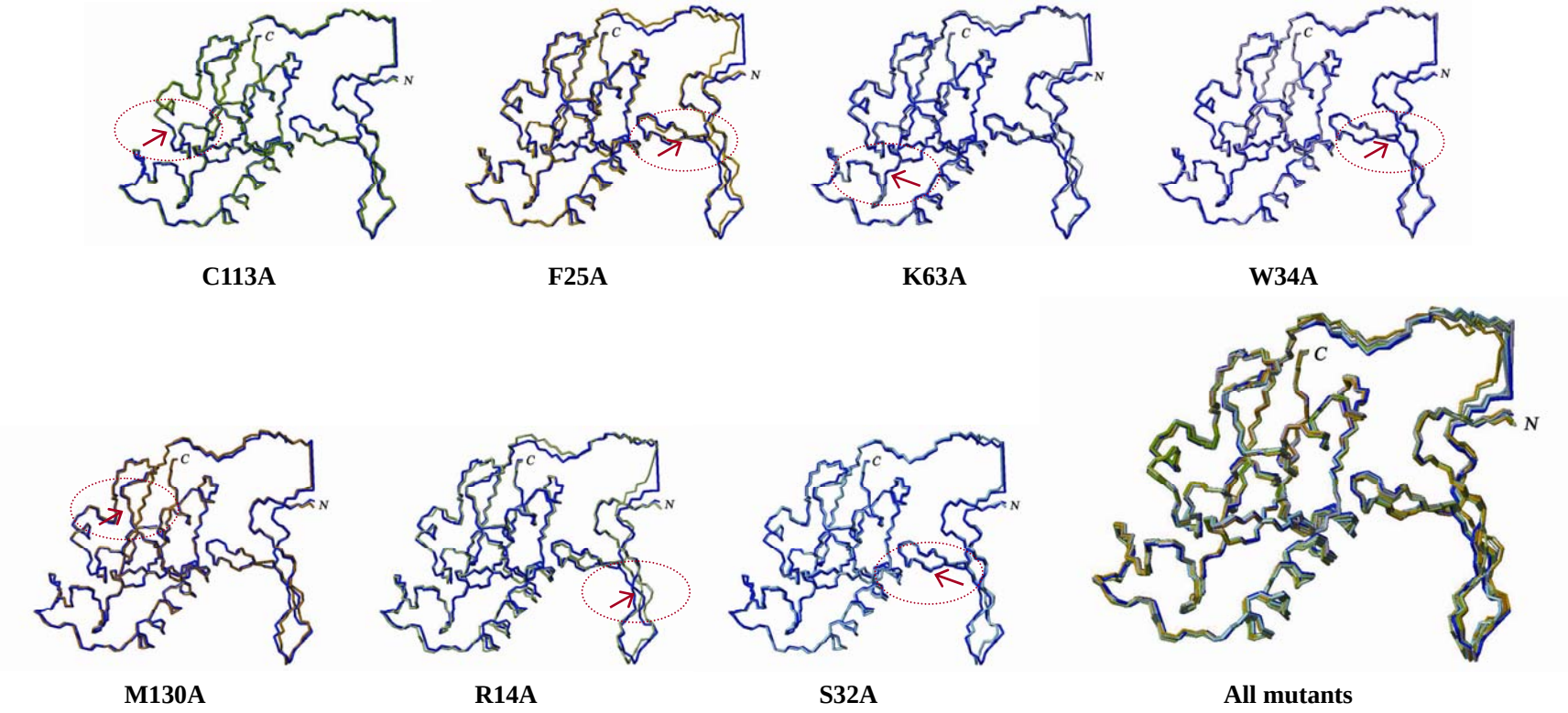

Figure 4-21: Pin1 mutant backbone structures superimposed on the wild-type structure. Backbone structure in blue colour denotes wild-type structure. Red arrows indicate the mutated sites. RMSDs for the mutant structures are in reference to the wild type structure: M130A—0.316; R14A—0.642; S32A—0.442; W34A—0.292; C113A—0.272; F25A—0.645; K63A—0.454. Figures were generated by MOLMOL.

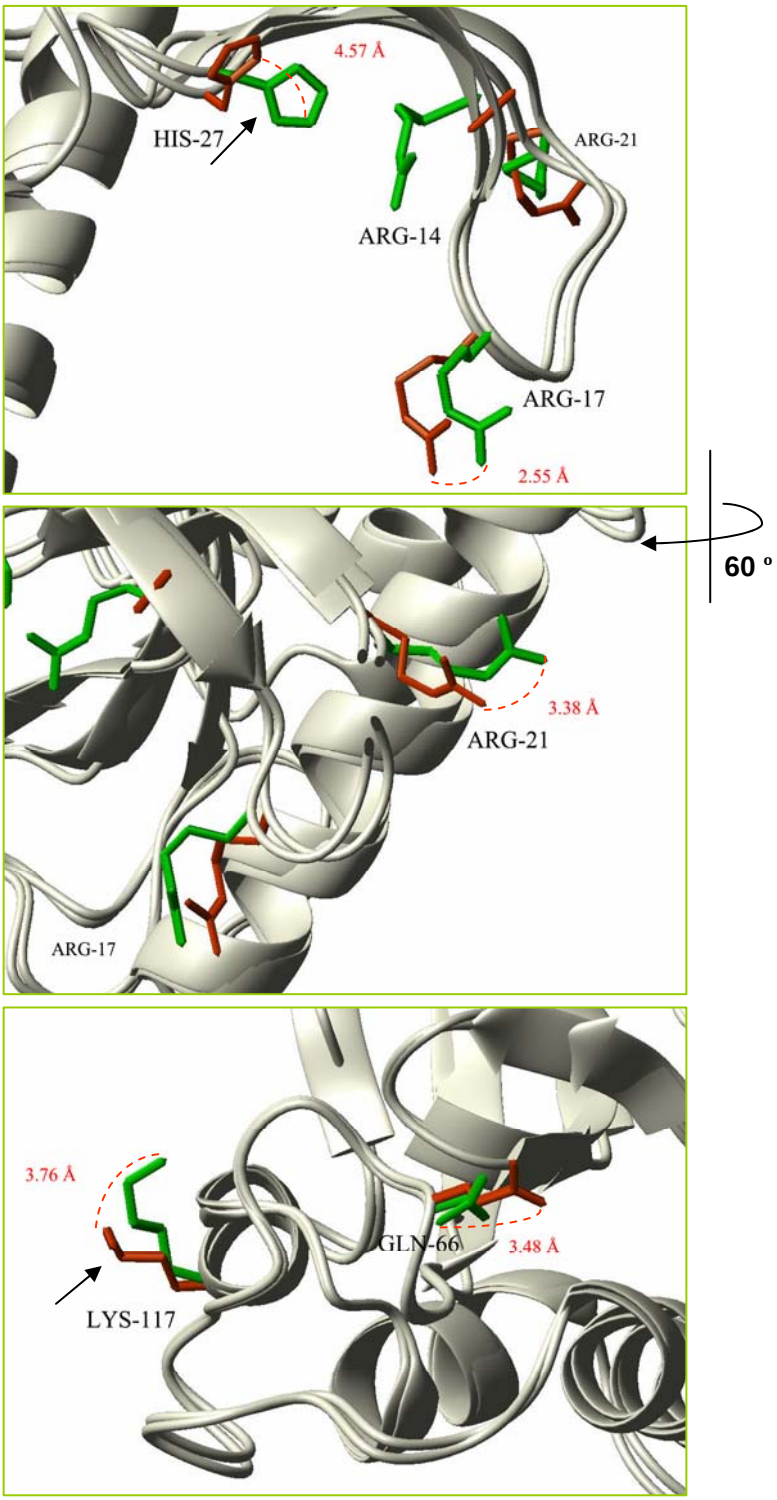

Figure 4-22: Side chain shifts in the R14A mutant. Side chains in wild type and mutant proteins were coloured in green and red, respectively. Residues His-27, Gln-66, and Lys-117 exhibited significant side chain shifts (> 3.4 Å, as indicated by black arrows). Figures were generated by MOLMOL.

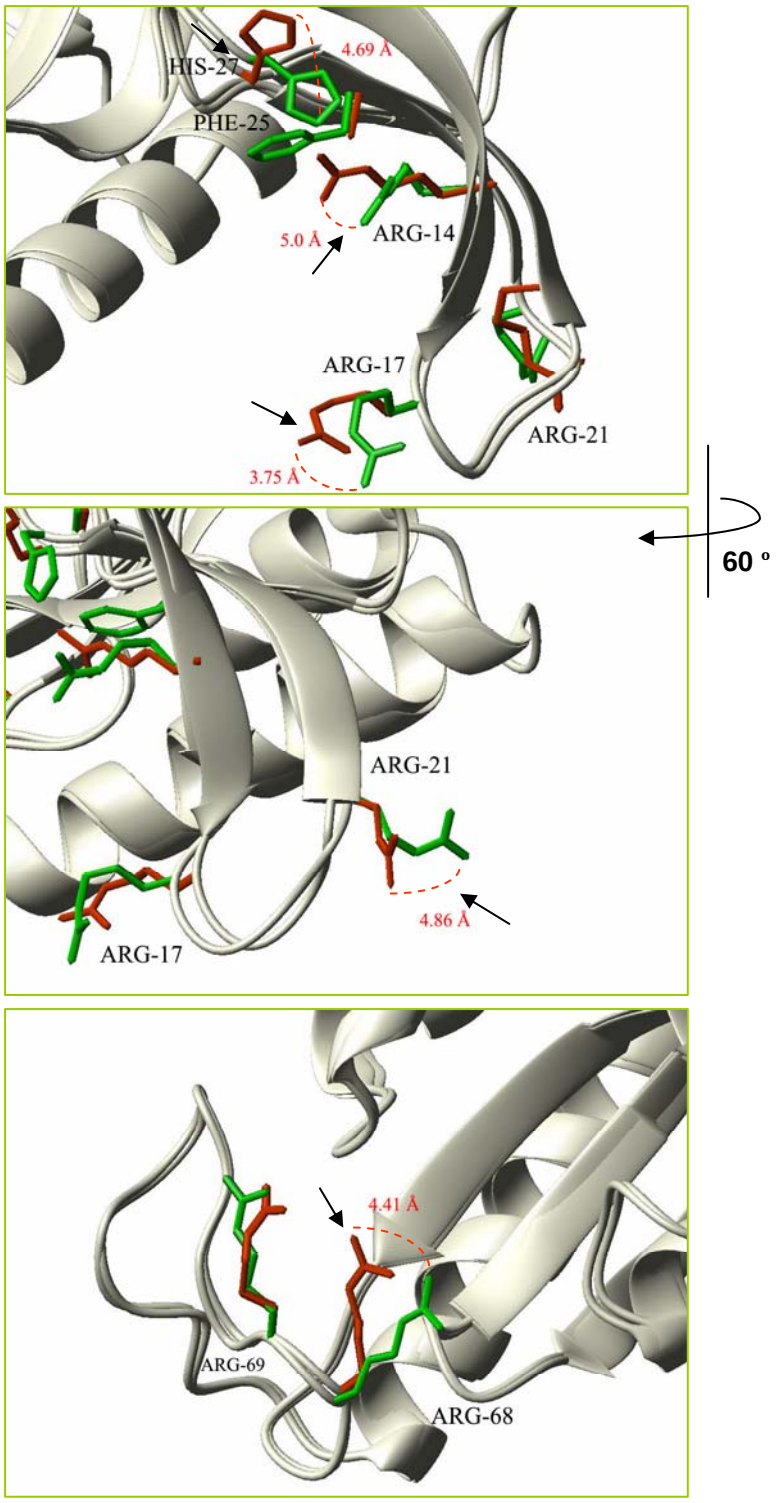

Figure 4-23: Side chain shifts in the F25A mutant. Side chains in wild type and mutant proteins were coloured in green and red, respectively. Residues Arg-14, Arg-17, Arg-21, His-27, and Arg-68 exhibited significant side chain shifts (> 2.7 Å, as indicated by black arrows). Figures were generated by MOLMOL.

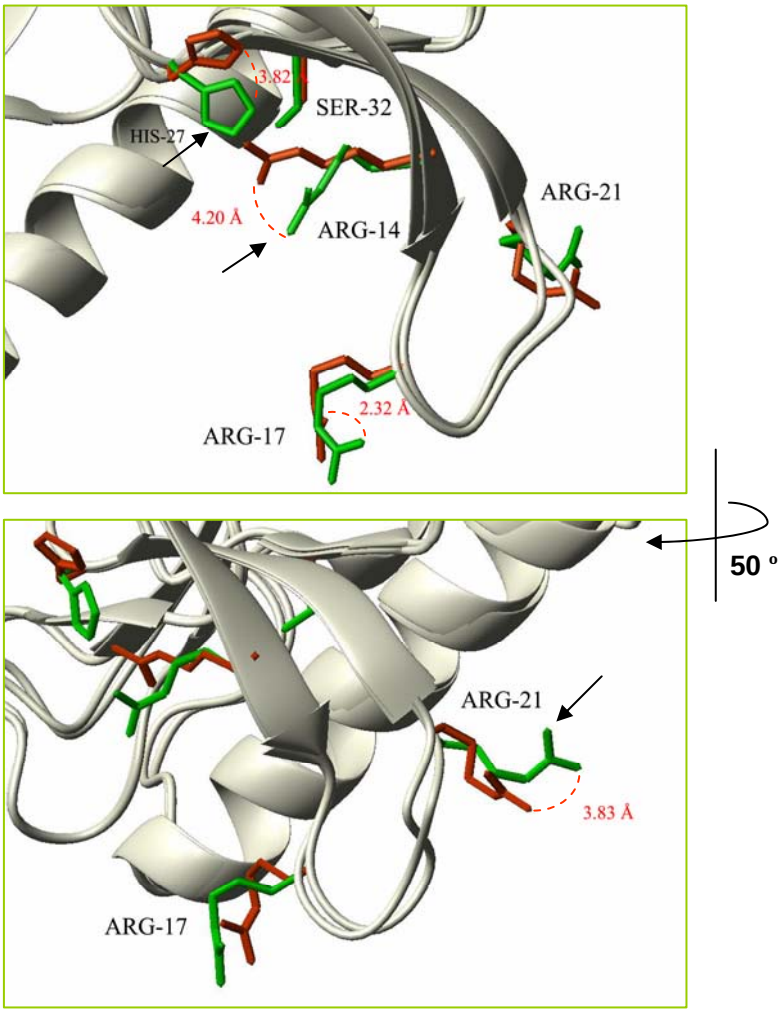

Figure 4-24: Side chain shifts in the S32A mutant. Side chains in wild type and mutant proteins were coloured in green and red, respectively. Residues Arg-14, His-27, and Arg-21 exhibited significant side chain shifts (> 2.5 Å, as indicated by black arrows). Figures were generated by MOLMOL.

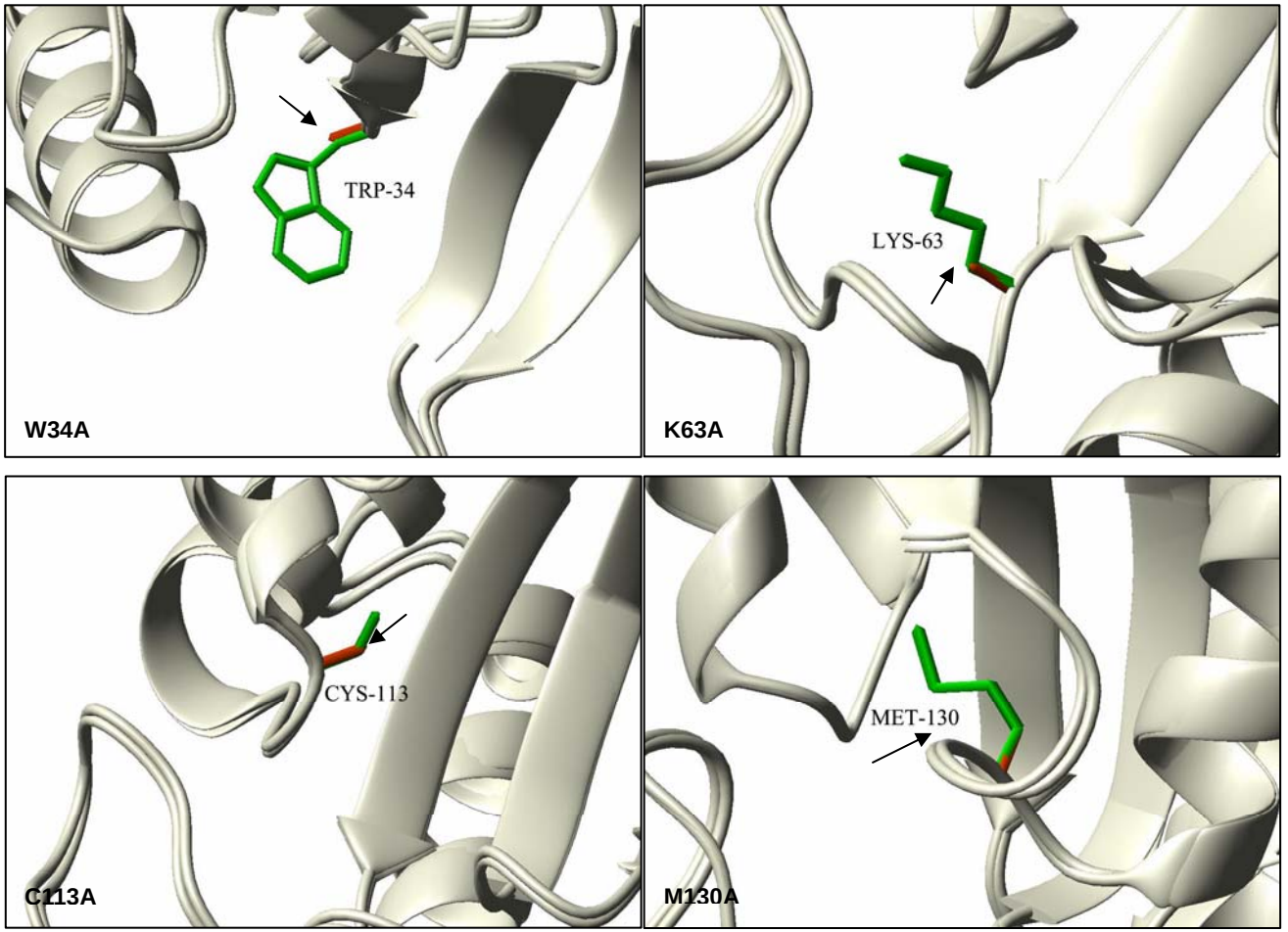

Figure 4-25: Side chains of mutated residues for the W34A, K63A, C113A, and M130A mutants. W34A, K63A, C113A, and M130A mutants did not show significant side chain difference compared with the wild type, except at the mutated sites changed to alanine (indicated by black arrows). Only the mutated sites were shown, with side chains in wild type and mutant proteins coloured in green and red, respectively. Figures were generated by MOLMOL.

Table 4-5: Summary of side chain shift comparisons between mutants and wild-type Pin1 (PDB code: 1PIN). Significant side chain shifts (> 2.0 Å) were indicated [in angstrom (Å)]. A blank entry indicates that insignificant or no side chain shifts were observed. "--" indicates corresponding residue mutated.

Mutants	R14A	F25A	C113A	K63A	W34A	S32A	M130A
WW Domain							
R14	--	**5.00**				**4.20**	
S16							
R17	**2.55**	**3.75**				**2.32**	
Y23							
F25		--					
S32						--	
W34					--		
PPIase Domain							
H59							
K63				--			
R68		**4.41**					
R69							
C113			--				
L122							
M130							--
S154							
H157							
Residues not reported in previous studies							
E12							
K13							
R21	**3.38**	**4.86**				**3.83**	
H27	**4.57**	**4.69**				**3.82**	
Q33							
E35							
Q66	**3.48**						
E87							
E100							
K117	**3.76**						

4.7 Speculation on the important Pin1 residues for substrate binding

The crystal structures of mutants R14A, F25A, S32A, W34A, K63A, C113A, and M130A were all very similar to that of wild type (PDB code: 1PIN) in both the backbone fold and side chain orientation. However, there were some observable shifts in side chain orientation in R14A, F25A, and S32A.

In F25A, Arg-14, Arg-17, Arg-68, Arg-21, and His-27 are the most significantly shifted, apparently because these residues reside at the substrate binding site. Arg-14 and Arg-17 are important residues in CTD peptide binding (Verdecia et al., 2000). Arg-14 are in van der Waals contact with Pro-3' of the peptide whereas Arg-17, together with Ser-16 and Tyr-23, constitute the full binding module for the phosphate group on Ser-5'. As discussed earlier in the review of the WW domain studies (section 1.8.2), residue Arg-14 may not be as important as Arg-17 in substrate binding specificity because it is also conserved in Group I WW domains which have no substrate preference for pSer/Thr-Pro motifs. Residue Arg-17 is important in substrate binding and specificity, but the side chain shift observed in the mutant structures may not sufficiently support this view for the following reasons. Firstly, Arg-17 lies in the loop between β1' and β2' which is rather flexible. As seen in the superposition of the mutant structures with wild type 1PIN, deviations were mainly observed in this region, although the overall structure deviations were insignificant (Figure 4-21). Secondly, the mutant structures were obtained with protein not in complex with any substrate peptide. Thus, it remains interesting to examine in future whether the Arg-17 side

chain shift indeed affects substrate binding. Nevertheless, previous studies using NMR titration with Cdc25 have mapped the peptide binding site at the β1' and β2' loop region, with chemical shift perturbations observed particularly at residues Arg-17 and Typ-34 (Wintjens et al., 2001).

Arg-68 resides in the α1/β1 loop in the PPIase domain and is involved in peptide binding and substrate selectivity. Mutation of Phe-25 to Ala causing side chain shift at Arg-68 suggests that Phe-25 could be one of the residues, if there are any other residues, causing the conformational change in the α1/β1 loop when CTD peptide was in complex with the WW domain (from "closed" conformation to "open" conformation), as observed in the crystal structure of Verdecia et al. (Verdecia et al., 2000). Residue His-27 was not previously reported as one that is in direct interaction with substrate peptide. Structurally, His-27 resides near the peptide binding interface at the WW domain, adjacent to Phe-25. Phe-25, together with Arg-14, is in van der Waals contact with Pro-3' of CTD peptide. His-27 could therefore conceivably be involved in substrate binding. Other WW domain residues with observable shifts in side chain orientation include Arg-21. This residue, although not residing near any previously reported functional domains, may also participate in substrate binding. Interestingly, four out of five shifted residues observed are arginine residues (Arg-14, Arg-17, Arg-68, and Arg-21). Thus, deletion of Phe-25 affects the orientation of these positively charged residues, which in turn may disturb the binding of phosphosubstrates through these positively charged residues. This suggests the

important role of these charged residues in Pin1 function. However, these speculations need to be verified through binding assay and Pin1 structure in complex with substrate.

In S32A mutant structure, similar with F25A, significant side chain shifts in Arg-14, Arg-21, and His-27 were observed. For R14A mutant, interestingly, besides His-27, mutation of Arg-14 also caused side chain shifts in Gln-66 and Lys-117. Same as Arg-68, Gln-66 resides in the α1/β1 loop in the PPIase domain. This suggested that besides Phe-25 as discussed earlier, Arg-14 could also be one of the residues causing the conformational change in the α1/β1 loop when CTD peptide was in complex with the WW domain. However, the resolution of R14A mutant structure (3.4 Å) was barely sufficient for the observation of side chain interaction (3.4 Å) so that the side chain shifts might not be significant.

Among all our Pin1 mutants, previous studies showed that mutations at Trp-34 abolished the substrate binding ability *in vitro* to the greatest extent. The affinity of the W34A mutant protein (as measured by Kd) towards CTD, drops from 10 μM of wild type to 180μM (Verdecia et al., 2000). A recent *in vivo* study done by Behrsin et al., has also demonstrated the importance of this residue, in which the W34A mutant failed to complement the function of ESS1 in ess1$^-$ strain of *S. cerevisiae* (Behrsin et al., 2006). Trp-34 is indeed in van der Waals contact with Pro-6' in CTD peptide and hydrogen bonds with the side chain hydroxyl group of Ser-7' (Verdecia et al., 2000). This residue is also highly conserved amongst the Pin1 homologues, as well as

amongst the Group IV WW domains. In our W34A mutant structure, no any side chain shift was observed. Thus, this indicates that the single localized perturbation of Trp-34 by alanine substitution is sufficient to abolish substrate binding, reinforcing the key role of Trp-34 in Pin1 function.

Despite of these speculations, it is difficult to conclude on the importance of residues involved in substrate recognition from structures of the free mutant proteins alone. This is substantiated in studies on the W34A mutant, which shows that side change shifts in structures of the free protein may not directly correlate to the effects of the mutation on Pin1 function. This would require some complexes with substrate, multi-site mutations, and binding assays. Indeed interestingly, our preliminary data shows that the substrate peptide binding capacity of F25A and R17A mutants was abolished to a greater extent than W34A mutant (unpublished data). Arg-17 would be an interesting residue to investigate. Unfortunately we could not have grown its protein crystal under the same condition as the other mutants. Different properties of R17A mutant may partly explain its different crystallization condition. These remain to be further investigated.

4.8 Speculations on the roles of residues in the PPIase domain

Mutations to alanine at Cys-113 and Met-130 at the PPIase domain did not affect the global as well as local conformation of Pin1 (these mutant structures were solved with a resolution of 2.0) (Figure 4-26). It is noteworthy to point out that the original wild type structure is in complex with Ala-Pro dipeptide at the PPIase active site

(PDB code: 1PIN). Without complex with any peptide at the active site, our mutant structures can be considered as the "real" wild type structure. We should expect to see the bound and unbound forms. However, surprisingly, we did not find any difference in the catalytic binding region. In other words, the dissociation or binding of Ala-Pro dipeptide did not induce any conformational change in this region. This suggests that this binding groove in the PPIase domain could be very rigid. In this way, the binding groove could serve as a sort of selectivity filter for the substrates.

The rigidity of the binding groove in the PPIase domain is consistent with the CD analyses. The CD analyses show that C113A, M130A, H59A, H157A, and L122A mutant proteins are all apparently less stable as revealed by their lower melting temperature (Figure 4-14). Hence, speculatively, disruption of these residues could have destroyed the core structure of the binding groove and rendered Pin1 unstable, thus diminishing its PPIase activity (Pastorino et al., 2006; Ranganathan et al., 1997; Ryo et al., 2001; Zhou et al., 2000), in addition to their direct role in Pin1's catalytic mechanism as proposed (Ranganathan et al., 1997; Behrsin et al., 2006). As a minor point, these mutants may not be appropriate as catalytic inactive mutants for functional comparisons. It would be essential to address this concern in the future studies.

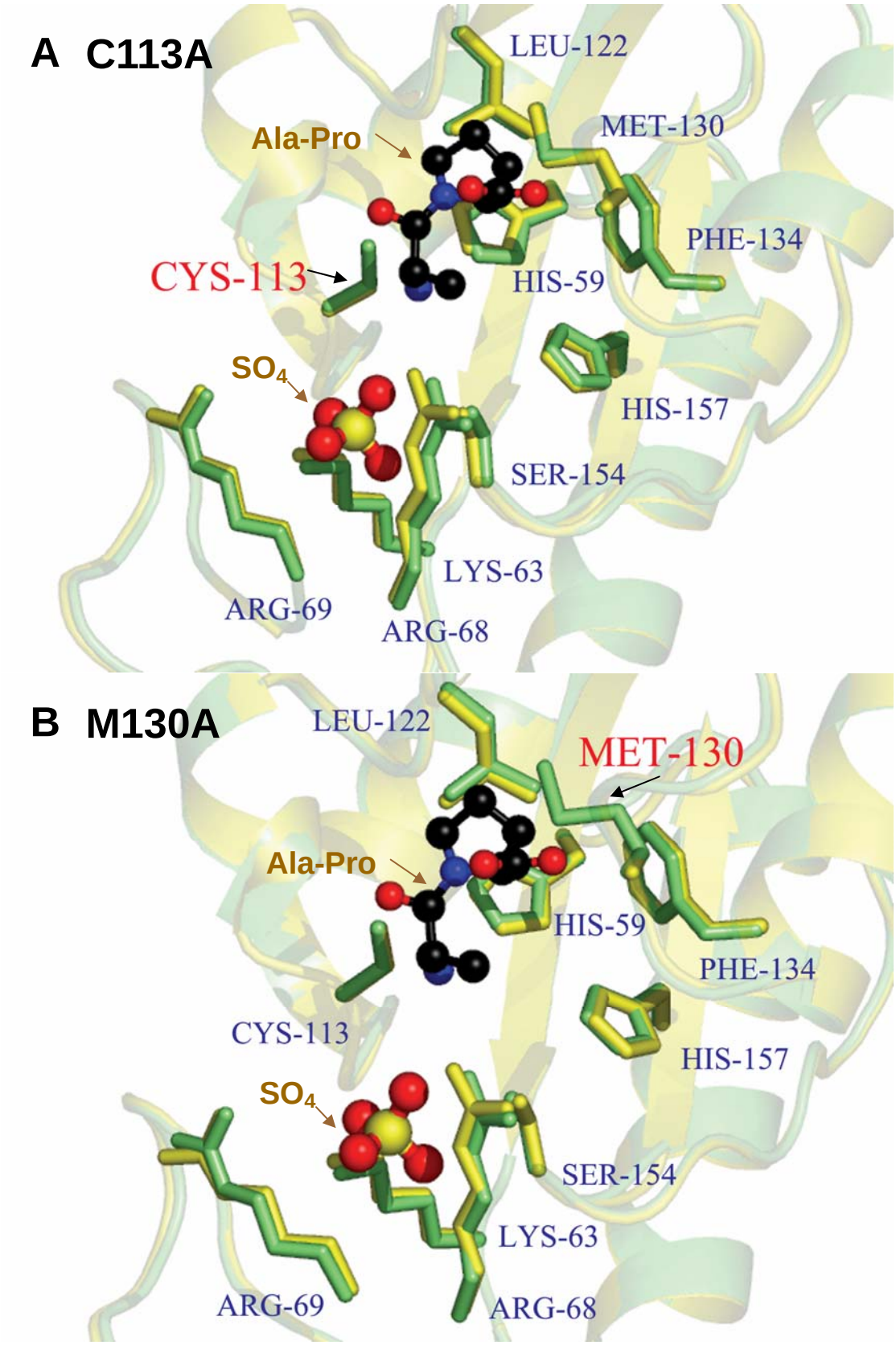
A C113A
LEU-122
MET-130
Ala-Pro
PHE-134
CYS-113
HIS-59
SO4
HIS-157
SER-154
LYS-63
ARG-69
ARG-68
B M130A
LEU-122
MET-130
Ala-Pro
HIS-59
PHE-134
CYS-113
HIS-157
SO4
SER-154
LYS-63
ARG-69
ARG-68

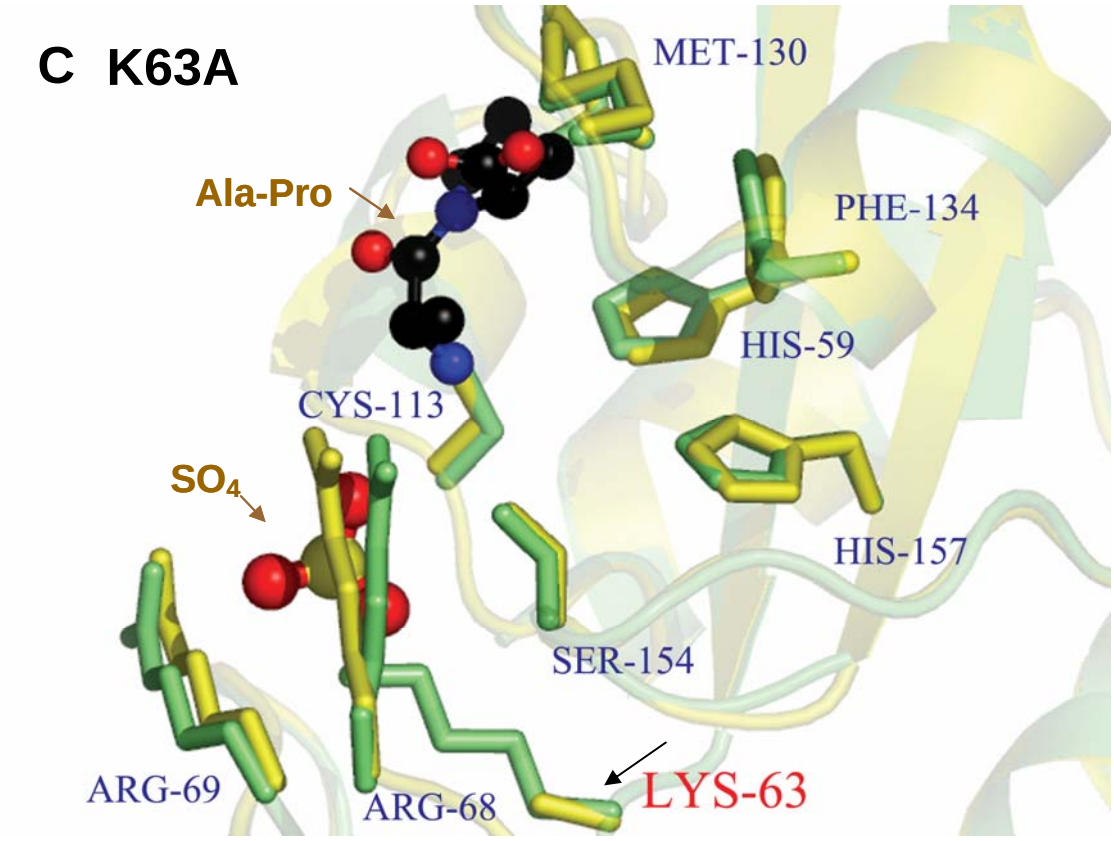

Figure 4-26: Catalytic site of PPIase domain mutants. PPIase domain mutants C113A (A), M130A (B), and K63A (C) were superimposed with wild type structure 1PIN for comparison on the sulphate group and Ala-Pro dipeptide binding. Previously reported important side chain were shown with wild type and mutant side chains represented as green and yellow, respectively. Besides the mutated residues (indicated by black arrows), no other side chains shifts were observed. Figures were generated by PyMOL.

On the other hand, mutation of Lys-63 to alanine did not affect the conformation of Pin1 as well (Figure 4-26). However, such a mutation did not lower Pin1 melting temperature (Figure 4-14), ruling out the possibility that the lost of function of K63A mutant was due to protein instability. This suggests that Lys-63, like Trp-34, may be functionally important to Pin1 in itself. This is consistent with the recent *in vivo* data reported by Behrsin *et al.* (Behrsin et al., 2006). Along the same line of investigation, Behrsin *et al.* have also reported that the negative charges of both Arg-68 and Arg-69 are essential for Pin1 function. Our data showed that double mutant R68A/R69A does

not destabilize Pin1 (Figure 4-14), thus vindicating the previously reported data, although crystal structures of the R68A/R69A mutant is unfortunately not available.

4.9 Modeling of Pin1 WW domain mutants in complex with the CTD peptide

Modeling of the WW domain Pin1 mutant structures in complex with the CTD peptide was next carried out based on the published wild type Pin1 crystal structure (PDB code: 1F8A) (Verdecia et al., 2000). 1F8A is the structure in which the Pin1 WW domain is in complex with the doubly phosphorylated CTD peptide (Tyr-pSer2'-Pro-Thr-pSer5'-Pro-Ser). By comparing these mutant structures with 1F8A, some generalized predictions on the phosphopeptide binding site of the WW domain mutants would be possible.

First, the backbone structures of the Pin1 WW domain mutants, including R14A, F25A, S32A, and W34A, were superimposed with 1F8A. All these mutants have a similar folding compared to 1F8A, except at the regions of α1/β1 loop and β1'/β2' loop, as reported previously for 1PIN (Figure 4-27, highlighted by dotted red circles). This is expected since 1PIN was the model structure used for molecular replacement to solve all the mutant structures in this study, and the mutants show identical folding as 1PIN as described earlier (Figure 4-21).

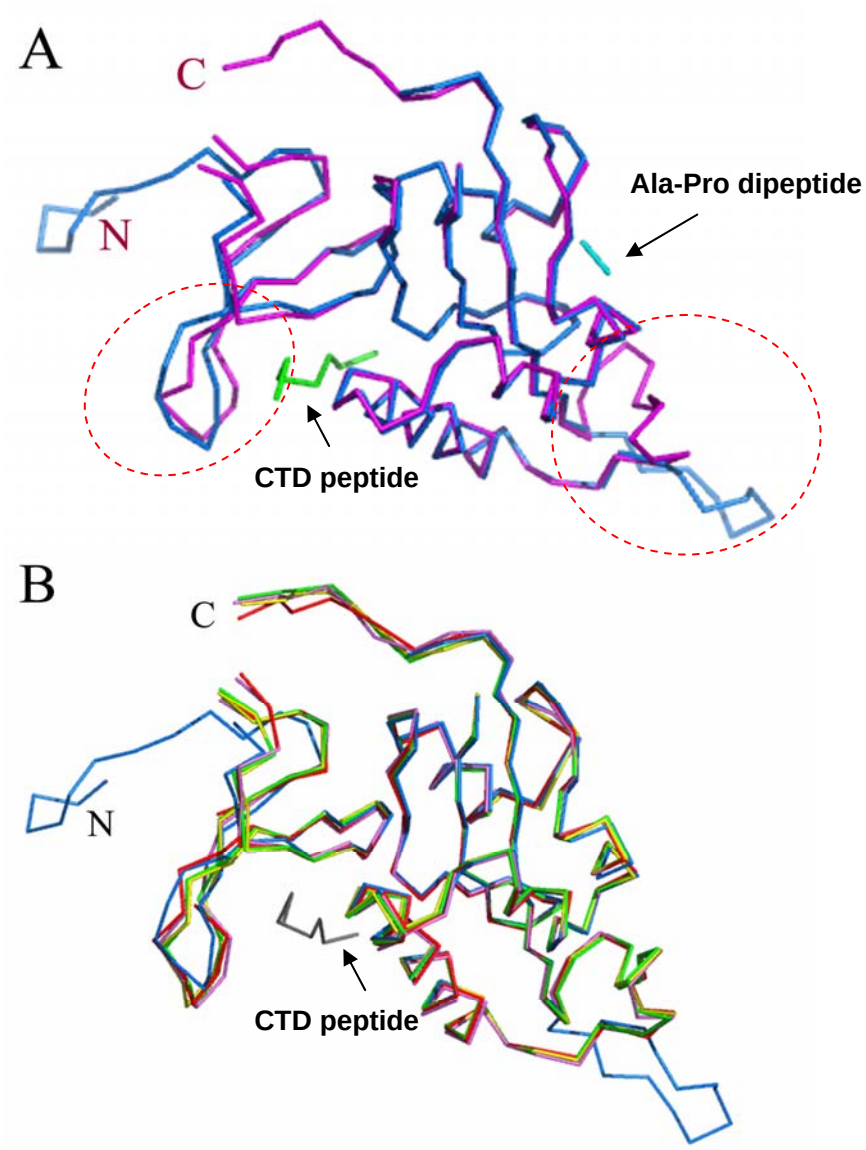

Figure 4-27: Backbone superposition of Pin1 crystal structures with 1F8A. (A) Superposition of wild-type structure 1PIN with 1F8A. 1PIN is the Pin1 crystal structure (magenta) in which the PPIase domain is in complex with Ala-Pro dipeptide (cyan), whereas 1F8A is the Pin1 crystal structure (blue) that the WW domain is in complex with CTD phosphopeptide (green). (B) Superposition of WW domain mutants R14A (magenta), F25A (red), S32A (cyan), and W34A (yellow) with 1F8A. Dotted line red circles indicate regions with structural deviations. Figures were generated by PyMOL.

Comparison of the side chains at the CTD binding site of of 1F8A with wild type Pin1 (PDB code: 1PIN) revealed several side chain shifts, including residues Arg-14, Ser-16, Arg-17, and Tyr-23 (Table 4-6). In comparing the various WW domain mutants and 1F8A, the same set of side chain shifts was observed (Table 4-6). Most of the shifts were similar to that of 1PIN. However, shifts of residue Arg-14 in F25A and S32A mutants, as well as that of residue Arg-17 in R14A, F25A and S32A mutants, were significantly different from that of 1PIN. The orientation of residue His-27 was observed to be shifted significantly in R14A, F25A, and S32A mutants (Figure 4-28). Since residue His-27 in the native structure is outside of the CTD binding region, whether it is involved in the substrate binding could not be addressed in this modeling exercise. However, residue His-27 could potentially be involved in substrate binding based on its location near to the CTD binding groove. As discussed before, although Arg-14 and Arg-17 reside in the binding groove, whether their side chain shifts in the mutants are biologically relevant is inconclusive.

4.10 Cellular localization of Pin1

The Pin1 mutants were expressed in mammalian cells to study the effect of the mutations on their biological functions *in vivo*, particularly to examine their cellular localization. Previous studies have revealed that Pin1 is predominantly localized in the nucleus or nuclear speckles. Moreover, an intact WW domain and an active catalytic site are essential for this nuclear localization (Lu et al., 1996b; Rippmann et al., 2000). There is no defined nuclear localization signal (NLS) in Pin1's sequence

(Lu et al., 2002a; Ranganathan et al., 1997). Thus, nuclear localization or nuclear import of Pin1, could have resulted from its interaction with cellular substrates (Lu et al., 2002a; Lu, 2003; Rippmann et al., 2000). Studying the localization of Pin1 mutants might therefore delineate the important residues in Pin1 function and substrate interaction *in vivo*.

Table 4-6: Summary of side chain comparison between mutants and wild-type Pin1 (PDB code: 1F8A). Significant side chain shifts (> 2.0 Å) were indicated [in angstrom (Å)]. A blank entry indicates that insignificant or no side chain shifts were observed. "--" indicates corresponding residue mutated. Side chain orientations which are significantly different from WT are underlined and highlighted in bold letters.

WT / Mutants	WT (1PIN)	R14A	F25A	C113A	K63A	W34A	S32A	M130A
Previously reported residues important for substrate binding at WW Domain								
R14	2.61	--	**3.87**	5.48	5.51	4.77	**3.48**	5.70
S16	3.78	5.12	4.13	3.57	4.46	7.04	6.00	3.61
R17	10.09	**8.30**	**7.65**	9.84	8.81	9.92	**7.85**	9.84
Y23	2.88	2.46	2.67		2.33			2.30
F25			--					
S32							--	
W34						--		
Residues not reported in previous studies								
E12	4.57	3.53	2.98		3.15	4.43	4.72	3.15
K13			4.18					
R21								6.21
H27	4.96	**0.71**	**0.38**	4.75	4.11	5.01	**2.18**	4.85
Q33					3.32			
E35								6.94
Q66								
E87	2.84	2.70	3.49		4.56	3.42	3.02	3.06
E100								
K117								

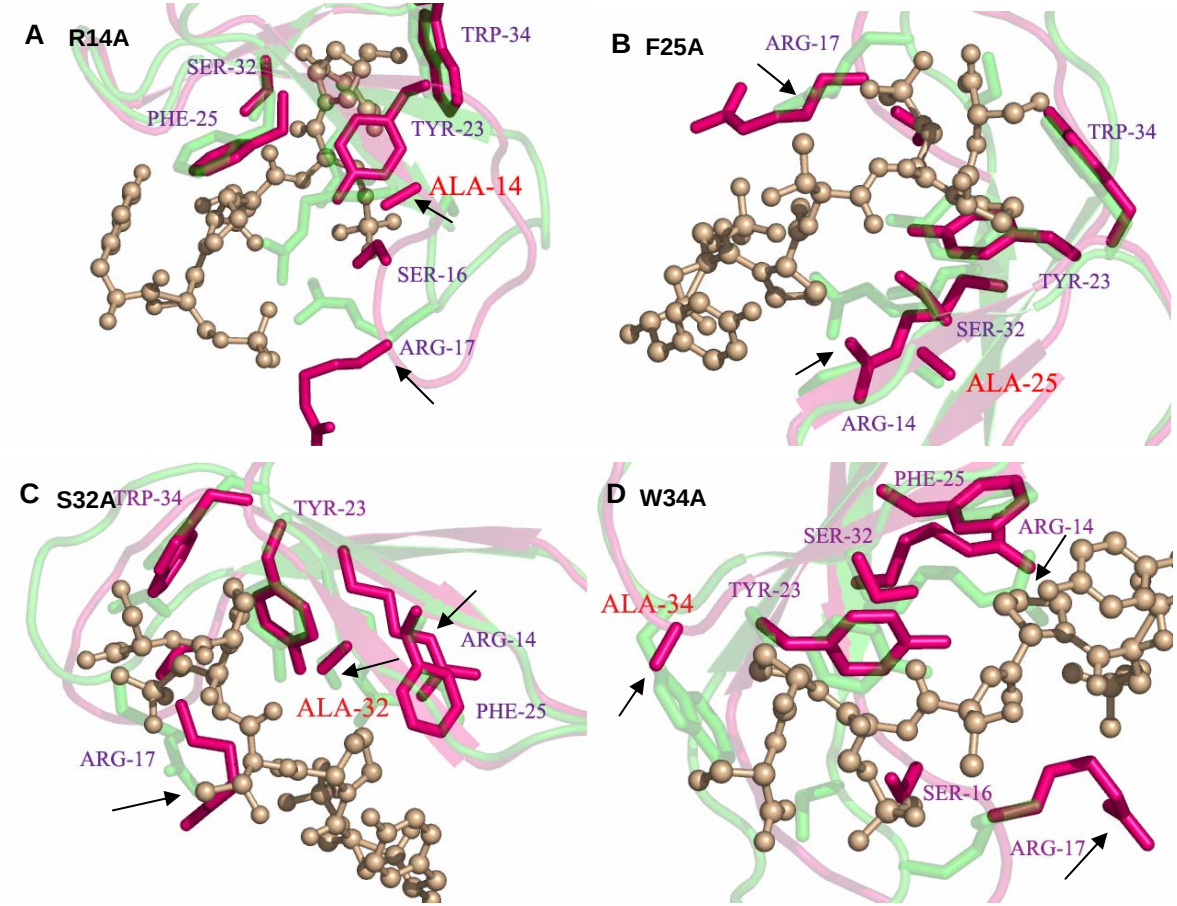

Figure 4-28: Superposition of Pin1 mutants with 1F8A at WW domain in complex with CTD peptide (Tyr-pSer2'-Pro-Thr-pSer5'-Pro-Ser). (A) R14A, (B) F25A, (C) S32A, and (D) W34A. Green denotes 1F8A; pink denotes mutants. Mutated side chains were shown. Besides the mutated site chains, site chain shifts at Arg-14 and Arg-17 were observed for all of these mutants (indicated by black arrows). Mutated residues were highlighted in red letters. Figures were generated by PyMOL.

Constructs of EGFP-tagged wild type Pin1 and the mutants (R14A, S16A, S16E, R17A, S32A, W34A, R68A/R69A, F25A, K63A, C113A, H59A, H157A, S154A, L122A, M130A) were first transiently expressed in HEK 293T cell lines. As shown by Western blot analysis of all lysates (Figure 4-29), all the EGFP-Pin1 constructs could be expressed in mammalian cells. The EGFP-Pin1 constructs were then transfected into HeLa cells and the subcellular localization of Pin1 was examined 20 hours after transfection by fluorescence microscopy. Consistent with previous findings, wild type Pin1 predominantly localized in the nucleus (Figure 4-30). Most of the mutations did not affect Pin1's nuclear localization, as shown in Figure 4-30 (only a few mutants were shown as representatives). However, W34A mutant had a diffused staining pattern of green fluorescence throughout the cells, thus validating the important role of residue Trp-34 in substrate binding *in vivo*. Interestingly, the C113A mutant protein was also preferentially localized in the nucleus, contradicting to the previous report (Rippmann et al., 2000). Moreover, for all mutants except W34A, it was observed that only some cells had Pin1 localization in the nuclear speckles. One possible explanation for this would be that the function and the cellular localization of Pin1 could be cell cycle dependent. Thus, cells were then synchronized to specific cell cycle stages using different drug treatments. Treatments with double thymidine and hydroxyurea block arrest cells at the early G1/S and late G1/S phase, respectively, whereas serum starvation arrests cells at G_0 phase. Cells that had a diffused green fluorescence pattern throughout the cells were quantified. As shown in Figure 4-31, mutation of Trp-34 to Ala (W34A) causes more mutant Pin1 to diffuse to the

cytoplasm compared to wild type in all the three cell cycle stage arrested populations. Translocation of C113A may also be cell cycle dependent. In addition, apoptosis in the majority of cells expressing the C113A mutant (which could induce apoptosis, consistent with previous report (Rippmann et al., 2000) could have biased the quantification. No obvious change in cellular localization was observed for the other mutants, namely R14A, S32A, F25A, K63A, and M130A.

Taken together, our data showed the importance of residue Trp-34 in Pin1 cellular function. Trp-34 may play a very critical role in substrate binding. Importantly, a single localized disruption of this residue, as discussed in session 4.7, would be sufficient to alter Pin1's function. However, whether the localization of wild type Pin1 is cell cycle specific is not conclusive from this study and remained to be further investigated.

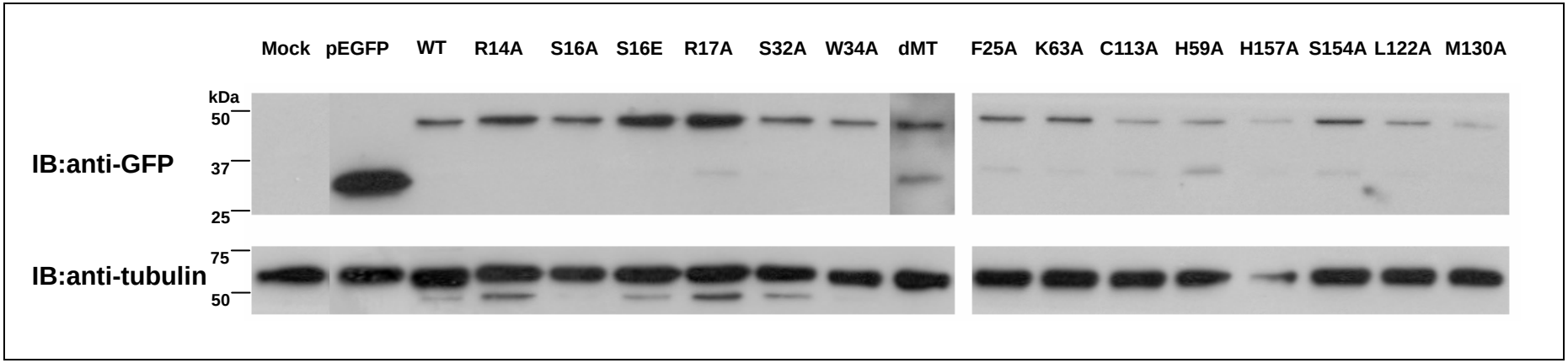

Figure 4-29: Pin1 overexpression in HEK 293T cells. 293T cells were transiently transfected with various EGFP-Pin1 constructs as indicated and the protein overexpressed were detected with Western blot by using anti-GFP antibody. All Pin1 mutant proteins were successfully expressed in the mammalian cells.

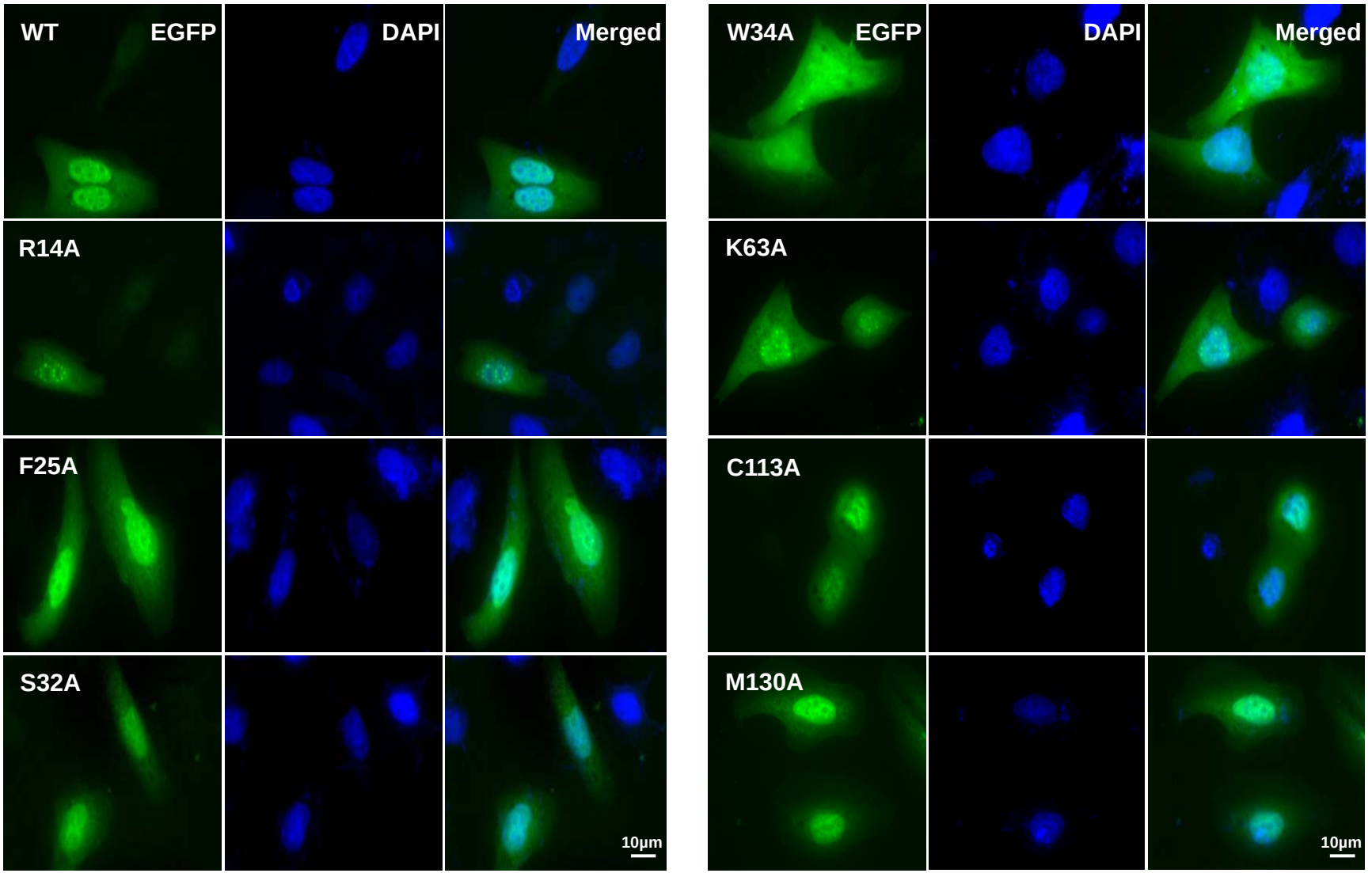
WT
EGFP
DAPI
Merged
W34A
EGFP
DAPI
Merged
R14A
K63A
F25A
C113A
S32A
M130A
10μm
10μm

Figure 4-30: Cellular localization of Pin1. Wild-type or mutant EGFP-Pin1 constructs were transiently transfected into HeLa cells. 20 hours after transfection, cells were fixed and stained with DAPI. Localization of Pin1 was imaged with a fluorescent microscope.

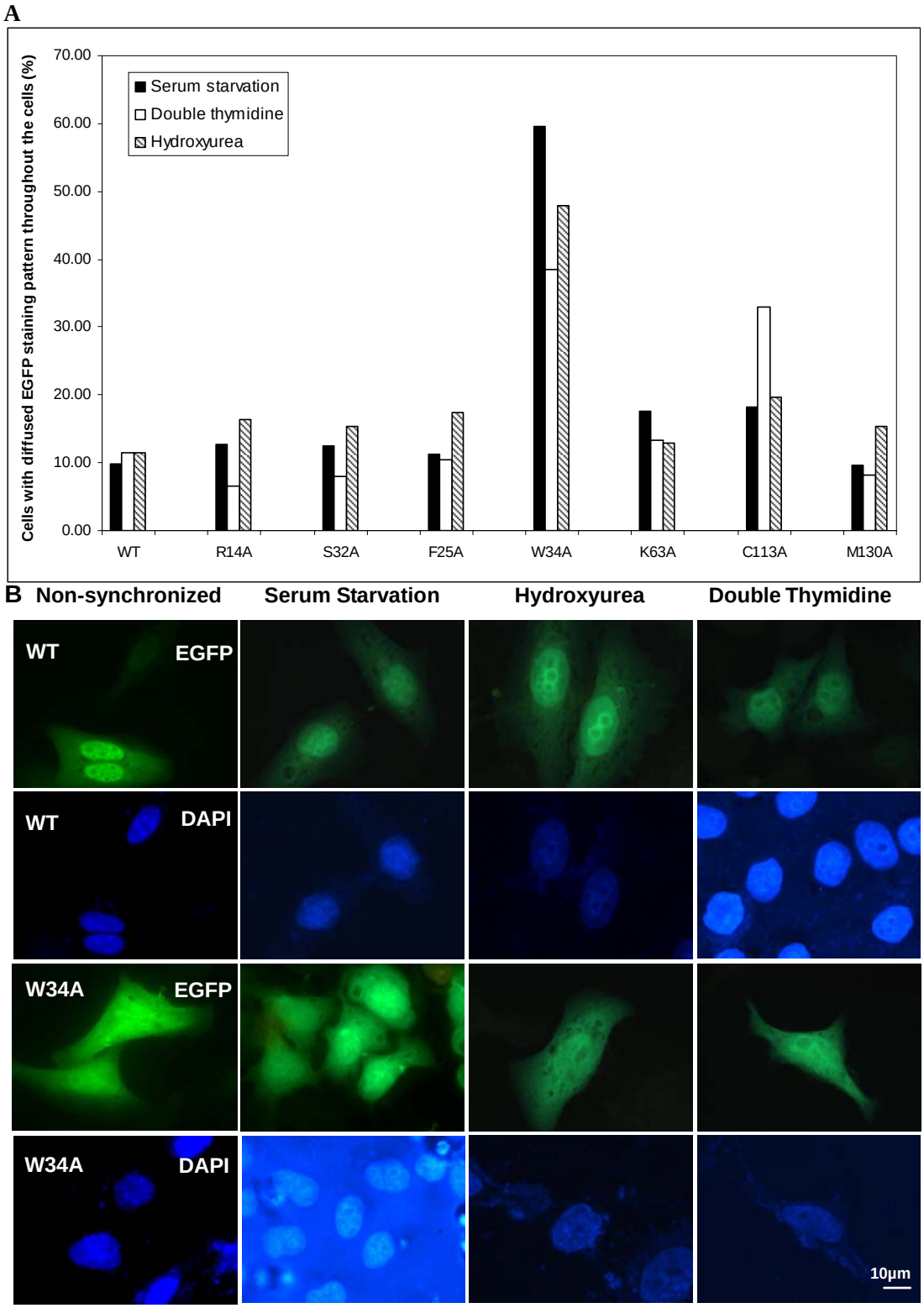

Figure 4-31: Subcellular localization of Pin1 during different cell cycle stages. HeLa cells grown on cover slips were transiently transfected with various EGFP-Pin1 constructs followed by serum starvation, double-thymidine block, and hydroxyurea treatments. Localization of Pin1 was observed and imaged under a fluorescence microscope. Numbers of cells showing more diffused green fluorescence to the cytosol in the various mutants were counted (A). Experiments were done twice and data shown are the averages of the two readings. (B) Fluorescence microscopy pictures of WT and W34A-construct transfected cells.

4.11 A proposed model for Pin1's mechanism of action—a new "two-step induced-fit" binding model

In the previous proposed "induced-fit" model based on the two available crystal structures of Pin1, 1PIN and 1F8A (Ranganathan et al., 1997; Verdecia et al., 2000), the α1/β1 loop with the tripartite basic cluster composing of Lys-63, Arg-68, and Arg-69 would act as a selectivity filter for phosphate. Upon phosphosubstrate binding to the catalytic site, the α1/β1 loop is induced to flip towards the bound substrate to adopt a "closed" conformation. Such a closed conformation encloses a cleft nicely fitting for a phosphorylated substrate (Ranganathan et al., 1997). According to this model, Pin1 would be in an "open" conformation when there is no substrate bound to the catalytic site. However and interestingly, the structures of the Pin1 mutants we have solved，which have no peptide recruited to the catalytic site, revealed a closed conformation. On the other hand, the Pin1 crystal structure 1F8A, which is in complex with CTD peptide at the WW domain, adopts an open conformation in the α1/β1 loop at the catalytic domain. A twist of the triple-stranded antiparallel β-sheet in WW domain was observed in this crystal structure as well (Verdecia et al., 2000). We also observed side chain shifts in the α1/β1 loop region when residues in the WW domain binding region were mutated (Arg-14 and Phe-25) (section 4.7). This has suggested an inherit mobility of this selectivity filter in solution through a twist in the WW domain upon binding or dissociation of a phosphopeptide at either the WW domain or PPIase domain, or both.

Taken together, these (the two reported crystal structures and our mutant structures)

suggest that peptide binding to the WW domain could stimulate the α1/β1 loop to be opened for the entering of substrate into the catalytic site (first step). The opening of the α1/β1 loop is through global conformational changes induced by the β-sheet twist in the WW domain, particularly involving Phe-25 and Arg-14. According to our data, mutation of Arg-14 and Phe-25 caused side chain shifts in Gln-66 and Arg-68, which reside in the α1/β1 loop region. Thus, peptide binding to the WW domain and particularly its interaction with Arg-14 and Phe-25 could be critical to induce the conformational change of the α1/β1 loop for the entering of substrate into the catalytic site. The entering of substrate into the catalytic site in turn causes another conformational change, resulting in the "closed" positioning of the α1/β1 loop (second step). Hence, we propose a "two-step induced-fit" binding model (Figure 4-32). The closing of the α1/β1 loop could be driven by the electrostatic interaction between the phosphate and the three positively charge residues at the α1/β1 loop (Lys-63, Arg-68, Arg-69) when phosphopeptide binds to the catalytic site.

In the model proposed by Bayer *et al*. through NMR studies, the Pin1 WW domain and PPIase domain are non-interacting in solution prior to substrate binding. These two domains are connected by a flexible linker comprising of Asn-40 to Gly-49. Upon substrate binding to the concave binding site in the WW domain (mainly through the hydrophobic and electrostatic interactions), the two domains are then brought together to interact with each other (Bayer et al., 2003). In accordance with our proposed "two-step induced-fit" binding model, the β-sheet twist at WW domain and the

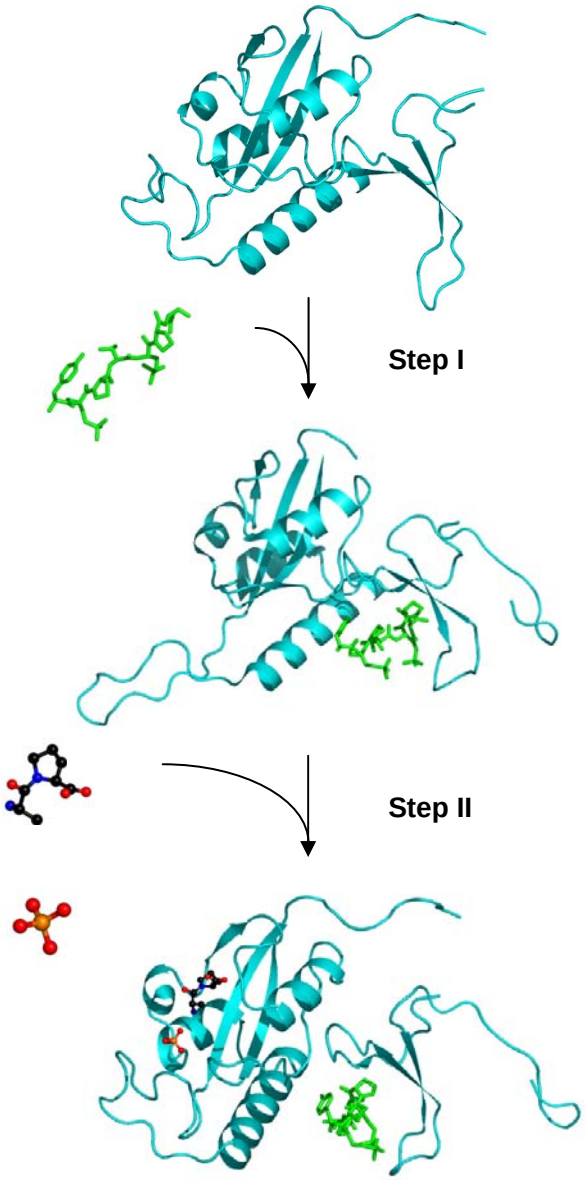

Figure 4-32: The "Two-step induced-fit" binding model. α1/β1 loop of Pin1 can adopt either closed or open conformation. Pin1 in itself is in closed conformation. Upon binding of substrate, as illustrated here with CTD peptide, the α1/β1 loop is induced to open (step I) to allow the binding of another substrate or another recognition motif within the same molecule, as illustrated with Ala-Pro dipeptide and sulphate ion. Recruitment of substrate at the PPIase active site induces a conformational change, causing α1/β1 loop to refold into a closed conformation (step II), followed by *cis-trans* isomerization of the oriented peptidyl prolyl bonds, leading to substrate conformation changes.

interaction of the two domains could be mediated through the flexible linker upon peptide binding to the concave binding site to trigger a global conformational change, leading to the α1/β1 loop to subsequently adopt an "open conformation" for substrate entering into PPIase catalytic site. Not only in all the NMR structures, the flexibility of the linker is also shown in the two crystal structures 1PIN and 1F8A, and all our seven mutant structures, in which no electron density map could be observed in this region.

The "two-step induced-fit" model may explain the case of the Pin1 homologue Ca-Ess1, which adopts a closed conformation without any phosphate recruited to the catalytic site (Li et al., 2005). Compared to the Pin1 crystal structure 1PIN (with a PEG molecule recruited to the WW domain), the Ca-Ess1 structure is one without any bound substrate. Thus, the recruitment of a PEG molecule in 1PIN may mimic substrate binding to the WW domain, inducing the α1/β1 loop to open up and enabling the Ala-Pro dipeptide and sulphate to enter the catalytic site, followed by the closure of the loop. In the case of Ca-Ess1, the α1/β1 loop is not induced to open to grant the entry of phosphate. This can also explain the NMR data reported by Bayer *et al.*, which showed that in either the presence or absence of sulphate ion, the α1/β1 loop remained in the closed conformation (Bayer et al., 2003).

In our model, the second step of peptide binding to the catalytic site and the closure of the α1/β1 loop may trigger second time of the β-sheet twist in the WW domain. This may cause the release of the substrate peptide from the WW domain, getting ready for the recruitment of another substrate peptide. The recruitment of second substrate

peptide in turn causes the opening of the α1/β1 loop to release the substrate peptide with its isomerized peptidyl prolyl bond from the catalytic site. This would allow the entering of another substrate peptide for isomerization. In this way, the cycle repeats for the carrying out Pin1's function in *cis*/*trans*-isomerization of its substrates. This has also pointed out that Pin1 may work on different peptidyl prolyl bonds within the same protein molecule, or different molecules interacting as a complex.

On the other hand, as discussed earlier based on our mutant structures and melting temperature analyses, the core catalytic site itself would be a very rigid structure. Thus, the catalytic site could act as a sort of selectivity filter for the substrates (section 4.8). The substrate selectivity in this binding groove for Ala-Pro dipeptide could even be more important than the phosphate selectivity at the α1/β1 loop. From our preliminary data, full-length Pin1 do not necessarily bind phosphorylated peptides better than the non-phosphorylated counterparts, although phosphorylated peptides are in general more favoured by the Pin1 WW domain (not published). This also raises the same question whether both the WW and PPIase domains work on the same peptidyl prolyl bond sequentially, or they work on different peptidyl prolyl bonds within the same protein molecule, or different molecules interacting as a complex. If the selectivity of this binding groove at the PPIase domain core region is critical, this could also explain why it is difficult for researchers to come out with a consensus sequence around the Ser/Thr-Pro motif.

At a more fundamental level of understanding, whether Pin1 could catalyze the

isomerization of the proline bond in the sequence of pSer/Thr-Pro remains debatable. The idea of pSer/Thr-Pro being the preferred substrate of Pin1 came from the Pin1 crystal structure in complex with the Ala-Pro dipeptide and a sulphate ion (Ranganathan et al., 1997). The vicinity and orientation of the dipeptide and sulphate ion suggested a substrate preference for pSer/Thr-Pro motifs. However, there is no direct evidence or direct visualization of this substrate preference. Frequently, another proline residue could be found a few amino acid residues downstream of the Ser/Thr-Pro motif in Pin1's substrates (Table 1-2). Hence it would be interesting to examine also whether the peptidyl prolyl bond orientated at the binding groove in the core catalytic site is the proline residue in the so-called Ser/Thr-Pro motif or is the proline lying downstream of the motif. In the later scenario, the pSer/Thr-Pro motif itself may bind to the WW domain, whereas the basic cluster at the α1/β1 loop can serve as second layer for substrate specificity towards the pSer/Thr-Pro motif. However, the PPIase domain would catalyze the isomerization of the prolyl bond downstream of pSer/Thr-Pro motif and not within.

Thus, in future studies, it would be important to work on Pin1 structure in complex with longer peptides or even the whole substrate protein that interact with the PPIase catalytic domain as well as WW domain peptide binding site to address all those uncertainties. A detailed peptide screen for optimized binding to full-length Pin1, and the WW or the PPIase domain alone would be helpful to further define the full recognition motif for Pin1.

CHAPTER 5: CONCLUSION AND FUTURE PERSPECTIVES

Pin1 is known to play important roles in a diverse array of cellular processes including cell cycle control, transcription and splicing regulation, DNA replication checkpoint control, DNA damage response, neuronal survival, and germ cell development. It functions by catalyzing peptidyl-prolyl isomerization and causes conformational changes of its substrates. Deregulation of Pin1 has been implicated in pathological conditions including cancers and neurodegenerative diseases. Structurally and functionally, Pin1 is a novel prolyl isomerase that specifically catalyzes the *cis*/*trans*-isomerization of proline within the sequence of phosphorylated Ser/Thr-Pro. In spite of knowledge in the wide range of its substrates, very little is known about its catalytic mechanism and how exactly it interacts with its biological substrates.

Structural studies on Pin1 mutants in this project aim to better understand Pin1's mechanism of action. Several Pin1 WW domain and PPIase domain mutants have been generated, cloned and expressed in *E. coli*. Large scale protein expression and purification were carried out for subsequent CD analysis and X-ray crystallography.

Melting temperature (Tm) analysis by CD revealed that only the PPIase domain mutants, including C113A, H59A, H157A, L122A, and M130A, but not the WW domain mutants, had lowered Tm. Interestingly, these residues reside at the core structure of the active site in the PPIase domain, and they might contribute to the

stability to the core structure of Pin1. Loss of PPIase activity in these PPIase domain mutants could thus be due either to the direct participation of these residues in Pin1's catalytic activity, or simply a result of the destabilization of the Pin1 core structure. Further investigation to verify the nature of these PPIase domain mutants is necessary before classifying them as PPIase-dead mutants. Moreover, CD data also supported the role of Pin1 residues Arg-14, Arg-17, Lys-63, Arg-68, and Arg-69 in phosphopeptide binding.

The structures of seven Pin1 mutants, including R14A, F25A, S32A, W34A, K63A, C113A, and M130A, were solved by molecular replacement analysis. The structures of these mutants were in general grossly similar to wild type Pin1. The R14A, F25A, and S32A mutant structures exhibited side chain shifts in residues Arg-14, Arg-17, Arg-21 His-27, Gln-66, Arg-68, and Lys-117, suggesting their possible involvement in substrate binding. Interestingly, side chain shifts observed in the PPIase domain (Gln-66 and Arg-68) in R14A and F25A mutants suggested that Arg-14 and Phe-25 in the WW domain could be important to cause a conformational change at the α1/β1 loop upon substrate binding to the WW domain. The Trp-34 in the WW domain was previously identified as an important residue in substrate binding. On the other hand, Lys-63, together with another two basic residues Arg-68 and Arg-69, resides in the α1/β1 loop, acting as the selectivity filter for phosphopeptide. Interestingly, deleterious mutations of Trp-34 and Lys-63 did not perturb the structural positioning of any other nearby residues. This implies that single, localized perturbations of Trp-34 or Lys-63

would be sufficient to abolish Pin1 function. These data further support the critical role of these two residues in Pin1 function. The biological importance of Trp-34 was further revealed by Pin1 localization studies, in which substitution of Trp-34 with Ala caused Pin1 to translocate from the nucleus to the cytoplasm.

It is noteworthy to point out that X-ray structures of free proteins are not sufficient to describe the properties of mutants and to conclude the importance of residues involved in substrate recognition. This would require some complexes with substrate, multi-site mutations, and binding assays. *In vivo* studies would also help to verify the biological significance of those important residues. Nevertheless, our information on these side chain shifts would be useful in future studies and aid in identifying potential residues important in substrate binding.

Superpositions of mutant structures with 1PIN (in which Pin1 is in complex with Ala-Pro dipeptide at the PPIase domain catalytic site) and with 1F8A (in which Pin1 is in complex with CTD phosphopeptide at WW domain) provided little information on the role of various side chains in peptide binding. However, in our mutant structures, where there was no Ala-Pro dipeptide bound to the catalytic site, did not exhibit any conformational difference at the catalytic site when compared which 1PIN. This observation suggested that the catalytic site could be a very rigid structure to serve as a selectivity filter for substrates.

Our crystal structures of Pin1 mutants revealed a closed conformation of the α1/β1

loop in all the mutants, although there is no sulphate or phosphate ion recruited to the PPIase catalytic site. This result contradicts the previously proposed "induced-fit" model. Thus, together with our mutant structures, a "two-step induced-fit" model is proposed to explain Pin1's mechanism of action. In our model, the Pin1 WW domain and PPIase domain interact weakly, and the α1/β1 loop is in a closed conformation. Upon binding of substrate to the WW domain, the two domains were promoted to interact with each other and the β-sheet twist in WW domain triggers a global conformational change, causing the α1/β1 loop to open (step I). This open conformation allows the binding of another substrate or another recognition motif within the same molecule. Recruitment of substrate to the PPIase active site then induces another conformational change, causing the α1/β1 loop to refold into a closed conformation (step II). This is then followed by *cis-trans* isomerization of the peptidyl prolyl bonds, leading to substrate conformation change for the regulation of substrate activity. We also proposed that the core catalytic site itself could be a very rigid structure to serve as a critical selectivity filter for substrates. It could even be more critical than the phosphate selectivity at the α1/β1 loop.

Together, these studies provide a deeper understanding of how Pin1 interacts with its biological target proteins. Although X-ray crystal structures alone are not sufficient to describe the properties of mutantsSeveral speculative points remained to be addressed: I) whether both WW and PPIase domains work on the same peptidyl prolyl bond sequentially, or they act simultaneously on different peptidyl prolyl bonds within

the same protein molecule or in different molecules interacting as a complex; and II) whether Pin1 catalyzes the isomerization of the proline bond in the sequence of pSer/Thr-Pro motif itself. To address these issues in the future, more Pin1 structures in complex with its biological substrates or longer peptides would be necessary. It would also be necessary to further verify our hypothesized "two-step induced-fit" binding model by titrating Pin1 with CTD peptide and Ala-Pro dipeptide for the examination of the resonance change at the α1/β1 and β1'/β2' loop regions. Alternatively, enzyme kinetics studies would be useful. Tools, such as NMR-based methods, could be developed to visualize the dynamic movements of the functional domains upon the binding of longer peptides or even the whole substrate molecule. Lastly, a detailed peptide screen for optimal binding to full-length Pin1, WW domain, or PPIase domain alone would also be helpful to further define the substrate recognition motif of Pin1.

BIBLIOGRAPHY

Albert,A.L., Lavoie,S.B., and Vincent,M. (2004). Multisite phosphorylation of Pin1-associated mitotic phosphoproteins revealed by monoclonal antibodies MPM-2 and CC-3. BMC. Cell Biol. *5*, 22.

Basu,A., Das,M., Qanungo,S., Fan,X.J., DuBois,G., and Haldar,S. (2002). Proteasomal degradation of human peptidyl prolyl isomerase pin1-pointing phospho Bcl2 toward dephosphorylation. Neoplasia. *4*, 218-227.

Basu,A. and Haldar,S. (2002). Signal-induced site specific phosphorylation targets Bcl2 to the proteasome pathway. Int. J. Oncol. *21*, 597-601.

Bayer,E., Goettsch,S., Mueller,J.W., Griewel,B., Guiberman,E., Mayr,L.M., and Bayer,P. (2003). Structural analysis of the mitotic regulator hPin1 in solution: insights into domain architecture and substrate binding. J. Biol. Chem. *278*, 26183-26193.

Becker,E.B. and Bonni,A. (2006). Pin1 mediates neural-specific activation of the mitochondrial apoptotic machinery. Neuron *49*, 655-662.

Behrsin,C.D., Bailey,M.L., Bateman,K.S., Hamilton,K.S., Wahl,L.M., Brandl,C.J., Shilton,B.H., and Litchfield,D.W. (2006). Functionally Important Residues in the Peptidyl-prolyl Isomerase Pin1 Revealed by Unigenic Evolution. J. Mol. Biol.

Berger,M., Stahl,N., Del,S.G., and Haupt,Y. (2005). Mutations in proline 82 of p53 impair its activation by Pin1 and Chk2 in response to DNA damage. Mol. Cell Biol. *25*, 5380-5388.

Bradford,M.M. (1976). A rapid and sensitive method for the quantitation of microgram quantities of protein utilizing the principle of protein-dye binding. Anal. Biochem. *72*, 248-254.

Brondani,V., Schefer,Q., Hamy,F., and Klimkait,T. (2005). The peptidyl-prolyl isomerase Pin1 regulates phospho-Ser77 retinoic acid receptor alpha stability. Biochem. Biophys. Res. Commun. *328*, 6-13.

Brown,N.R., Noble,M.E., Endicott,J.A., and Johnson,L.N. (1999). The structural basis for specificity of substrate and recruitment peptides for cyclin-dependent kinases. Nat. Cell Biol. *1*, 438-443.

Brunger,A.T., Adams,P.D., Clore,G.M., DeLano,W.L., Gros,P., Grosse-Kunstleve,R.W., Jiang,J.S., Kuszewski,J., Nilges,M., Pannu,N.S., Read,R.J., Rice,L.M., Simonson,T., and Warren,G.L. (1998). Crystallography & NMR system: A new software suite for macromolecular structure determination. Acta Crystallogr. D. Biol. Crystallogr. *54*, 905-921.

Campaner,S., Kaldis,P., Izraeli,S., and Kirsch,I.R. (2005). Sil phosphorylation in a Pin1 binding domain affects the duration of the spindle checkpoint. Mol. Cell Biol. *25*, 6660-6672.

Campbell,H.D., Webb,G.C., Fountain,S., and Young,I.G. (1997). The human PIN1 peptidyl-prolyl cis/trans isomerase gene maps to human chromosome 19p13 and the closely related PIN1L gene to 1p31. Genomics *44*, 157-162.

Chen,J., Li,L., Zhang,Y., Yang,H., Wei,Y., Zhang,L., Liu,X., and Yu,L. (2006). Interaction of Pin1 with Nek6 and characterization of their expression correlation in Chinese hepatocellular carcinoma patients. Biochem. Biophys. Res. Commun. *341*, 1059-1065.

Collaborative Computational Project Number 4 (1994). The CCP4 suite: programs for protein crystallography. Acta Crystallogr. D. Biol. Crystallogr. *50*, 760-763.

Crenshaw,D.G., Yang,J., Means,A.R., and Kornbluth,S. (1998). The mitotic peptidyl-prolyl isomerase, Pin1, interacts with Cdc25 and Plx1. EMBO J. *17*, 1315-1327.

Dougherty,M.K., Muller,J., Ritt,D.A., Zhou,M., Zhou,X.Z., Copeland,T.D., Conrads,T.P., Veenstra,T.D., Lu,K.P., and Morrison,D.K. (2005). Regulation of Raf-1 by direct feedback phosphorylation. Mol. Cell *17*, 215-224.

Eckerdt,F., Yuan,J., Saxena,K., Martin,B., Kappel,S., Lindenau,C., Kramer,A., Naumann,S., Daum,S., Fischer,G., Dikic,I., Kaufmann,M., and Strebhardt,K. (2005). Polo-like kinase 1-mediated phosphorylation stabilizes Pin1 by inhibiting its ubiquitination in human cells. J. Biol. Chem. *280*, 36575-36583.

Fischer,G., Tradler,T., and Zarnt,T. (1998). The mode of action of peptidyl prolyl cis/trans isomerases in vivo: binding vs. catalysis. FEBS Lett. *426*, 17-20.

Fujimori,F., Takahashi,K., Uchida,C., and Uchida,T. (1999). Mice lacking Pin1 develop normally, but are defective in entering cell cycle from G(0) arrest. Biochem. Biophys. Res. Commun. *265*, 658-663.

Gerez,L., Mohrmann,K., van,R.M., Jongeneelen,M., Zhou,X.Z., Lu,K.P., and van Der,S.P. (2000). Accumulation of rab4GTP in the cytoplasm and association with the peptidyl-prolyl isomerase pin1 during mitosis. Mol. Biol. Cell *11*, 2201-2211.

Hani,J., Stumpf,G., and Domdey,H. (1995). PTF1 encodes an essential protein in Saccharomyces cerevisiae, which shows strong homology with a new putative family of PPIases. FEBS Lett. *365*, 198-202.

Harrison,R.K. and Stein,R.L. (1990). Substrate specificities of the peptidyl prolyl cis-trans isomerase activities of cyclophilin and FK-506 binding protein: evidence for the existence of a family of distinct enzymes. Biochemistry *29*, 3813-3816.

Hashemzadeh-Bonehi,L., Phillips,R.G., Cairns,N.J., Mosaheb,S., and Thorpe,J.R. (2006). Pin1 protein associates with neuronal lipofuscin: potential consequences in age-related neurodegeneration. Exp. Neurol. *199*, 328-338.

He,J., Lau,A.G., Yaffe,M.B., and Hall,R.A. (2001). Phosphorylation and cell cycle-dependent regulation of Na+/H+ exchanger regulatory factor-1 by Cdc2 kinase. J. Biol. Chem. *276*, 41559-41565.

Hong,J.W., Ryu,M.S., and Lim,I.K. (2005). Phosphorylation of serine 147 of tis21/BTG2/pc3 by p-Erk1/2 induces Pin-1 binding in cytoplasm and cell death. J. Biol. Chem. *280*, 21256-21263.

Hsu,T., McRackan,D., Vincent,T.S., and Gert de,C.H. (2001). Drosophila Pin1 prolyl isomerase Dodo is a MAP kinase signal responder during oogenesis. Nat. Cell Biol. *3*, 538-543.

Huang,H.K., Forsburg,S.L., John,U.P., O'Connell,M.J., and Hunter,T. (2001). Isolation and characterization of the Pin1/Ess1p homologue in Schizosaccharomyces pombe. J. Cell Sci. *114*, 3779-3788.

Huang,X., Poy,F., Zhang,R., Joachimiak,A., Sudol,M., and Eck,M.J. (2000). Structure of a WW domain containing fragment of dystrophin in complex with beta-dystroglycan. Nat. Struct. Biol. *7*, 634-638.

Jacobs,D.M., Saxena,K., Vogtherr,M., Bernado,P., Pons,M., and Fiebig,K.M. (2003). Peptide binding induces large scale changes in inter-domain mobility in human Pin1. J. Biol. Chem. *278*, 26174-26182.

Jones,T.A., Zou,J.Y., Cowan,S.W., and Kjeldgaard,M. (1991). Improved methods for building protein models in electron density maps and the location of errors in these models. Acta Crystallogr. A *47 (Pt 2)*, 110-119.

Kamimoto,T., Zama,T., Aoki,R., Muro,Y., and Hagiwara,M. (2001). Identification of a novel kinesin-related protein, KRMP1, as a target for mitotic peptidyl-prolyl isomerase Pin1. J. Biol. Chem. *276*, 37520-37528.

Kato,Y., Ito,M., Kawai,K., Nagata,K., and Tanokura,M. (2002). Determinants of ligand specificity in groups I and IV WW domains as studied by surface plasmon resonance and model building. J. Biol. Chem. *277*, 10173-10177.

Kato,Y., Nagata,K., Takahashi,M., Lian,L., Herrero,J.J., Sudol,M., and Tanokura,M. (2004). Common mechanism of ligand recognition by group II/III WW domains: redefining their functional classification. J. Biol. Chem. *279*, 31833-31841.

Katzman,R. and Saitoh,T. (1991). Advances in Alzheimer's disease. FASEB J. *5*, 278-286.

Ke,H.M., Zydowsky,L.D., Liu,J., and Walsh,C.T. (1991). Crystal structure of recombinant human T-cell cyclophilin A at 2.5 A resolution. Proc. Natl. Acad. Sci. U. S. A *88*, 9483-9487.

Kerr,M.L. and Small,D.H. (2005). Cytoplasmic domain of the beta-amyloid protein precursor of Alzheimer's disease: function, regulation of proteolysis, and implications for drug development. J. Neurosci. Res. *80*, 151-159.

Kops,O., Eckerskorn,C., Hottenrott,S., Fischer,G., Mi,H., and Tropschug,M. (1998). Ssp1, a site-specific parvulin homolog from Neurospora crassa active in protein folding. J. Biol. Chem. *273*, 31971-31976.

Koradi,R., Billeter,M., and Wuthrich,K. (1996). MOLMOL: a program for display and analysis of macromolecular structures. J. Mol. Graph. *14*, 51-32.

Landrieu,I., Wieruszeski,J.M., Wintjens,R., Inze,D., and Lippens,G. (2002). Solution structure of the single-domain prolyl cis/trans isomerase PIN1At from Arabidopsis thaliana. J. Mol. Biol. *320*, 321-332.

Li,Z., Li,H., Devasahayam,G., Gemmill,T., Chaturvedi,V., Hanes,S.D., and Van,R.P. (2005). The structure of the Candida albicans Ess1 prolyl isomerase reveals a well-ordered linker that restricts domain mobility. Biochemistry *44*, 6180-6189.

Liou,Y.C., Ryo,A., Huang,H.K., Lu,P.J., Bronson,R., Fujimori,F., Uchida,T., Hunter,T., and Lu,K.P. (2002). Loss of Pin1 function in the mouse causes phenotypes resembling cyclin D1-null phenotypes. Proc. Natl. Acad. Sci. U. S. A *99*, 1335-1340.

Liu,W., Youn,H.D., Zhou,X.Z., Lu,K.P., and Liu,J.O. (2001). Binding and regulation of the transcription factor NFAT by the peptidyl prolyl cis-trans isomerase Pin1. FEBS Lett. *496*, 105-108.

Lu,K.P. (2003). Prolyl isomerase Pin1 as a molecular target for cancer diagnostics and therapeutics. Cancer Cell *4*, 175-180.

Lu,K.P., Hanes,S.D., and Hunter,T. (1996a). A human peptidyl-prolyl isomerase essential for regulation of mitosis. Nature *380*, 544-547.

Lu,K.P., Hanes,S.D., and Hunter,T. (1996b). A human peptidyl-prolyl isomerase essential for regulation of mitosis. Nature *380*, 544-547.

Lu,K.P. and Hunter,T. (1995). Evidence for a NIMA-like mitotic pathway in vertebrate cells. Cell *81*, 413-424.

Lu,K.P., Liou,Y.C., and Vincent,I. (2003a). Proline-directed phosphorylation and isomerization in mitotic regulation and in Alzheimer's Disease. Bioessays *25*, 174-181.

Lu,K.P., Liou,Y.C., and Vincent,I. (2003b). Proline-directed phosphorylation and isomerization in mitotic regulation and in Alzheimer's Disease. Bioessays *25*, 174-181.

Lu,K.P., Liou,Y.C., and Vincent,I. (2003c). Proline-directed phosphorylation and isomerization in mitotic regulation and in Alzheimer's Disease. Bioessays *25*, 174-181.

Lu,K.P., Liou,Y.C., and Zhou,X.Z. (2002a). Pinning down proline-directed phosphorylation signaling. Trends Cell Biol. *12*, 164-172.

Lu,P.J., Wulf,G., Zhou,X.Z., Davies,P., and Lu,K.P. (1999a). The prolyl isomerase Pin1 restores the function of Alzheimer-associated phosphorylated tau protein. Nature *399*, 784-788.

Lu,P.J., Zhou,X.Z., Liou,Y.C., Noel,J.P., and Lu,K.P. (2002b). Critical role of WW domain phosphorylation in regulating phosphoserine binding activity and Pin1 function. J. Biol. Chem. *277*, 2381-2384.

Lu,P.J., Zhou,X.Z., Shen,M., and Lu,K.P. (1999b). Function of WW domains as phosphoserine- or phosphothreonine-binding modules. Science *283*, 1325-1328.

Macias,M.J., Wiesner,S., and Sudol,M. (2002). WW and SH3 domains, two different scaffolds to recognize proline-rich ligands. FEBS Lett. *513*, 30-37.

Maleszka,R., Hanes,S.D., Hackett,R.L., de Couet,H.G., and Miklos,G.L. (1996). The Drosophila melanogaster dodo (dod) gene, conserved in humans, is functionally interchangeable with the ESS1 cell division gene of Saccharomyces cerevisiae. Proc. Natl. Acad. Sci. U. S. A *93*, 447-451.

Mantovani,F., Piazza,S., Gostissa,M., Strano,S., Zacchi,P., Mantovani,R., Blandino,G., and Del,S.G. (2004). Pin1 links the activities of c-Abl and p300 in regulating p73 function. Mol. Cell *14*, 625-636.

Metzner,M., Stoller,G., Rucknagel,K.P., Lu,K.P., Fischer,G., Luckner,M., and Kullertz,G. (2001). Functional replacement of the essential ESS1 in yeast by the plant parvulin DlPar13. J. Biol. Chem. *276*, 13524-13529.

Michnick,S.W., Rosen,M.K., Wandless,T.J., Karplus,M., and Schreiber,S.L. (1991). Solution structure of FKBP, a rotamase enzyme and receptor for FK506 and rapamycin. Science *252*, 836-839.

Min,S.H., Cho,J.S., Oh,J.H., Shim,S.B., Hwang,D.Y., Lee,S.H., Jee,S.W., Lim,H.J., Kim,M.Y., Sheen,Y.Y., Lee,S.H., and Kim,Y.K. (2005). Tau and GSK3beta dephosphorylations are required for regulating Pin1 phosphorylation. Neurochem. Res. *30*, 955-961.

Monje,P., Hernandez-Losa,J., Lyons,R.J., Castellone,M.D., and Gutkind,J.S. (2005). Regulation of the transcriptional activity of c-Fos by ERK. A novel role for the prolyl isomerase PIN1. J. Biol. Chem. *280*, 35081-35084.

Orlicky,S., Tang,X., Willems,A., Tyers,M., and Sicheri,F. (2003). Structural basis for phosphodependent substrate selection and orientation by the SCFCdc4 ubiquitin ligase. Cell *112*, 243-256.

Osmani,S.A., Pu,R.T., and Morris,N.R. (1988). Mitotic induction and maintenance by overexpression of a G2-specific gene that encodes a potential protein kinase. Cell *53*, 237-244.

Pastorino,L., Sun,A., Lu,P.J., Zhou,X.Z., Balastik,M., Finn,G., Wulf,G., Lim,J., Li,S.H., Li,X., Xia,W., Nicholson,L.K., and Lu,K.P. (2006). The prolyl isomerase Pin1 regulates amyloid precursor protein processing and amyloid-beta production. Nature *440*, 528-534.

Pathan,N., ime-Sempe,C., Kitada,S., Basu,A., Haldar,S., and Reed,J.C. (2001). Microtubule-targeting drugs induce bcl-2 phosphorylation and association with Pin1. Neoplasia. *3*, 550-559.

Proteau,A., Blier,S., Albert,A.L., Lavoie,S.B., Traish,A.M., and Vincent,M. (2005). The multifunctional nuclear protein p54nrb is multiphosphorylated in mitosis and interacts with the mitotic regulator Pin1. J. Mol. Biol. *346*, 1163-1172.

Rahfeld,J.U., Rucknagel,K.P., Schelbert,B., Ludwig,B., Hacker,J., Mann,K., and Fischer,G. (1994a). Confirmation of the existence of a third family among peptidyl-prolyl cis/trans isomerases. Amino acid sequence and recombinant production of parvulin. FEBS Lett. *352*, 180-184.

Rahfeld,J.U., Schierhorn,A., Mann,K., and Fischer,G. (1994b). A novel peptidyl-prolyl cis/trans isomerase from Escherichia coli. FEBS Lett. *343*, 65-69.

Ranganathan,R., Lu,K.P., Hunter,T., and Noel,J.P. (1997). Structural and functional analysis of the

mitotic rotamase Pin1 suggests substrate recognition is phosphorylation dependent. Cell *89*, 875-886.

revalo-Rodriguez,M., Cardenas,M.E., Wu,X., Hanes,S.D., and Heitman,J. (2000). Cyclophilin A and Ess1 interact with and regulate silencing by the Sin3-Rpd3 histone deacetylase. EMBO J. *19*, 3739-3749.

Rippmann,J.F., Hobbie,S., Daiber,C., Guilliard,B., Bauer,M., Birk,J., Nar,H., Garin-Chesa,P., Rettig,W.J., and Schnapp,A. (2000). Phosphorylation-dependent proline isomerization catalyzed by Pin1 is essential for tumor cell survival and entry into mitosis. Cell Growth Differ. *11*, 409-416.

Rudd,K.E., Sofia,H.J., Koonin,E.V., Plunkett,G., III, Lazar,S., and Rouviere,P.E. (1995). A new family of peptidyl-prolyl isomerases. Trends Biochem. Sci. *20*, 12-14.

Ryo,A., Liou,Y.C., Wulf,G., Nakamura,M., Lee,S.W., and Lu,K.P. (2002). PIN1 is an E2F target gene essential for Neu/Ras-induced transformation of mammary epithelial cells. Mol. Cell Biol. *22*, 5281-5295.

Ryo,A., Nakamura,M., Wulf,G., Liou,Y.C., and Lu,K.P. (2001). Pin1 regulates turnover and subcellular localization of beta-catenin by inhibiting its interaction with APC. Nat. Cell Biol. *3*, 793-801.

Ryo,A., Suizu,F., Yoshida,Y., Perrem,K., Liou,Y.C., Wulf,G., Rottapel,R., Yamaoka,S., and Lu,K.P. (2003). Regulation of NF-kappaB signaling by Pin1-dependent prolyl isomerization and ubiquitin-mediated proteolysis of p65/RelA. Mol. Cell *12*, 1413-1426.

Ryo,A., Togo,T., Nakai,T., Hirai,A., Nishi,M., Yamaguchi,A., Suzuki,K., Hirayasu,Y., Kobayashi,H., Perrem,K., Liou,Y.C., and Aoki,I. (2006). Prolyl-isomerase Pin1 accumulates in lewy bodies of parkinson disease and facilitates formation of alpha-synuclein inclusions. J. Biol. Chem. *281*, 4117-4125.

Saitoh,T., Tun-Kyi,A., Ryo,A., Yamamoto,M., Finn,G., Fujita,T., Akira,S., Yamamoto,N., Lu,K.P., and Yamaoka,S. (2006). Negative regulation of interferon-regulatory factor 3-dependent innate antiviral response by the prolyl isomerase Pin1. Nat. Immunol. *7*, 598-605.

Schiene,C. and Fischer,G. (2000). Enzymes that catalyse the restructuring of proteins. Curr. Opin. Struct. Biol. *10*, 40-45.

Schutkowski,M., Bernhardt,A., Zhou,X.Z., Shen,M., Reimer,U., Rahfeld,J.U., Lu,K.P., and Fischer,G. (1998). Role of phosphorylation in determining the backbone dynamics of the serine/threonine-proline motif and Pin1 substrate recognition. Biochemistry *37*, 5566-5575.

Shaw,P.E. (2002). Peptidyl-prolyl isomerases: a new twist to transcription. EMBO Rep. *3*, 521-526.

Shen,M., Stukenberg,P.T., Kirschner,M.W., and Lu,K.P. (1998). The essential mitotic peptidyl-prolyl isomerase Pin1 binds and regulates mitosis-specific phosphoproteins. Genes Dev. *12*, 706-720.

Smet,C., Sambo,A.V., Wieruszeski,J.M., Leroy,A., Landrieu,I., Buee,L., and Lippens,G. (2004). The peptidyl prolyl cis/trans-isomerase Pin1 recognizes the phospho-Thr212-Pro213 site on Tau. Biochemistry *43*, 2032-2040.

Stukenberg,P.T. and Kirschner,M.W. (2001). Pin1 acts catalytically to promote a conformational change in Cdc25. Mol. Cell *7*, 1071-1083.

Suizu,F., Ryo,A., Wulf,G., Lim,J., and Lu,K.P. (2006). Pin1 regulates centrosome duplication, and its overexpression induces centrosome amplification, chromosome instability, and oncogenesis. Mol. Cell Biol. *26*, 1463-1479.

Uchida,T., Fujimori,F., Tradler,T., Fischer,G., and Rahfeld,J.U. (1999). Identification and characterization of a 14 kDa human protein as a novel parvulin-like peptidyl prolyl cis/trans isomerase. FEBS Lett. *446*, 278-282.

Van Duyne,G.D., Standaert,R.F., Karplus,P.A., Schreiber,S.L., and Clardy,J. (1991). Atomic structure of FKBP-FK506, an immunophilin-immunosuppressant complex. Science *252*, 839-842.

Verdecia,M.A., Bowman,M.E., Lu,K.P., Hunter,T., and Noel,J.P. (2000). Structural basis for phosphoserine-proline recognition by group IV WW domains. Nat. Struct. Biol. *7*, 639-643.

Wang,X.J. and Etzkorn,F.A. (2006). Peptidyl-prolyl isomerase inhibitors. Biopolymers *84*, 125-146.

Weiwad,M., Kullertz,G., Schutkowski,M., and Fischer,G. (2000). Evidence that the substrate backbone conformation is critical to phosphorylation by p42 MAP kinase. FEBS Lett. *478*, 39-42.

Wells,N.J., Watanabe,N., Tokusumi,T., Jiang,W., Verdecia,M.A., and Hunter,T. (1999). The C-terminal domain of the Cdc2 inhibitory kinase Myt1 interacts with Cdc2 complexes and is required for inhibition of G(2)/M progression. J. Cell Sci. *112 (Pt 19)*, 3361-3371.

Winkler,K.E., Swenson,K.I., Kornbluth,S., and Means,A.R. (2000). Requirement of the prolyl isomerase Pin1 for the replication checkpoint. Science *287*, 1644-1647.

Wintjens,R., Wieruszeski,J.M., Drobecq,H., Rousselot-Pailley,P., Buee,L., Lippens,G., and Landrieu,I. (2001). 1H NMR study on the binding of Pin1 Trp-Trp domain with phosphothreonine peptides. J. Biol. Chem. *276*, 25150-25156.

Wu,R.C., Qin,J., Yi,P., Wong,J., Tsai,S.Y., Tsai,M.J., and O'Malley,B.W. (2004). Selective phosphorylations of the SRC-3/AIB1 coactivator integrate genomic reponses to multiple cellular signaling pathways. Mol. Cell *15*, 937-949.

Wu,X., Wilcox,C.B., Devasahayam,G., Hackett,R.L., revalo-Rodriguez,M., Cardenas,M.E., Heitman,J., and Hanes,S.D. (2000). The Ess1 prolyl isomerase is linked to chromatin remodeling complexes and the general transcription machinery. EMBO J. *19*, 3727-3738.

Wulf,G., Finn,G., Suizu,F., and Lu,K.P. (2005). Phosphorylation-specific prolyl isomerization: is there an underlying theme? Nat. Cell Biol. *7*, 435-441.

Wulf,G.M., Liou,Y.C., Ryo,A., Lee,S.W., and Lu,K.P. (2002). Role of Pin1 in the regulation of p53 stability and p21 transactivation, and cell cycle checkpoints in response to DNA damage. J. Biol. Chem. *277*, 47976-47979.

Wulf,G.M., Ryo,A., Wulf,G.G., Lee,S.W., Niu,T., Petkova,V., and Lu,K.P. (2001). Pin1 is overexpressed in breast cancer and cooperates with Ras signaling in increasing the transcriptional activity of c-Jun towards cyclin D1. EMBO J. *20*, 3459-3472.

Yaffe,M.B., Schutkowski,M., Shen,M., Zhou,X.Z., Stukenberg,P.T., Rahfeld,J.U., Xu,J., Kuang,J., Kirschner,M.W., Fischer,G., Cantley,L.C., and Lu,K.P. (1997). Sequence-specific and phosphorylation-dependent proline isomerization: a potential mitotic regulatory mechanism. Science *278*, 1957-1960.

Ye,X.S., Xu,G., Pu,R.T., Fincher,R.R., McGuire,S.L., Osmani,A.H., and Osmani,S.A. (1995). The NIMA protein kinase is hyperphosphorylated and activated downstream of p34cdc2/cyclin B: coordination of two mitosis promoting kinases. EMBO J. *14*, 986-994.

Yeh,E., Cunningham,M., Arnold,H., Chasse,D., Monteith,T., Ivaldi,G., Hahn,W.C., Stukenberg,P.T., Shenolikar,S., Uchida,T., Counter,C.M., Nevins,J.R., Means,A.R., and Sears,R. (2004). A signalling pathway controlling c-Myc degradation that impacts oncogenic transformation of human cells. Nat. Cell Biol. *6*, 308-318.

Yeh,E.S., Lew,B.O., and Means,A.R. (2006). The loss of PIN1 deregulates cyclin E and sensitizes mouse embryo fibroblasts to genomic instability. J. Biol. Chem. *281*, 241-251.

Yi,P., Wu,R.C., Sandquist,J., Wong,J., Tsai,S.Y., Tsai,M.J., Means,A.R., and O'Malley,B.W. (2005). Peptidyl-prolyl isomerase 1 (Pin1) serves as a coactivator of steroid receptor by regulating the activity of phosphorylated steroid receptor coactivator 3 (SRC-3/AIB1). Mol. Cell Biol. *25*, 9687-9699.

Yu,L., Mohamed,A.J., Vargas,L., Berglof,A., Finn,G., Lu,K.P., and Smith,C.I. (2006). Regulation of Bruton tyrosine kinase by the peptidylprolyl isomerase Pin1. J. Biol. Chem. *281*, 18201-18207.

Zacchi,P., Gostissa,M., Uchida,T., Salvagno,C., Avolio,F., Volinia,S., Ronai,Z., Blandino,G., Schneider,C., and Del,S.G. (2002). The prolyl isomerase Pin1 reveals a mechanism to control p53 functions after genotoxic insults. Nature *419*, 853-857.

Zarrinpar,A. and Lim,W.A. (2000). Converging on proline: the mechanism of WW domain peptide recognition. Nat. Struct. Biol. *7*, 611-613.

Zheng,H., You,H., Zhou,X.Z., Murray,S.A., Uchida,T., Wulf,G., Gu,L., Tang,X., Lu,K.P., and Xiao,Z.X. (2002). The prolyl isomerase Pin1 is a regulator of p53 in genotoxic response. Nature *419*, 849-853.

Zhou,X.Z., Kops,O., Werner,A., Lu,P.J., Shen,M., Stoller,G., Kullertz,G., Stark,M., Fischer,G., and Lu,K.P. (2000). Pin1-dependent prolyl isomerization regulates dephosphorylation of Cdc25C and tau proteins. Mol. Cell *6*, 873-883.

Zhou,X.Z., Lu,P.J., Wulf,G., and Lu,K.P. (1999). Phosphorylation-dependent prolyl isomerization: a novel signaling regulatory mechanism. Cell Mol. Life Sci. *56*, 788-806.

APPENDICES

A Matlab script--Analyzing and plotting graphs for Pin1's melting temperature

(Written by Mr. Xu Yuhong)

```
%read data into column vectors
[a,b,c]=textread('H:\Research Project\CD spectra\For Matlab\WT hepes 20-90
a.txt','%f%f%f');
b=111.92*b/(10*0.1*0.18)

%cubic smoothing spline with appropriate smoothing parameter
f=csaps(a,b,0.001); %0.01 is a smoothing parameter

%find the minimum and maximum value
m1=fnmin(f,[min(a) max(a)]); %minimum
g=f;
g.coefs=-f.coefs;
m2=-fnmin(g,[min(a) max(a)]); %maximum

%find the roots of eqn f(x)=(m1+m2)/2
mean=(m1+m2)/2;
h=f;
h.coefs(:,4)=h.coefs(:,4)-mean;
rts=fnzeros(h,[min(a) max(a)]);

%display the value of the roots; show the plot
disp('the root is:'); disp(rts);
%subplot(1,2,1);
fnplt(f,2), hold on, plot(a,b,'x'),hold on;
plot([min(a) max(a)],[m1 m1],'--'),hold on;
plot([min(a) max(a)],[m2 m2],'--'),hold on;
plot([min(a) max(a)],[mean mean],'--'),hold on;
set(gca,'xlim',[20 90]);
xlabel('Temperature (^o C)');ylabel('deg.cm^2.dmol^{-1}');
legend(strcat('Tm = ', num2str(rts(1))));
%title('Thermo-unfolding Curve of WT');
%subplot(1,2,2);
%fnplt(f,2);
%set(gca,'xlim',[20 90]);
%xlabel('Temperature (^o C)');ylabel('degcm^2dmol{-1}');
title('Thermo-unfolding Curve of WT');
```